THE EFFECT OF BASIN PHYSIOGRAPHY ON THE SPATIAL DISTRIBUTION OF SNOW WATER EQUIVALENT AND SNOW DENSITY NEAR PEAK ACCUMULATION

by

Karl Bruno Wetlaufer

A thesis submitted in partial fulfillment
of the requirements for the degree

of

Master of Science

in

Earth Sciences

MONTANA STATE UNIVERSITY
Bozeman, Montana

April 2013

© COPYRIGHT

by

Karl Bruno Wetlaufer

2013

All Rights Reserved

APPROVAL

of a thesis submitted by

Karl Bruno Wetlaufer

This thesis has been read by each member of the thesis committee and has been found to be satisfactory regarding content, English usage, format, citation, bibliographic style, and consistency and is ready for submission to The Graduate School.

Dr. Jordy Hendrikx

Approved for the Department of Earth Sciences

Dr. David Mogk

Approved for The Graduate School

Dr. Ronald W. Larsen

STATEMENT OF PERMISSION OF USE

In presenting this thesis in partial fulfillment of the requirements for a master's degree at Montana State University, I agree that the Library shall make it available to borrowers under rules of the Library.

If I have indicated my intention to copyright this thesis by including a copyright notice page, copying is allowable only for scholarly purposes, consistent with "fair use" as prescribed in the U.S. Copyright Law. Requests for permission for extended quotation from or reproduction of this thesis in whole or in parts may be granted only by the copyright holder.

Karl Bruno Wetlaufer

April 2013

ACKNOWLEDGEMENTS

I would like to thank the following for helping me make this research possible. First of all I would like to thank my committee members, Dr. Jordy Hendrikx (primary advisor), Dr. Lucy Marshall, and Stuart Challender for invaluable insight and encouragement. I would also like to thank the Montana Institute on Ecosystems, The Montana Water Center, and the Montana State University College of Letters and Science for funding which allowed me to complete this research and present it at several professional conferences. In addition, I would also like to acknowledge and thank my field assistants who helped in gathering a very substantial data set: Alex Marienthal, Chris Ebeling, Christine Miller, Ryan McClure, Sam Swanson, Olivia Buchanan, Zach Rich, Tom Matthews, Gaelen Rhinard, Rebecca Kurnick, James Hadfield, and the Yellowstone Club Ski Patrol. Big Sky Resort, The Yellowstone Club, and Lone Mountain Ranch provided access to private land to sample on as well as access to public portions of the basin otherwise inaccessible. For data contributions I would like to thank Dr. Rick Lawrence of the Montana State University Spatial Sciences Center for quality land cover data. Last but certainly not least I would like to thank all of my family and friends for unending support through all of my endeavors.

TABLE OF CONTENTS

1. INTRODUCTION 1

2. STUDY AREA 9

3. METHODS 11

Defining Sampling Areas 11
Data Collection 18
Data Processing 20
Data Analysis 21
Mixed Effects Multiple Regression Analysis 22
Binary Regression Tree Analysis 23
Conditional Inference Tree Analysis 24
Model Implementation 24
Modeling the Spatial Distribution of Snow Density 25

4. RESULTS 26

Representative Sampling 26
Field Observations 30
Modeling the Spatial Distribution of Snow Water Equivalent 31
Mixed Effects Multiple Regression Analysis 31
Binary Regression Tree Analysis 35
Conditional Inference Tree Analysis 38
Model Comparisons 41
Modeling the Spatial Distribution of Snow Density 50
Multiple Linear Regression 51
Binary Regression Tree 53
Comparison of Modeled and Measured Snow Densities 55
The effect of Density Parameterization on Estimates of Total Basin SWE 57
Comparisons to the Lone Mountain SNOTEL Site 59

5. DISCUSSION 61

Spatial Distribution of Snow Water Equivalent 61
Spatial Distribution of Snow Density 68

6. CONCLUSIONS 71

TABLE OF CONTENTS CONTUNUED

7. CHALLENGES, IMPROVEMENTS, AND RECOMMENDATIONS 73

Sampling Plan 73
Lack of Access due to Low Snowpack 73
Avalanche Hazard 74
Access to Sample on Private Land 74
Changing Weather Throughout Sampling Campaign 75
Precisely Defining Sampling Areas 75
Analysis and Modeling 76
Recommendations for Similar Future Research 77

REFERENCES CITED 79

APPENDICES 83

APPENDIX A: Data Used For Analysis 84
APPENDIX B: Conditional Statements 112

LIST OF TABLES

Table Page

1. Reclassification Parameters for Defining Sampling Strata....12

2. Justification of Physiographically Proportional Sampling Areas by Percent of Each Strata in the Whole Basin to that in the Sampling Areas....17

3. Summary of Results of the Sampling Plan by Strata....29

4. Summary of Observed SWE and Snow Density Data....31

5. Summary of Results of Mixed Effects Multiple Regression Analysis for Models Utilizing One Explanatory Variable....31

6. Summary of Results of Mixed Effects Multiple Regression Analysis for Models Utilizing Three Explanatory Variables....34

7. Summary of Modeled SWE Values from all Model Structures....41

8. Summary of the Results of SLR of Physiographic Parameters on Snow Density....51

9. Results of MLR Models for Snow Density....52

10. The effect of varying depth and density parameterizations on estimates of total basin SWE....58

11. Comparisons of modeled and measured values to that measured at the Lone Mountain SNOTEL site....60

LIST OF FIGURES

Figure Page

1. Comparison of the Elevation Range and Spatial Extent of Similar Studies....8

2. West Fork of the Gallatin River Basin in Southwest Montana....10

3. Hypsometry of the West Fork of the Gallatin River Basin....10

4. Parameters used for Defining Physiographic Strata 13

5. Sampling areas 14

6. Percent of whole basin in elevation bands used to define strata compared to percent of sampling areas in these elevation bands 15

7. Percent of whole basin in radiation bands used to define strata compared to percent of sampling areas in these radiation band 15

8. Percent of whole basin in landcover classes used to define strata compared to percent of sampling areas in these classes 16

9. Comparison of Percentage of Area Covereved by each Physiographic Strata in Defined Sampling Areas to the Basin as a Whole....16

10. Example of the Field Data Collection Plan....19

11. Locations of All Sampled Points in the Basin 20

12. Comparison of Percentage of Basin area to Percentage of Sampled Points by Elevation Band 26

13. Comparison of Percentage of Basin to Percentage of Sampled Points by Relative Incoming Solar Radiation Levels 27

14. Comparison of Percentage of Whole Basin to Percentage of Sampled Points by Land Cover 28

15. Comparisons of Percent of Basin Area to Percent of Sampled Points by Physiographic Strata 29

LIST OF FIGURES CONTINUED

Figure Page

16. Relation between slope angle and radiation....34

17. Modeled Spatial Distribution of SWE Using the MEMR Model....35

18. Binary Regression Tree Model for SWE....36

19. Modeled Spatial Distribution of SWE Using the Binary Regression Tree Model....37

20. Modeled Spatial Distribution of SWE Using the Conditional Inference Tree Model....39

21. Conditional inference tree model structure for SWE....40

22. Comparison of the Three Models of the Spatial Distribution of SWE Compared to Their Average....42

23. Boxplot Comparisons of Measured and Modeled Values of SWE....43

24. Comparisons of Measured and Modeled SWE Values at the Locations of Measured Points, by Elevation....44

25. Observed vs. modeled values of SWE....45

26. Comparison of residuals of modeled SWE values from measured values at measured points....46

27. Comparison of Modeled SWE Values to Their Average, by Elevation....48

28. Comparison of the spatial distributions of SWE models to their average....49

29. The Spatial Distribution of Snow Density Using a Multiple Linear Regression Model....53

LIST OF FIGURES CONTINUED

Figure Page

30. Binary Regression Tree for Snow Density Utilizing Nine Terminal Nodes....54

31. Modeled Spatial Distribution of Snow Density Using a Nine Node Regression Tree....55

32. Boxplot Comparisons of Measured and Modeled Snow Densities....56

33. Comparison of the Distributions of Measured to Modeled Snow Densities....57

ABSTRACT

This study quantifies the effect of the physiography (elevation, potential incoming solar radiation, land cover, etc.) of a large (207 km^2) and complex mountainous basin on the spatial distribution of snow water equivalence (SWE) and snow density during peak SWE accumulation. SWE and snow density were sampled in areas of the basin that were physiographically representative (based on unique combinations of elevation, incoming solar radiation, and land cover) to the basin as a whole. Sampling took place over a variety of spatial scales (10m-400m) in a semi-random and structured manner acquiring over 1,000 direct measurements of SWE and snow density. Three modeling approaches were used in the analysis of the SWE data; regression tree, conditional inference tree, and mixed effects multiple regression. The three modeling approaches were similar in their estimates of total basin SWE (approximately within 1% of their averages) but provided very different patterns of how SWE is spatially distributed throughout the basin. All three methods showed elevation and potential incoming solar radiation to have the most significant influence on the spatial distribution of SWE, with land cover also being significant in the mixed effects and conditional inference tree models. Snow density was observed to vary widely throughout the basin with a standard deviation of 61 kg/m^3 around a mean of 349 kg/m^3. The spatial distribution of density was modeled using regression tree and multiple linear regression analysis. Both models estimated similar basin average snow density using elevation and radiation as explanatory variables, but displayed considerably different spatial distributions and ranges of value. This study demonstrates the importance of elevation and radiation for modeling the spatial distribution of SWE and snow density in a large and physiographically diverse basin and expresses the differences that exist between various methods of modeling these phenomena

1.0 INTRODUCTION

Much of the Western United States depends on the winter snowpack for water supply throughout the year, with about 60-75% of streamflow being derived from snowpack in mountainous regions [*Doeksen and Judson*, 1996]. Because of this, a thorough understanding of how much water is stored in the winter snowpack is of great importance to this region. The spatial distribution of snow water equivalence (SWE) in large and physiographically diverse watersheds is an important and poorly understood aspect of snow hydrology. One way of improving this understanding is by investigating correlations between basin physiography (e.g. elevation, land cover, incoming solar radiation, etc.) and SWE depths. An improved understanding of how SWE is spatially distributed throughout complex terrain, and the various methods of modeling it, can lead to improved accuracy and precision of water supply forecasting. More accurate estimates of the amount of water stored in the winter snowpack can positively influence agricultural planning, reservoir management (e.g. for applications in managing hydro-electric power, municipal water supply, agricultural water supply, and buffering potential flood waters), flood forecasting, and recreation (e.g. fishing, boating, and the local economic impacts thereof), among others.

The challenge of quantifying the spatial distribution of SWE in mountainous terrain has been approached by many previous studies using a variety of methods and over a wide range of spatial scales [*Clark et al.*, 2011]. Some of the common statistical methods used to approach this challenge include binary regression trees [e.g. *Molotch et al.*, 2005 and *Winstral et al.*, 2002] and binary regression trees in combination with the

kriging of the residuals between modeled and measured values [e.g. *Balk and Elder*, 2000 and *Erxleben et al.*, 2002]. In addition to various modeling methods, the influence of using varying input data for the same parameters has also been analyzed [e.g. *Molotch et al.*, 2005]. Most of the prior research done with regards to estimating the spatial distribution of SWE has used these methods to estimate the spatial distribution of snow depth (due to increased sampling efficiency) after which SWE is modeled using various parameterizations of snow density. While sampling efficiency may be increased using this method increased uncertainty is also introduced when extrapolating this data to make inferences about SWE, whereas if SWE is directly measured at each sampled point (as in this study) those particular uncertainties are avoided.

Recursive partitioning through binary regression tree analysis [*Breiman et al.*, 1984] has been a commonly used statistical tool for analysis of correlations between snow depth and physiographic parameters. Binary regression trees have been successfully used by many studies to quantify the effect of physiographic parameters (e.g. elevation, potential incoming solar radiation, vegetation, slope angle, and aspect) on the spatial distribution of SWE [e.g. *Elder et al.*, 1998; *Erxleben et al.*, 2002; *Winstral et al*., 2002; *Molotch et al.*, 2005] with varying results, explaining between 18-70% of observed variance depending on the study. In addition to the commonly used parameters, such as elevation, radiation, slope angle and land cover, *Winstral et al.* [2002] studied the effect of wind redistribution parameters in a regression tree model. These parameters substantially improved model performance (with an increase of 8-23% of explained variance by including wind related parameters) in the wind dominated 2.3 km^2 Green

Lakes Valley in Colorado. Here, the wind re-distribution parameters showed stronger correlation to SWE depth than any others, including elevation. The lack of correlation to elevation in *Winstral et al.* [2002] likely has relation to this basin having a relatively small elevation range (~425m) and being in a wind dominated alpine environment [*Winstral et al*, 2002; *Erickson et al.*, 2005]. *Molotch et al.* [2005] quantified the impact of the digital elevation data and independent variable selection when applied to analyzing field data of snow depth using binary regression trees. Their results indicate that the use of different digital elevation models (DEMs) can substantially affect snow distribution models, with the standard U.S. Geological Survey (USGS) DEM yielding the lowest overall model deviance and lowest error in snow depth prediction.

Geostatistical methods (kriging, co-kriging, inverse distance weighting, etc.) have been used in combination with regression tree models as an attempt to improve model performance, but with mixed results. In a study of three different 1 km^2 plots in Colorado *Erxleben et al.* [2002] found regression trees to provide superior results compared to a combined method with geostatistics at two out of three sites with the combined modeling method being only slightly superior at the third. *Erxleben et al.* [2002] notes that while the regression tree models generated the most accurate results (compared to geostatistical methods and a combined method) these models still left substantial portion (70-82%) of the observed variability in snow depth unexplained. Also in Colorado, *Balk and Elder* [2000] found strong results from both a regression tree alone as well as a combined model of a regression tree and kriged estimates of residuals from measured points in the 6.9 km^2 Loch Vale watershed. The decision tree models explained 54-65% of observed

variance and the combined model explained 60-85% of observed variance. By utilizing the kriged residuals from measured points the model results were further refined in areas that were being either over or underestimated, leading to the increased percent of explained variance.

The sampling plan employed for a given study can have a substantial impact on the results [*Skøien and Blöschl*, 2006]. Many different types of sampling plans have been employed in studies of the spatial distribution of SWE [*Clark et al.*, 2011]. The issues of scale and scaling, as defined by *Blöschl and Sivapalan* [1995], in both measurement and modeling of snow hydrological phenomena is non-trivial and can have considerable effects on the outcome of a study [*Blöschl*, 1999; *Skøien and Blöschl*, 2006]. The concept of a scale triplet consisting of spacing, extent, and support can be used to define the spatial dimensions of a field study (or monitoring network) where spacing is the average distance between samples, extent is the size of the domain sampled, and support is the averaging area of one sample [*Skøien and Blöschl*, 2006]. *Blöschl* [1999] gives a detailed treatment of issues that can arise when extrapolating or interpolating between spatial scales of natural processes, measurements, or models in snow hydrology. In this he discusses why close attention must be given to these issues, particularly with regards to the importance of designing a sampling plan that is spatially congruent with the proposed analysis and modeling.

Simple random sampling (SRS) was used by Elder et al. (1991) with success in a relatively small (1.2 km^2) watershed, but noted that statistical analysis showed partitioning the watershed based on topography and radiation does produce superior

results over SRS. While SRS can be a practical approach in small watersheds it poses logistical challenges for sampling larger areas due to time constraints involved with accessing randomly assigned points. Steep terrain and avalanche hazard can limit data collection to safe and accessible areas [*Winstral et al.,* 2002]. Sampling using transects in portions of the basin deemed to be characteristic of the whole have also been used [*Elder et al.,* 1998; *Clark et al.,* 2011], with samples generally taken at regular intervals in each transect. Sampling an entire basin on a relatively evenly spaced grid [*Balk and Elder,* 2000 *Molotch et al.* 2005] allows for complete coverage of a basin in a manageable time period [*Molotch et al.,* 2005]. Other sampling strategies that have been used include collecting samples at regular intervals while travelling through all safe and accessible areas of a basin [*Winstral et al.,* 2002] and utilizing both transects and random sampling within the confines of pre-defined grid cells [*Erxleben et al.,* 2002].

Many studies have also attempted to sample areas of a basin that are physiographically proportional to the whole basin on a qualitative level, but few have quantified this prior to sampling. *Jost et al.* [2007] stratified the Cotton Creek (17.4 km^2) watershed in British Columbia, Canada into 19 strata defined by elevation, aspect, and forest cover. Within each of these strata two perpendicular transects of 30 depth measurements were taken, along with 12 density measurements. In Yellowstone National Park, WY *Watson et al.* [2006] utilized a sampling plan that accounted for quantification of both fixed effects (i.e. due to elevation, vegetation, radiation, etc.) and random effects on how SWE is distributed throughout the landscape. The study area was stratified based on elevation, radiation, vegetation, and time (treated as the different sampling campaigns

throughout the winter and spring) and samples were acquired on a range of spatial scales in a five stage nested design (on scales of approximately1000m, 250m, 100m, 10m, and 1m) with random starting points within each strata. The nested sampling plan utilized by *Watson et al.* [2006] minimized random effects compared to sampling cost (with regards to time, money, and energy expenditure).

Most of the sampling plans and modeling efforts mentioned above are primarily for snow depth, while the sampling and modeling of snow density (necessary for estimating SWE) has been approached through a variety of means. Studies have attempted to correlate basin physiography to the spatial distribution of snow density [*Molotch et al.*, 2005; *Erxleben et al.*, 2002], but found no significant relations based on the density samples taken and applied the average measured density basin wide to calculate SWE. While *Clark et al.* [2011] took at least one density measurement in each transect of snow depth their analysis still only focused on snow depth as opposed to SWE, due in part to both a small number of density measurements and that snow density varied minimally between transects. The spatial distribution of snow density was calculated by *Elder et al.* [1998] to estimate basin SWE from snow depth measurements, but was done using only n=10 density measurements. *Watson et al*. [2006] collected all samples (average of ~200 per sampling campaign) with a Federal Sampler, providing direct measurements of SWE, snow depth, and snow density at all locations.

This study utilized a sampling plan which identified sampling areas of a large (207 km^2) and physiographically diverse drainage basin in Southwest Montana (USA) which were physiographically proportional to the basin as a whole. Within these

sampling areas over 1,000 direct measurements of SWE, snow depth, and therefore density were acquired in a semi-random structured manner and at spatial scales of 10-400m. All measurements were taken using federal SWE samplers near the time of peak accumulation (around April, 1 2012). The spatial distribution of SWE was modeled using regression tree, mixed effects multiple regression (MEMR), and conditional inference (CI) tree analysis. The spatial distribution of snow density was modeled using multiple linear regression and regression tree analysis.

This research builds upon prior work regarding the spatial distribution of SWE in several ways. First, it develops a sampling plan structure that provides a physiographically proportional data set that can be replicated over a wide range of spatial scales and landscape types. These methods were developed for a substantially larger watershed than studied in most similar ground based studies of the spatial distribution of SWE (Figure 1).

The use of a watershed of this size furthers the understanding of how the spatial distribution of SWE varies over a wide range of spatial scales and makes steps towards being able to more accurately model it from the catchment to the regional scale (as defined by *Blöschl and Sivapalan*, 1995). Second, this research also provides a comparison between a well accepted method of modeling the spatial distribution of SWE (binary regression tree) and two methods that were previously unused for this type of research (MEMR and CI tree analysis). Lastly, with over 1,000 direct measurements of snow density a more accurate quantification of the effect of physiography on the spatial distribution of snow density was obtained than has been possible in previous research.

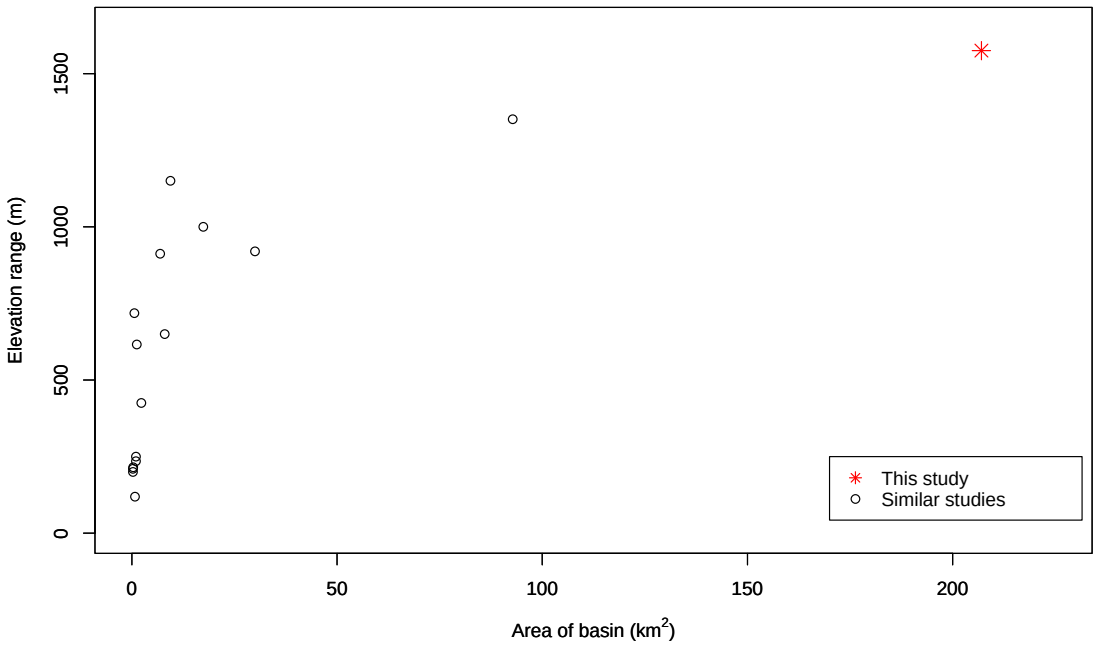


Figure 1. Comparison the elevation range and spatial extent of similar studies of the spatial distribution of SWE in mid-latitude mountainous basins. Based on data from *Clark et al*. [2011].

2.0 STUDY AREA

This study was conducted in the West Fork of the Gallatin River Basin (West Fork Basin) in Southwest Montana, approximately 45° 16'N, 111° 26'W, (Figure 2). The elevation ranges from 1830m at the confluence of the West Fork of the Gallatin with the Gallatin River to 3405m at the top of Lone Peak (1575m of total vertical relief) and covers an area of 207 km^2. A hypsometric profile of the basin is shown in Figure 3. The West Fork Basin is very physiographically diverse ranging from low elevation grass and sagebrush cover, to mid elevation conifer forests, to high elevation steep rocky alpine terrain. Approximately 52% of the basin contains conifer forests with the landcover in the remaining areas consisting primarily of grass and sagebrush in the lower elevations and rocky alpine terrain at the higher elevations. The basin is partially developed, containing a small community (Big Sky, MT) and ski resorts on Lone Peak and Pioneer mountains in the western portion of the basin. Currently the only automated SWE data for the basin is provided by the Lone Mountain Snow Telemetry (SNOTEL) site which is located in a small meadow in the west-central portion of the basin at an elevation of 2706m. As of April 1, 2012 (the time of sampling) the Lone Mountain SNOTEL site was reporting 93% of average SWE based on a 21-year record (1991-2012), at 450mm.

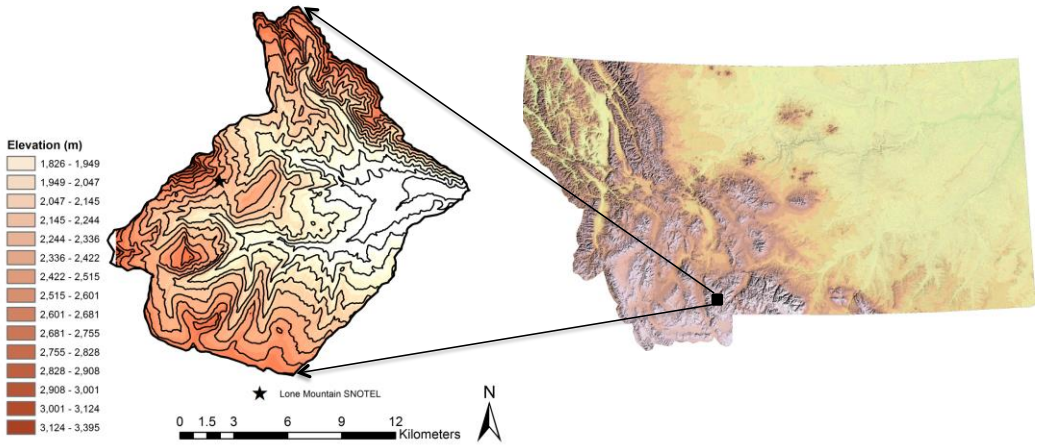


Figure 2. West Fork of the Gallatin River Basin in Southwest Montana, 100m contour interval.

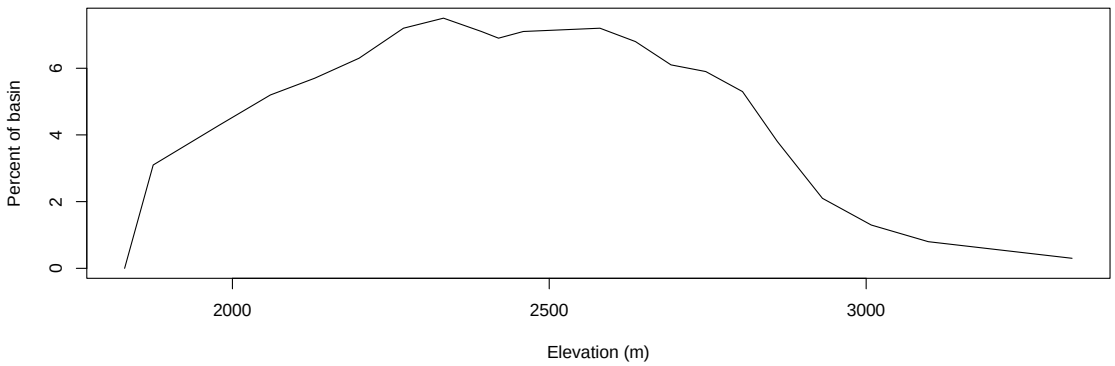


Figure 3. Hypsometric profile of the West Fork Basin.

3.0 METHODS

3.1 Defining Sampling Areas

A primary goal of the sampling plan was to sample smaller areas of this relatively large (compared to previous similar studies) basin that were physiographically proportional to the basin as a whole. These defined smaller portions of the basin are where all SWE samples were collected and are termed 'sampling areas' herein. The methods developed for this study were also designed so the same approach can be easily replicated over a wide range of spatial scales and landscape types to maximize comparisons between future studies. The determination of physiographic proportionality was done by defining strata within the basin that consist of unique combinations of elevation, potential incoming solar radiation, and landcover. These three parameters were chosen because it is well accepted that they have a strong influence on the spatial distribution of SWE [*Clark et al.,* 2011]. Elevation data was derived from a USGS 30m Digital Elevation Model (DEM). Potential incoming solar radiation was calculated from this DEM as total potential accumulated radiation from December 1st 2011 through April 1st 2012 using the area solar radiation calculation in *ArcGIS 10.0*. Land cover data was derived from Landsat imagery (30m resolution) that had been classified for the study site with high accuracy [*Campos et al.,* 2011].

Elevation and potential incoming solar radiation were reclassified into five (~equal interval) and four (by Jenks Natural Breaks) distinct categories, respectively, while the land cover data was reclassified as forested or un-forested, all in separate

rasters. Physiographic strata were defined through the use of map algebra applied to reclassified raster datasets of the aforementioned parameters through raster addition. Each parameter was reclassified on a different order of magnitude so when added together provided unique identifiers of which combination of parameters comprise each strata (Table 1).

Table 1. Reclassification parameters for defining sampling strata.

Parameter	Original Value(s)	Reclassified Value
Elevation (m)	1820 - 2139	1000
	2140 - 2453	2000
	2454 - 2767	3000
	2768 - 3081	4000
	3082 - 3395	5000
Radiation (WH/m^2)	63,919 - 176,897	100
	176,898 - 228,251	200
	228,252 - 279,604	300
	279,605 - 391,299	400
Land Cover	Unforested	0
	Forested	10

For example, if a given strata had an identifier of 1410, that strata is in the lowest elevation band (1000), receives the highest levels of solar radiation (0400), and is forested (0010). Through this process 36 unique strata were defined (Figure 4) to identify and justify which portions of the basin were to be sampled. Sampling areas were chosen based on both accessibility and physiographic representativeness of the basin as a whole.

The physiographic representativeness of the sampling areas (Figure 5) was assessed by comparing the percent of the whole basin to the percent of the sampling areas lying within each of the classifications of the physiographic parameters used to define the

strata, as well as the strata themselves. Figure 6 shows this comparison with the five elevation bands.

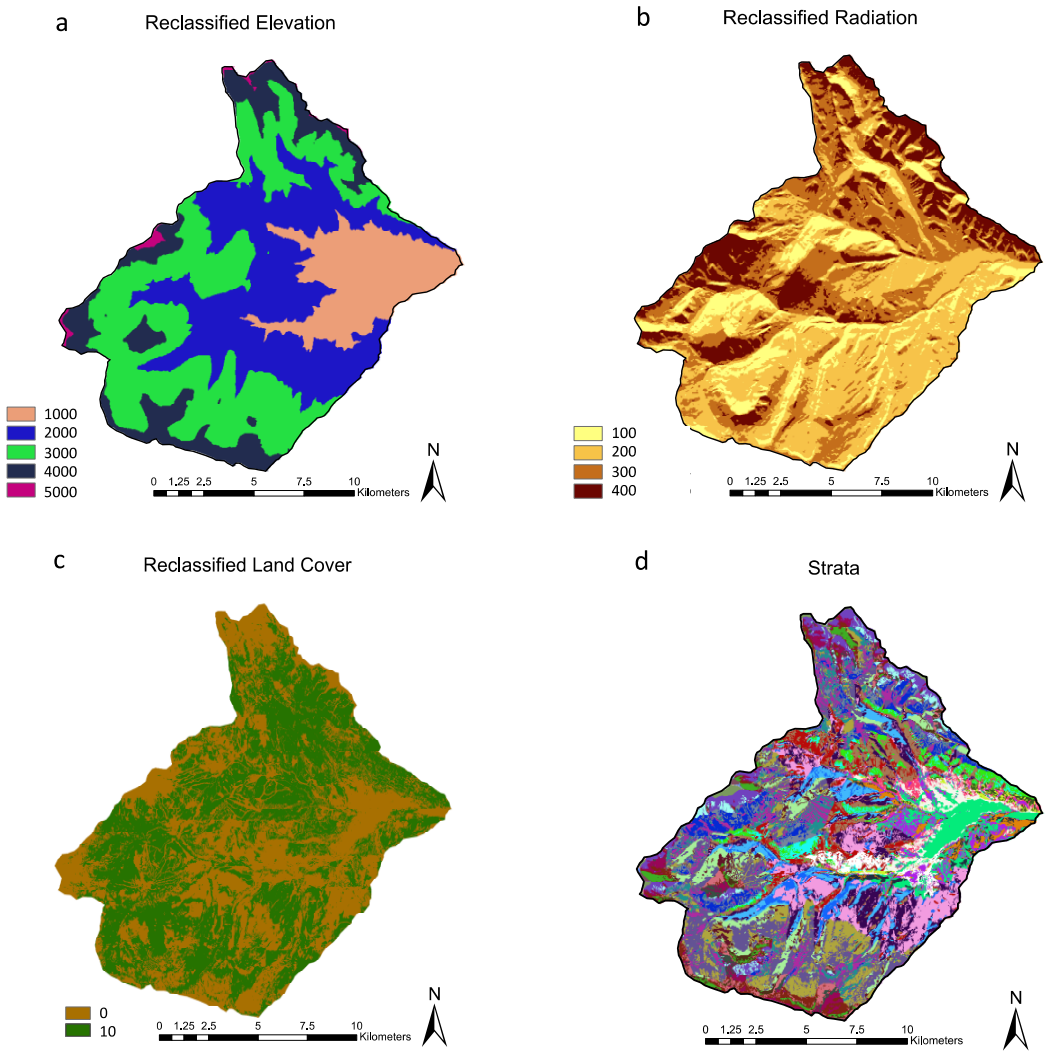


Figure 4. Parameters used for defining physiographic strata. Five elevation bands (a), four levels of potential incoming solar radiation (b), and land cover (c) were used to define the physiographic strata (d) which aided in determining the sampling areas. While a legend is not included for figure 4d each color represents an individual strata resulting from unique combinations of the reclassified physiographic parameters.



Figure 5. The sampling areas are shown by the yellow polygons.

The representativeness of the sampling areas with regard to the various radiation levels (Figure 7) provides a closer match than that of the elevation bands, but with the largest relative differences also existing in the middle of the range and a very close match in areas of that receive the highest levels of potential incoming solar radiation. Figure 8 shows this same comparison for forested and un-forested areas with the match being almost identical.

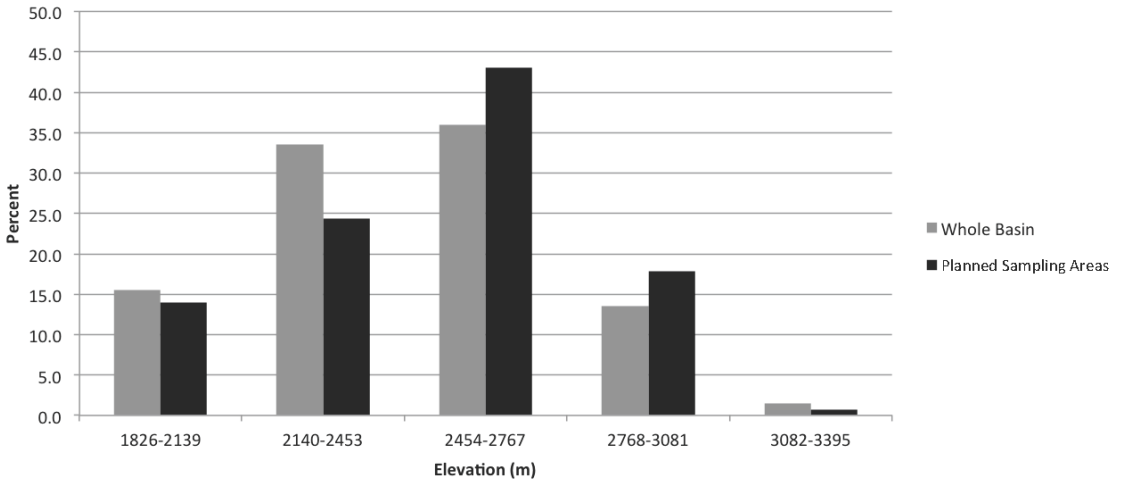


Figure 6. Percent of whole basin in elevation bands used to define strata compared to percent of planned sampling areas in each elevation band.

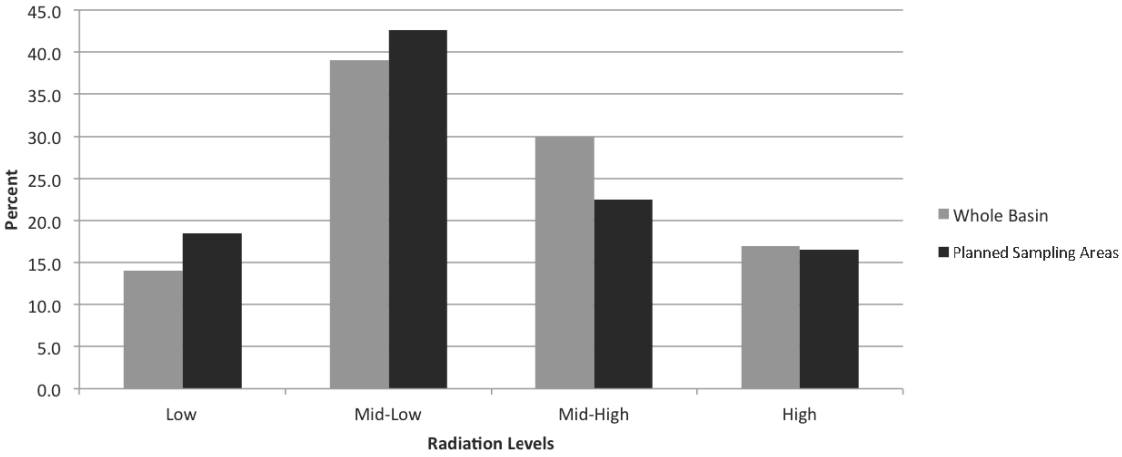


Figure 7. Percent of whole basin in radiation bands used to define strata compared to percent of planned sampling areas in each radiation band.

Overall representativeness of the sampling areas was determined by comparing the percent of pixels of the various classified ranges of physiographic parameters as well as the defined strata within the sampling areas to that of the whole basin, the results for the comparison by strata are shown in Figure 9 and Table 2.

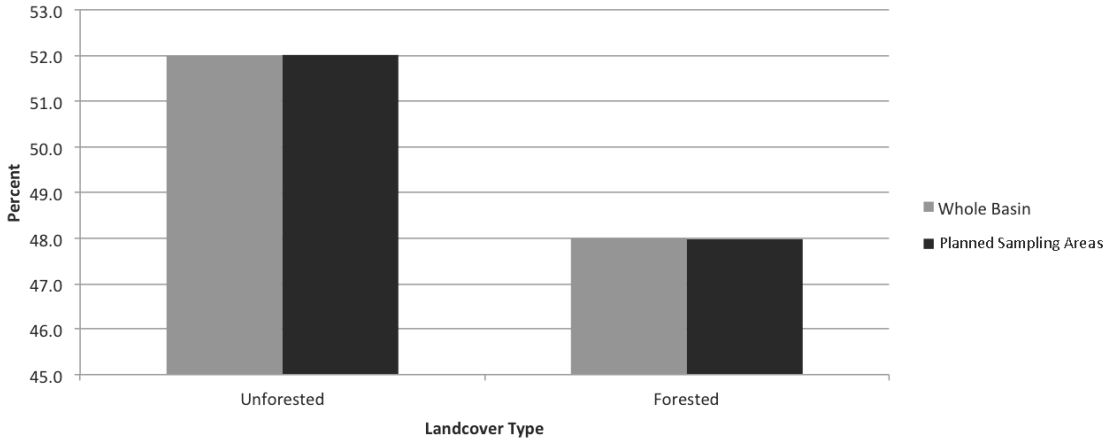


Figure 8. Percent of whole basin in landcover classes used to define strata compared to percent of planned sampling areas in each land cover class.

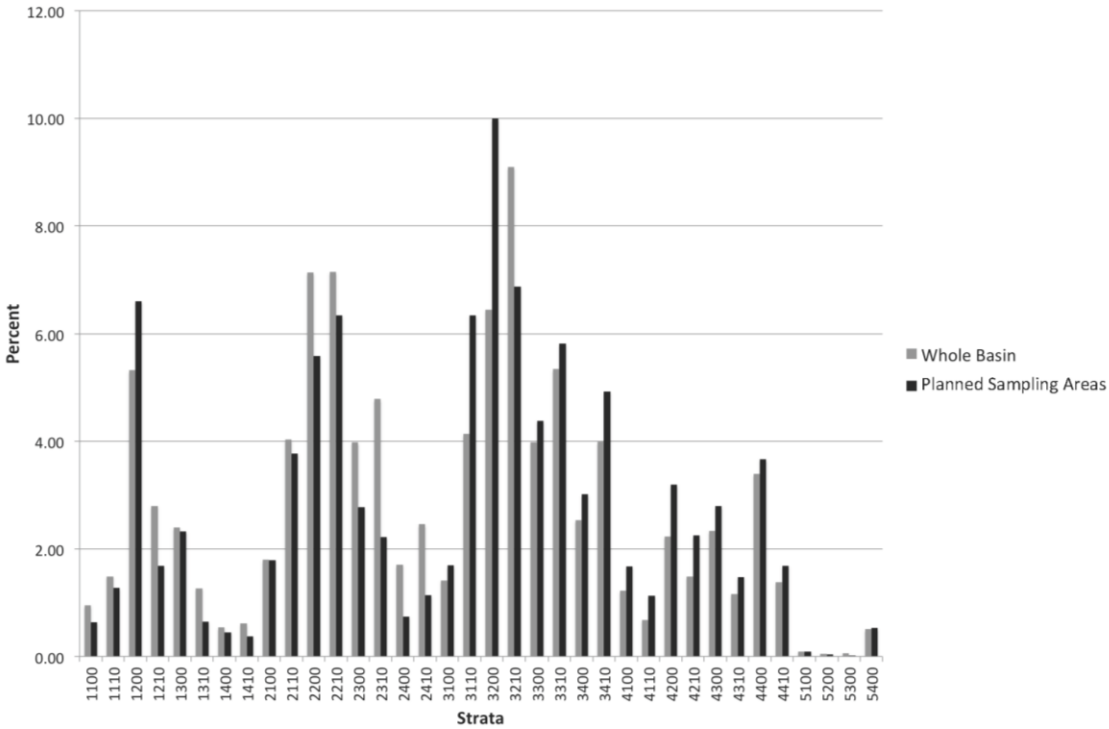


Figure 9. Comparison of percentage of area covereved by each physiographic strata in the planned sampling areas to the basin as a whole.

As would be expected from the results of the elevation and radiation bands, the largest discrepancies by strata exist in the those that represent the mid-elevations (e.g. strata 2xxx and 3xxx) and mid-levels of radiation (strata x2xx and x3xx).

Table 2. Justification of physiographically proportional sampling areas by percent of each strata in the whole basin to that in the sampling areas.

Strata	Percent of Whole Basin	Percent of Sampling Areas	Absolute % Difference	Ratio of Basin Area to Sampled Points
1100	0.95	0.64	0.31	1.48
1110	1.49	1.27	0.22	1.17
1200	5.32	6.6	-1.28	0.81
1210	2.8	1.69	1.11	1.66
1300	2.4	2.33	0.07	1.03
1310	1.27	0.65	0.62	1.95
1400	0.54	0.45	0.09	1.20
1410	0.61	0.37	0.24	1.65
2100	1.8	1.79	0.01	1.01
2110	4.03	3.77	0.26	1.07
2200	7.14	5.59	1.55	1.28
2210	7.15	6.34	0.81	1.13
2300	3.98	2.77	1.21	1.44
2310	4.79	2.23	2.56	2.15
2400	1.71	0.75	0.96	2.28
2410	2.46	1.14	1.32	2.16
3100	1.41	1.69	-0.28	0.83
3110	4.14	6.34	-2.2	0.65
3200	6.45	9.99	-3.54	0.65
3210	9.09	6.87	2.22	1.32
3300	3.98	4.38	-0.4	0.91
3310	5.35	5.82	-0.47	0.92
3400	2.53	3.01	-0.48	0.84
3410	3.99	4.92	-0.93	0.81
4100	1.23	1.68	-0.45	0.73
4110	0.68	1.13	-0.45	0.60
4200	2.23	3.19	-0.96	0.70
4210	1.49	2.26	-0.77	0.66
4300	2.33	2.79	-0.46	0.84
4310	1.16	1.48	-0.32	0.78
4400	3.4	3.67	-0.27	0.93

Table 2 Continued

4410	1.38	1.69	-0.31	0.82
5100	0.09	0.09	0	1.00
5200	0.05	0.03	0.02	1.67
5300	0.06	0.02	0.04	3.00
5400	0.51	0.53	-0.02	0.96

3.2 Data Collection

The field data collection campaign took place over the course of several days encompassing April 1st, 2012, near the time of peak SWE accumulation as recorded at the Lone Mountain SNOTEL site. SWE and snow depth measurements were acquired using Federal SWE Samplers. Sets of three samples were taken as 10 meter equilateral triangles to minimize bias due to anisotropy [*Watson et al.*, 2006]. These sets of three samples were acquired at randomly assigned distances that varied from 30m to 400m (as best estimated by sampling teams) between them (Figure 10) as teams of two travelled throughout a defined sampling areas. The goal of the sampling teams was to travel throughout an assigned area through all of the strata lying within that area, continually sampling along their path. This range of spatial scales was chosen based on insight gathered from Watson et al. [2006] and the results of pilot studies to ensure sampling teams could adhere to the sampling plan while travelling throughout the entirety an assigned area. By sampling at random distances over spatial scales of 10m and 400m variation in snow depth were captured within multiple frequency intervals in snow depth variation (as observed by *Trujillo et al.*, 2007) allowing for the capture of interactions between SWE depth and the surrounding physiography over both small and large spatial extents. Additionally, given that any point some distance away from a random starting

point (previously sampled location) is equally as representative as any other point the same distance away, the effect of random sampling was achieved through the systematic sampling of a random field [*Lohr,* 1999; *Watson et al.*, 2006].

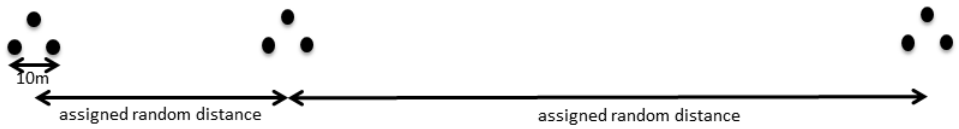


Figure 10. Example of the field data collection plan.

The randomization of the distances at which samples are taken allows for a more robust statistical analysis [*Kronholm and Birkeland,* 2007]. Much of this sampling theory was also influenced by the importance of the scale triplet in spatial sampling, where spacing, extent, and support are used to define the spatial dimensions of a field study [*Blöschl and Skøien*, 2006; *Blöschl and Sivapalan*, 1995]. In total 1043 direct measurements of SWE and snow depth (and therefore density) were measured and recorded, the locations of which are shown in Figure 11, with approximately 25% of the basin area being sampled.

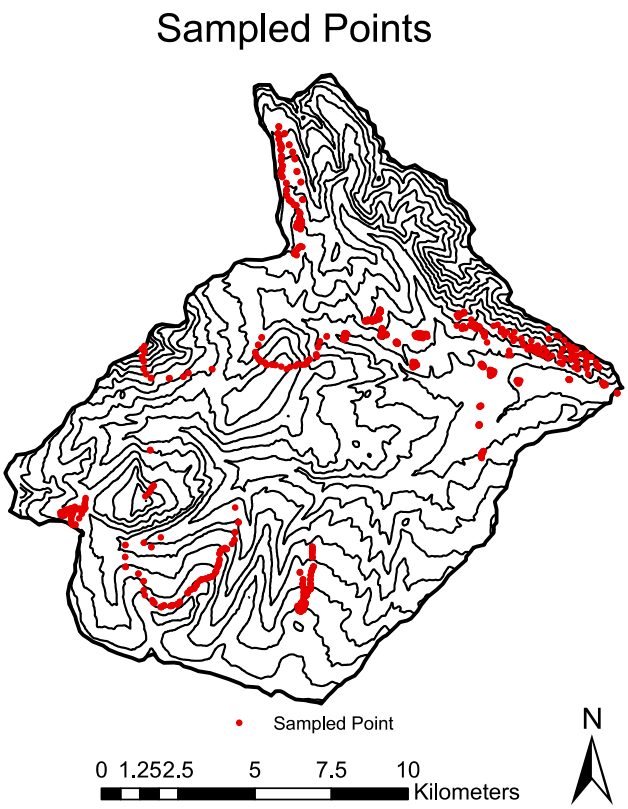


Figure 11. The locations of all sampled points in the basin, 100m contour interval.

3.3 Data Processing

The GPS data collected during the field campaign was post processed against the Montana State University Continuously Operating Reference Station to ensure maximum positional accuracy of the data points. Sub-meter accuracy is important if the data are to be analyzed using high resolution DEMs (e.g. 1m LiDAR derived data, although the analysis described herein utilized 30m data). After post processing the data for this project had an average of approximately 0.6m accuracy. All GPS data collected in the field was exported as a single shapefile with SWE and snow depth values attached to each point feature as an attribute. Using GIS, the various physiographic attributes of the

point where a sample was collected were added to the attributes of the point feature. These included elevation, potential incoming solar radiation (total accumulated from December 1st through April 1st as WH/m^2), land cover (as forested or not), slope angle, aspect, and degree of curvature of the land surface. Curvature was calculated as the second derivative of the surface for each pixel in the basin (utilizing the elevations of adjacent cells), with positive values indicating concavity and negative values indicating convexity. While no direct indices related to wind redistribution or wind exposure were included, as observed by *Golding* [1974] and *Woo et al.* [1983] the degree of curvature was thought to possibly have relation to wind with snow being removed from convex areas and re-deposited in concave areas.

Samples that were assumed to be inaccurate due to measurement or recording error were identified and removed from the data set by calculating the density for each sample and applying a 95% prediction interval to a simple linear regression of elevation on snow density. Observations that occurred outside the prediction interval were assumed to have error in either measurement or recording and were removed from the data set, representing 26 data points. The data set used for analysis consisted of 1017 measurements of SWE, snow depth, snow density, and the associated physiographic attributes of each point.

3.4 Data Analysis

Three types of models were used to quantify the effect of physiographic parameters on the spatial distribution of SWE. These were mixed effects multiple

regression [*Zuur et al.*, 2009], binary regression tree [*Breiman et al.*, 1984], and conditional inference tree analysis [*Hothorn et al.*, 2004]. Two types of analysis were used to quantify the effect of physiography on the spatial distribution of snow density, multiple linear regression (MLR) and binary regression tree. This allowed for a comparison of how the various model structures estimate total basin SWE, its spatial distribution, and that of snow density. All statistical analysis was performed using the *R* statistical software package.

3.4.1 Mixed Effects Multiple Regression

Field data in earth and environmental sciences often does not fully comply with all of the assumptions of multiple linear regression (in this case, constant variance of the residuals [*Ramsey and Shafer*, 2002]). MEMR models provide an additional way to analyze these datasets that do not require a data transformation, where information about important interactions of the explanatory variables may be blurred or lost [*Zuur et al*., 2009]. For this study, a fixed variance model structure was chosen because it accounts for non-constant (increasing) variance in the residuals of SWE depth as elevation increases which is a violation of an important assumption of multiple linear regression [*Zuur et al.*, 2009; *Ramsey and Shafer*, 2002]. Within this framework, various model structures were systematically constructed and evaluated based on their respective Akaike Information Criterion (AIC), Bayesian Information Criterion (BIC), Residual Standard Error (RSE), F-statistics, p-values, and qualitative scientific judgment. This process involved looking at all criteria, both direct statistical output and how that related to scientific knowledge of

the primary drivers of the spatial distribution of SWE, to determine the ideal model structure given the selected parameters.

Each explanatory variable (physiographic parameter) was first individually regressed against SWE depth to determine which had the strongest correlations. Elevation was shown to have the highest univariate correlation to SWE depth, therefore all mixed effects models included elevation. Subsequent model structures were then progressively developed until the best mixed effects models for this data were determined.

3.4.2 Binary Regression Tree Analysis

Binary regression trees have been widely used in studies concerning the spatial distribution of SWE in montane basins [*Balk and Elder,* 2000; *Elder et al.,*1998; *Erxleben et al.*; 2002; *Winstral et al.*, 2002; *Molotch et al.*, 2005]. The binary regression tree analysis that was utilized in this study is based on the algorithms described by *Breiman et al.* [1984]. Using this method (the *rpart* function in *R* for this study), a large regression tree is first built through the use of binary splits in the data based on multiple explanatory variables (physiographic parameters) that will minimize the sum of squared residuals in the estimates of the response variable. The tree is pruned back to an optimal size as determined by the complexity parameter (CP) value for a given number of nodes at which there is no more substantial improvement to the 10-fold cross validated error. According to *Hothorn et al.* [2004] this class of regression tree can have two fundamental problems, overfitting and a selection bias towards covariates with many possible splits. Pruning can be utilized to alleviate the overfitting problem but interpretation of the tree can still be affected by the biased variable selection. For this reason a CI tree model

structure was also analyzed to evaluate its appropriateness for various applications in the study of snow hydrology.

3.4.3 Conditional Inference Tree Analysis

Conditional inference trees were utilized as a comparison to the more common binary regression trees because of the different ways they approach splitting and stopping criteria. The CI tree structure avoids overfitting by utilizing multiple test procedures to determine when no significant association between the covariates and the response variable can be stated and the recursion needs to stop [*Hothorn et al.,* 2004]. The size of a tree is determined by a defined significance level required for a split to occur, minimum number of observations for a split, and minimum number of observations required for a final node (in this study; 95%, 60, and 30 respectively), so cross validation and pruning are not necessary for determining final tree size [*Hothorn et al.*, 2004]. Biased variable selection is avoided by separating the variable selection from the splitting procedure. *Hothorn et al.* [2004] have shown that the CI method is not inferior to, and in some cases better than, the algorithms described by *Breiman et al.* [1984].

3.4.4 Model Implementation

The MEMR model was spatially distributed using map algebra by multiplying the estimated β coefficients by the raster datasets of physiographic parameters and adding these values together, along with an intercept value (β_0). The regression tree and conditional inference tree model structures were spatially distributed through the use of nested conditional statements applied to the raster data of their explanatory variables that

precisely describe the structure of the respective trees. Estimated total basin SWE was then calculated for each model by multiplying the modeled SWE depth (in meters) of each pixel in the basin by the area of the 30m pixel ($900m^2$) to provide the estimated total basin SWE as cubic meters of water. Comparisons were also between modeled values at the Lone Mountain SNOTEL site and values measured by the site, as well as sampled and modeled values throughout the strata (3310) that the SNOTEL site lies within.

3.4.5 Modeling the Spatial Distribution of Snow Density

Many prior studies concerning the spatial distribution of SWE on mountain basins have relied on modeling snow density throughout the basin of interest based on relatively few density measurements [e.g. *Elder et al.*, 1998] in order to estimate SWE based on modeled snow depth, or used a single density throughout the entire basin (generally as an average of measurements) [e.g. *Molotch et al.*, 2005; *Erxleben et al.*, 2002]. This study took direct measurements of SWE and snow depth at all sampling locations, providing an opportunity to more accurately analyze the effect of physiography on snow density near the time of maximum snow accumulation. This was done through both MLR and regression tree analysis.

4.0 RESULTS

4.1 Results of Representative Sampling

Comparisons of the percent of sampled points to the percent of the whole basin within the various classifications of physiographic parameters and strata used to define the sampling areas was performed as a means of assessing the effectiveness of the sampling plan and the physiographic representativeness of the data. Figure 12 shows these comparisons for the elevation bands used to define the physiographic strata. Low elevation areas were over-sampled likely due to ease of access and travel in these areas and some higher elevation areas (2768-3081m) were relatively under-sampled because many of these areas were steep and could not be sampled due to high avalanche hazard.

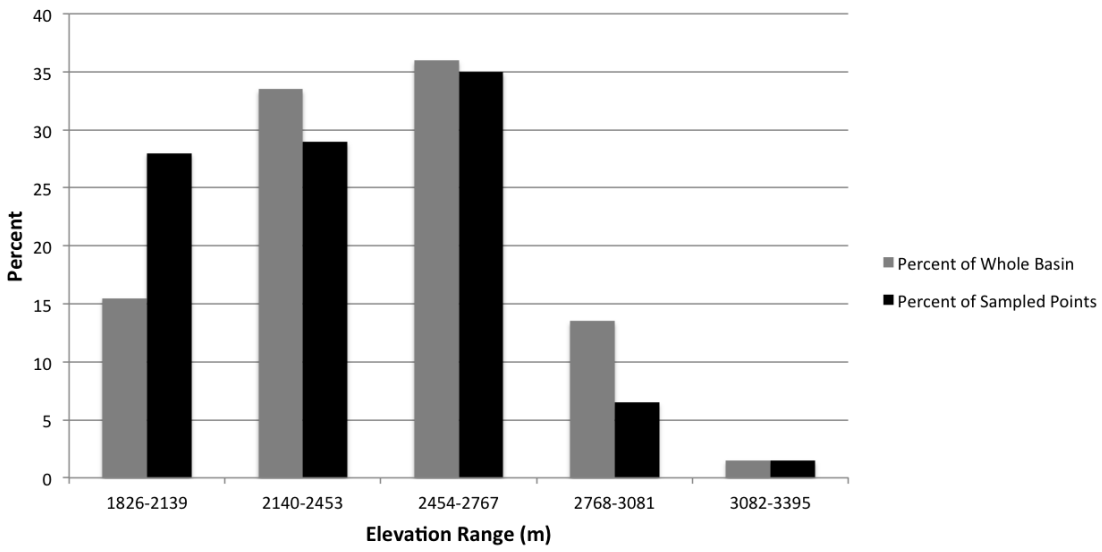


Figure 12. Comparison of percentage of basin area to percentage of sampled points by elevation band.

A similar comparison for the various radiation levels used to define the sampling areas is shown in Figure 13, with the largest relative discrepancies occurring in the middle radiation bands. The comparison of forested and un-forested portions of the basin is shown in Figure 14, with forested areas being under-sampled relative to un-forested areas. Comparisons to the physiographic strata used to define the sampling areas are shown in Figure 15 and Table 3.

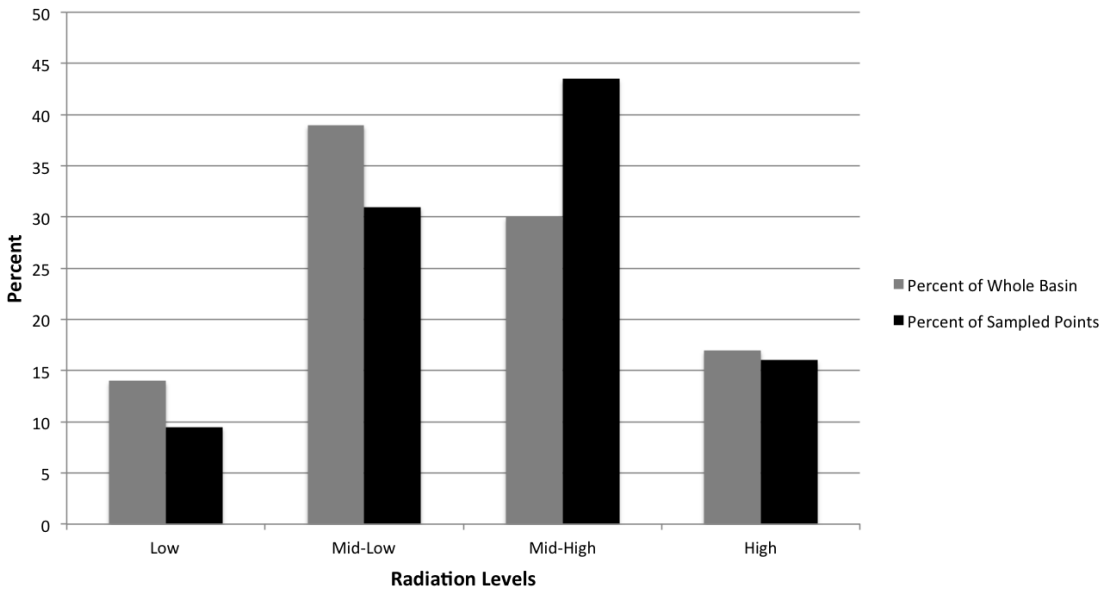


Figure 13. Comparison of percentage of basin to percentage of sampled points by relative incoming solar radiation levels.

In total five strata (1110, 4410, 5100, 5200, and 5300, see Table 1 for strata descriptions) remained un-sampled, which comprised approximately 3% of total basin area. Four of these strata were at high elevation and were likely not sampled due to a combination of the small area which they comprise and lack of access due to avalanche hazard. Strata 3200 (see Table 1 for strata description) was heavily sampled due to

assistance from the Montana State University Snow Dynamics and Accumulation class for an afternoon leading to a higher density of samples in that strata compared to the sampling density throughout the rest of the basin. While differences can be seen in Figure 15 and Table 3, the basin was considered to have been sampled in an overall physiographically proportional manner. Although the entirety of the defined sampling areas comprised slightly more, approximately 20% of the basin area was sampled. Through this 86% of strata were sampled which in total comprised 97% of total basin area.

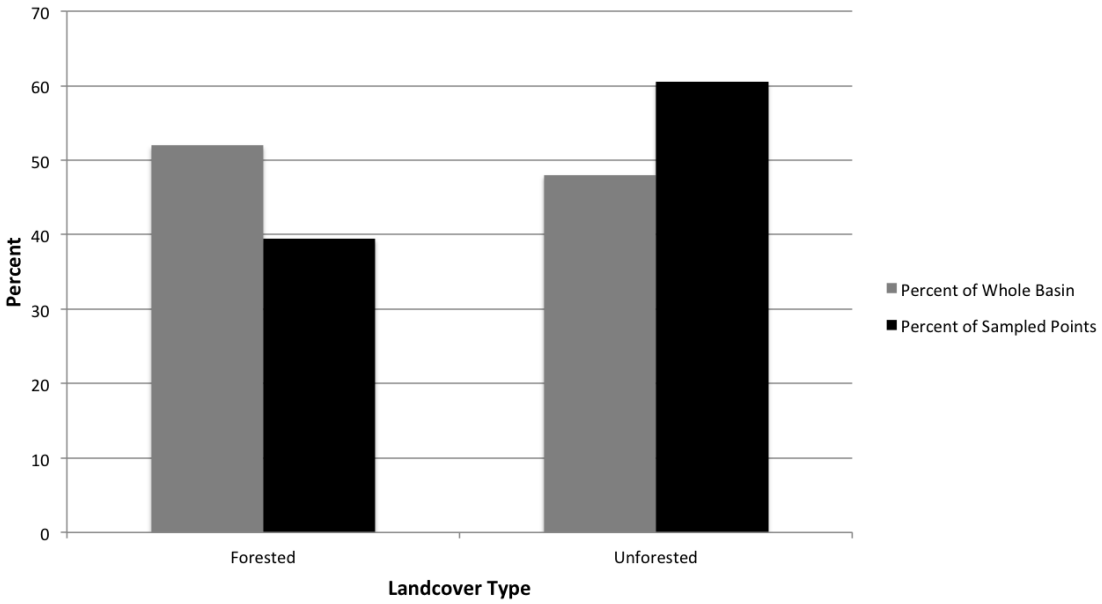


Figure 14. Comparison of percentage of whole basin to percentage of sampled points by land cover.

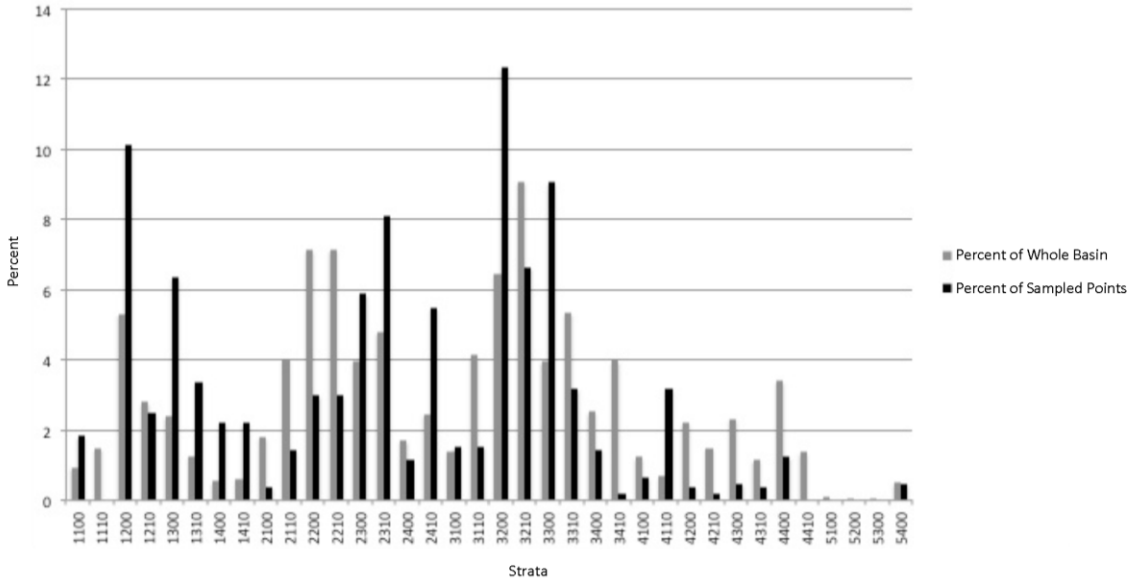


Figure 15. Comparisons of percent of basin area to percent of sampled points by physiographic strata.

Table 3. Summary of results of sampling plan by strata.

Strata	Percent of Whole Basin	Percent of Sampled Points	Absolute % Difference	Ratio of Basin Area to Sampled Points
1100	0.95	1.83	-0.88	0.52
1110	1.49	0	1.49	N/A
1200	5.32	10.12	-4.79	0.53
1210	2.8	2.5	0.29	1.12
1300	2.4	6.36	-3.96	0.38
1310	1.27	3.37	-2.11	0.38
1400	0.54	2.22	-1.68	0.24
1410	0.61	2.22	-1.6	0.27
2100	1.8	0.39	1.41	4.62
2110	4.03	1.45	2.59	2.78
2200	7.14	2.99	4.15	2.39
2210	7.15	2.99	4.17	2.39
2300	3.98	5.88	-1.89	0.68
2310	4.79	8.09	-3.31	0.59
2400	1.71	1.16	0.55	1.47
2410	2.46	5.49	-3.03	0.45
3100	1.41	1.54	-0.13	0.92
3110	4.14	1.54	2.6	2.69
3200	6.45	12.33	-5.88	0.52

Table 3 Continued

3210	9.09	6.65	2.44	1.37
3300	3.98	9.06	-5.07	0.44
3310	5.35	3.18	2.17	1.68
3400	2.53	1.45	1.09	1.74
3410	3.99	0.19	3.8	21.00
4100	1.23	0.67	0.55	1.84
4110	0.68	3.18	-2.5	0.21
4200	2.23	0.39	1.85	5.72
4210	1.49	0.19	1.29	7.84
4300	2.33	0.48	1.85	4.85
4310	1.16	0.39	0.78	2.97
4400	3.4	1.25	2.15	2.72
4410	1.38	0	0.9	N/A
5100	0.09	0	0.09	N/A
5200	0.05	0	0.05	N/A
5300	0.06	0	0.06	N/A
5400	0.51	0.48	0.03	1.06

4.2 Field Observations

A wide range of SWE and snow density values were observed during data collection. Generally, the lowest SWE depths and highest density values were found in the low elevation meadows of the basin and particularly on southerly aspects. Many low elevation areas of the basin were entirely snow free at the time of sampling, most commonly on steep south facing aspects but also in other isolated areas throughout the lower elevation portions of the basin. High elevation areas held the most SWE, while the influence of radiation was still evident it appeared to have less influence at high elevation than in lower portions of the basin. The lowest densities were observed in the higher elevations on northerly aspects. Summary statistics of the field data are shown in Table 4.

Table 4. Summary of observed SWE and snow density data.

Data Type	Minimum	Mean	Maximum	Standard Deviation	*n*
SWE (mm)	0	246	965	206	1017
Density (kg/m^3)	190	349	500	61	1017

4.3 Results of Modeling the Spatial Distribution of SWE

4.3.1 Mixed Effects Multiple Regression Analysis

Numerous MEMR models were developed and tested to determine which model structure provided to best representation of the data. Models were developed and compared in order of increasing complexity so the influence of each independent variable (and combination thereof) could be assessed for how it influenced overall model performance. First, SWE was regressed against individual independent variables (physiographic parameters). The results showed elevation to have the strongest single parameter correlation with SWE while radiation, land cover, and slope angle all were shown to have significant correlations at the $P < .05$ level as well. The results of these analyses are shown in Table 5 where lower AIC and BIC values indicate the best combination of model performance and model complexity [*Zuur et al*., 2009] and the RSE is a metric of model fit, with smaller indicating a better fit.

Table 5. Summary of the results of mixed effects multiple regression analysis for models utilizing one explanatory variable.

Model Structure	AIC	BIC	RSE
SWE~elevation	12593.2	12608.0	2.44
SWE~radiation	13658.0	13672.7	4.10
SWE~slope angle	13676.7	13691.5	4.17
SWE~land cover	13678.4	13693.2	4.18
SWE~ degree of curvature	13697.0	13711.8	4.21
SWE~aspect	13701.1	13715.8	4.21

Based on the results of the above analysis additional independent variables were subsequently added into the model structures. Elevation was clearly shown to have the strongest correlation with SWE so it was included in all subsequent MEMR models tested. Utilizing information obtained from more basic model structures, models with three independent variables as well as models utilizing interaction terms between the independent variables were developed and analyzed. Percent canopy cover data was also analyzed in place of land cover, but no significant improvement to model performance was gained. Models utilizing interaction terms did not significantly improve model performance and therefore are not discussed. The two model structures that were statistically strongest were (with land cover coded as 10=forested and 0=unforested):

$$SWE \sim \beta_0 + \beta_1 * elevation(m) + \beta_2 * radiation(WH/m^2) + \beta_3 * landcover + \varepsilon_i$$

$$SWE \sim \beta_0 + \beta_1 * elevation(m) + \beta_2 * slope\ angle(°) + \beta_3 * landcover + \varepsilon_{i.}$$

The model structure incorporating slope angle was statistically stronger based on AIC and BIC values (Table 6) and displayed a smaller but relatively similar RSE value to the model utilizing radiation. However, the model incorporating relative incoming solar radiation was chosen to use in the final analysis because they were both shown to be appropriate models for the data, but by utilizing incoming solar radiation the patterns observed in the field were better matched, as well as generally being more compliant with the authors perceptual model of the dominant influences on SWE depth in the terrain that comprises the majority of the West Fork Basin. Radiation also had substantially stronger correlation to SWE than did slope angle when tested individually, as seen in Table 5, indicating its strength as a better predictor of SWE. While slope angle alone can effect

the spatial distribution of SWE in steep terrain through agents such as sloughing and avalanching [*Kerr et al.,* 2013] its strength in the statistical models was decided against in favor of a stronger and more practical perceptual model of radiation having a larger influence on the spatial distribution of SWE basin wide. The statistical strength of the model including slope angle is possibly related to the correlation between slope angle and incoming solar radiation, which is also why they were not included in any model structures together. The relation between radiation and slope angle is shown in Figure 16, note that the highest and lowest radiation levels exist at the steepest slope angles and the moderate radiation levels occurring on low slope angles. Given that no samples were taken in areas steep enough for sloughing to be a dominant factor in snow re-distribution (~ >55°) this correlation provides additional support for radiation being the more practical choice for the model.

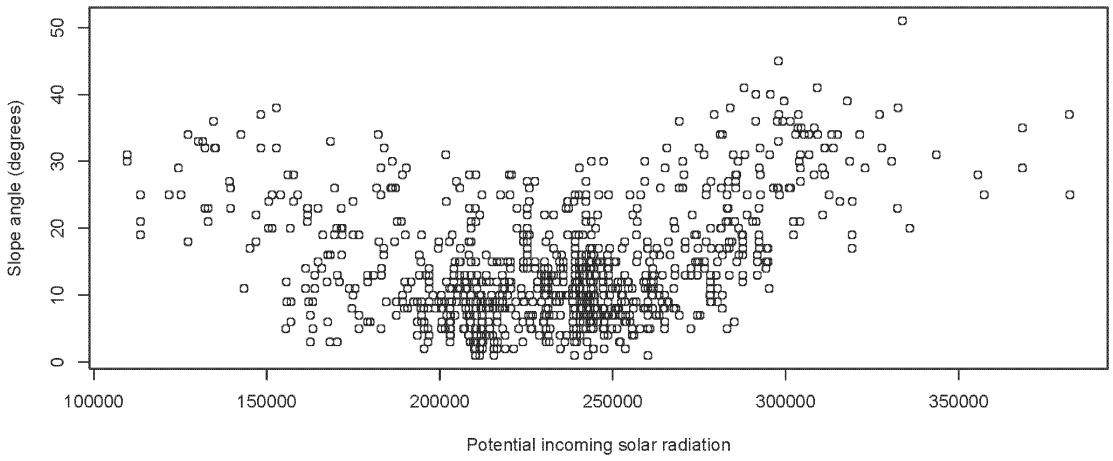


Figure 16. Relation between slope angles and potential incoming solar radiation (WH/m^2).

Table 6. Summary of results of mixed effects multiple regression analysis for models utilizing three explanatory variables.

Model Structure	AIC	BIC	RSE
SWE~elevation+radiation+land cover	12523.7	12548.3	2.33
SWE~elevation+slope angle+land cover	12451.9	12476.5	2.27

When spatially distributed through the use of raster algebra the mixed effects model structure provides unique values of SWE for each pixel in the basin (Figure 17), giving the most spatially explicit estimations of SWE distribution of any of the models. In this model elevation and radiation values were multiplied directly by their β coefficients and land cover was coded as 10 for forested, and 0 for unforested, essentially subtracting 54.4 mm of SWE in all areas of the basin that are forested.

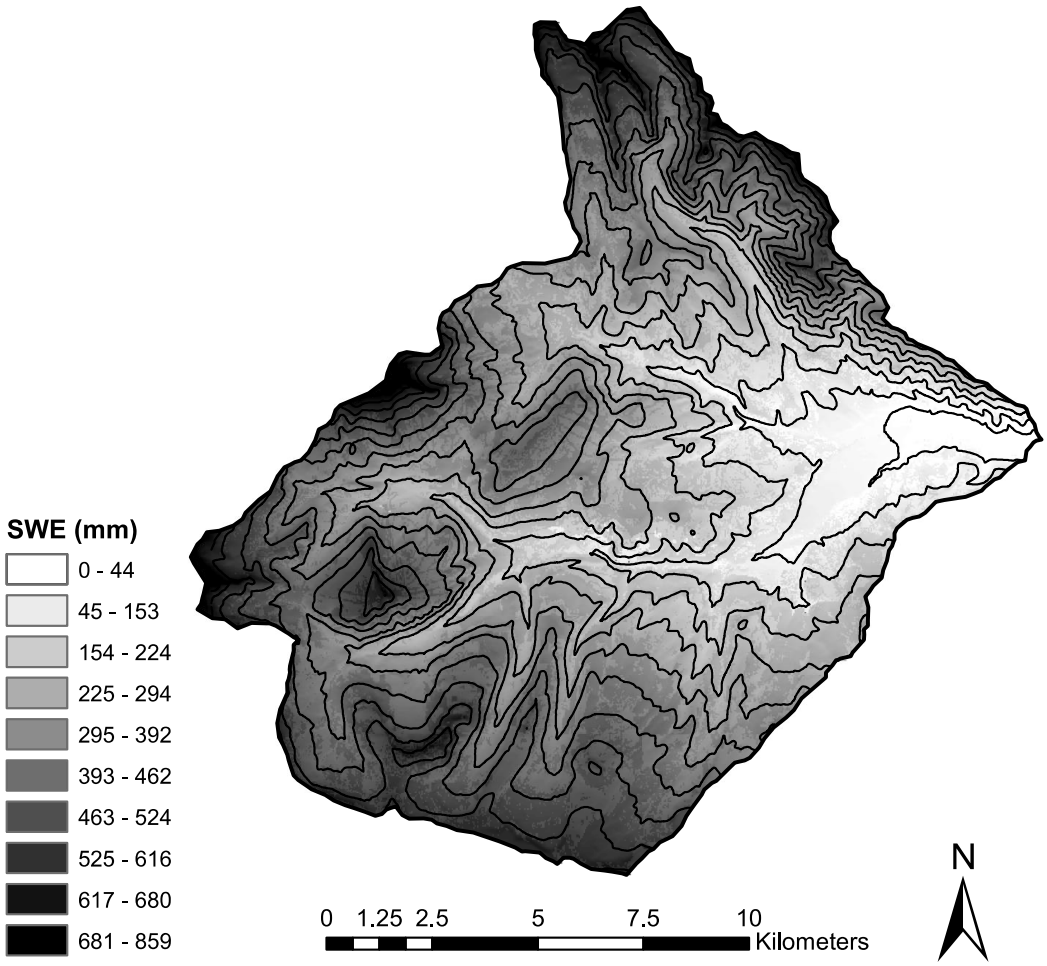


Figure 17. Modeled spatial distribution of SWE (mm) using the MEMR model: *SWE ~ -959.65 + 0.5683*elevation(m) + -0.0005*radiation(WH/m^2) + -5.44*land cover(0 or 10)*. 100m contour interval.

4.3.2 Results of Regression Tree Analysis

The 10 fold cross validated regression tree model for this data contained seven terminal nodes and utilized elevation and incoming solar radiation as the only significant parameters for adequately describing the data. This tree structure is shown in Figure 18 and includes the percentages of total basin area and total basin SWE represented by each terminal node.

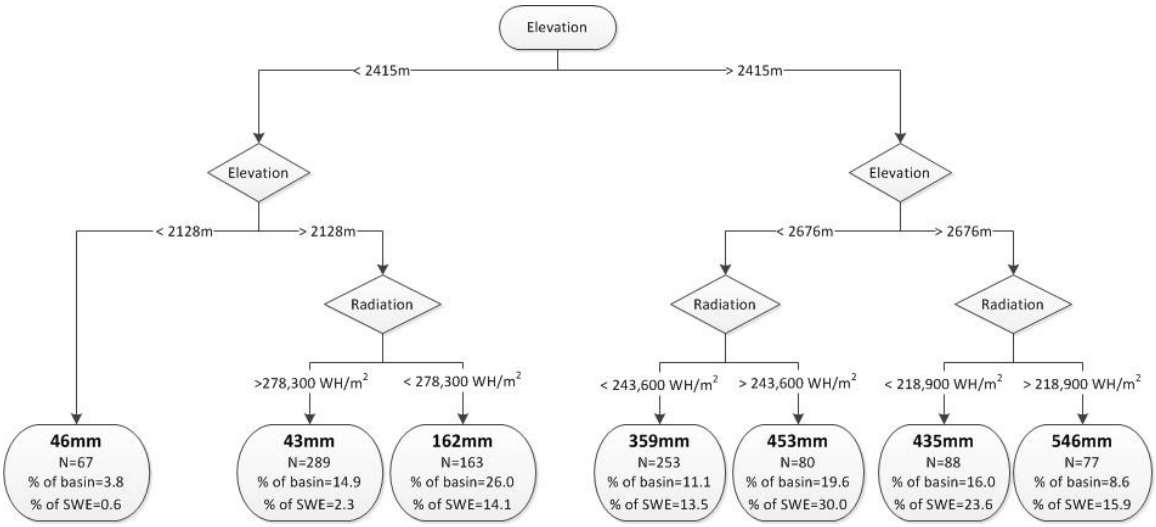


Figure 18. Binary regression tree model with seven terminal nodes utilizing elevation and potential incoming solar radiation.

This regression tree provided a 10-fold cross validated R^2 value of 0.71 (derived from a 10-fold cross validated error representing the percent variance in observations explained by the model). This is a relatively strong result in comparison to previous similar work (e.g. averages of $R^2 = 0.59$ for *Balk and Elder*, 2000; 0.25 for *Erxleben et al.*, 2002; and 0.37 for *Molotch et al.*, 2005), being mindful that comparisons of R^2 values between studies are not necessarily directly comparable due to varying sampling techniques and basin characteristics. The regression tree represented a substantial dichotomy in modeled SWE depths based on elevation, with all modeled SWE below 2415m being between 43.64mm and 161.8mm and all SWE above 2415m being between 359mm and 545.5mm of SWE. The modeled spatial distribution of SWE for this tree is shown in Figure 19.

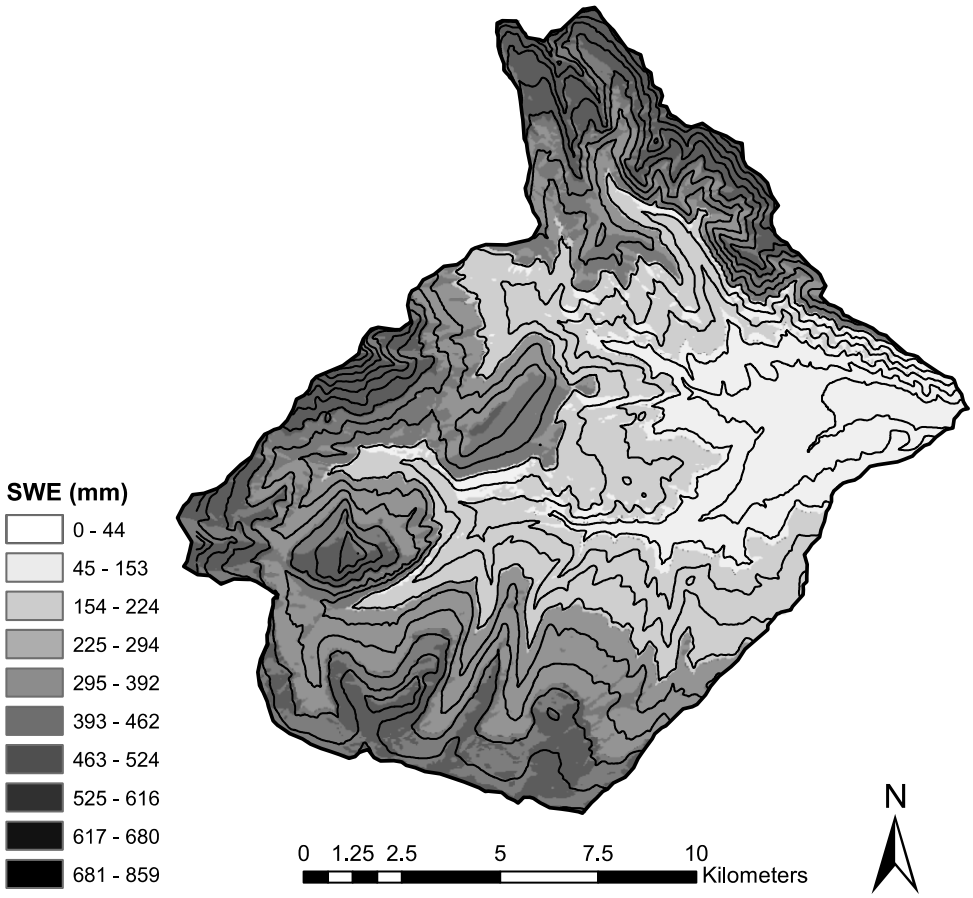


Figure 19. Modeled spatial distribution of SWE (mm) through the use of a binary regression tree with seven terminal nodes, 100m contour interval.

The area of the basin that was represented by each terminal node was also non-uniform (Table 5). The lowest and highest modeled values of SWE (43mm and 545mm, respectively) represented the smallest portions of the basin. The terminal node representing 161mm represented the largest portion of the basin covered, modeling nearly 26% of the basin as having 161mm of SWE, which represented 14% of total basin SWE. The important initial split on elevation at 2415m had a substantial impact on how SWE

was spatially distributed by elevation as well, with 83% of total basin SWE modeled as being above this elevation.

4.3.3 Conditional Inference Tree Analysis

A conditional inference tree with 16 terminal nodes was developed using the following for splitting and stopping criteria. For a split to be made model performance must have been improved at the 95% significance level. In addition, a minimum of n=60 observations were required for a split and therefore a minimum of n=30 observations were required for a terminal node to be defined. The minimum n values were chosen to maximize both the number of terminal nodes for the 95% significance level as well as the statistical viability of the tree by maintaining a sample of at least n=30 observations in each terminal node. As with the regression tree, certain terminal nodes represented substantially larger portions of the basin and total basin SWE than others, but with an even more pronounced effect. The spatial distribution of SWE as modeled by this conditional inference tree is shown in Figure 20 and the conditional inference tree structure in Figure 21.

The effect of certain terminal nodes having a larger impact than others is pronounced in this model with approximately 60% of the basin area and being represented by only four terminal nodes (185, 325, 453, and 486mm SWE), particularly given the larger number of terminal nodes for this model compared to the regression tree. The node representing the highest modeled value, 486mm, represents 24.55% of the basin area and 40.12% of the total basin SWE. The area above 2412m in elevation (represented by five terminal nodes) contains 81% of modeled total basin SWE and 56%

of total basin area, again showing the dominance of elevation on the spatial distribution of SWE.

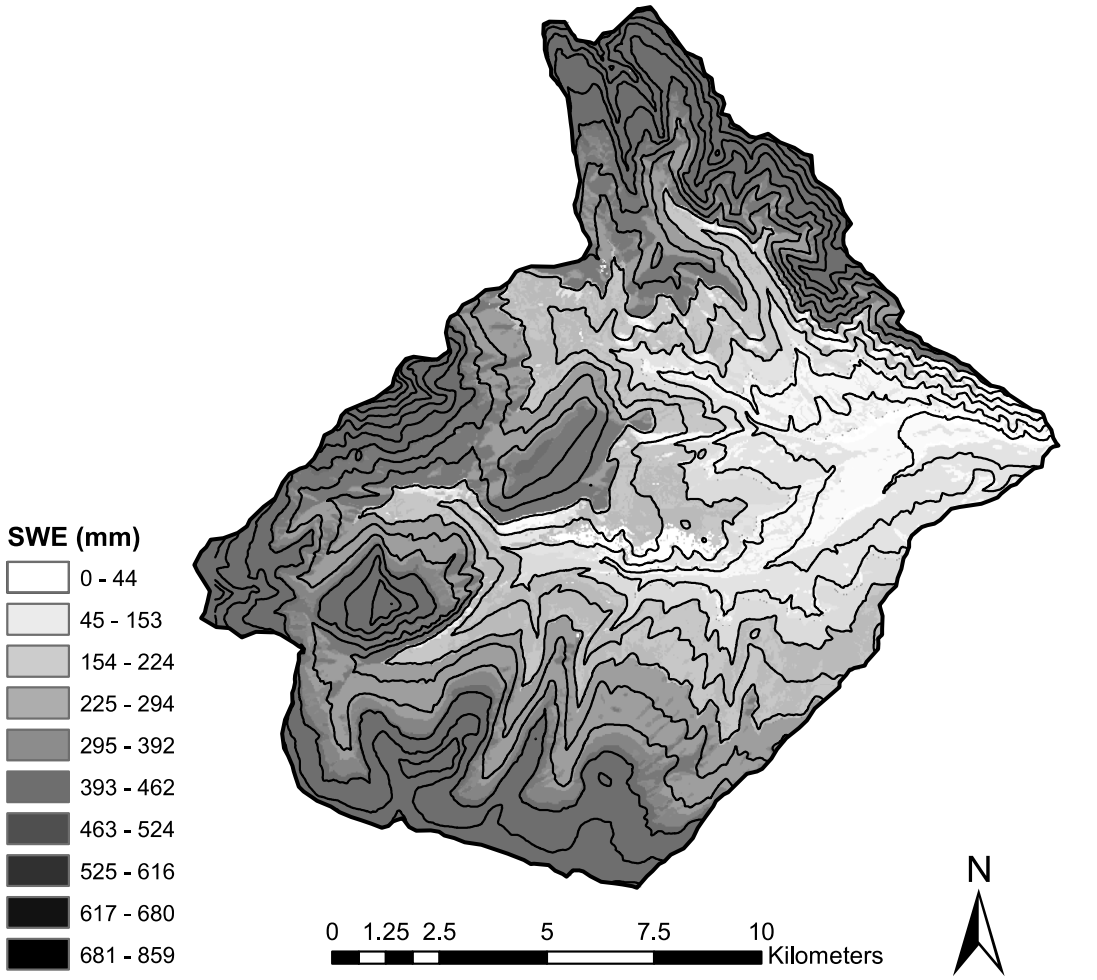


Figure 20. The spatial distribution of SWE as modeled by the conditional inference tree. 100m contour interval.

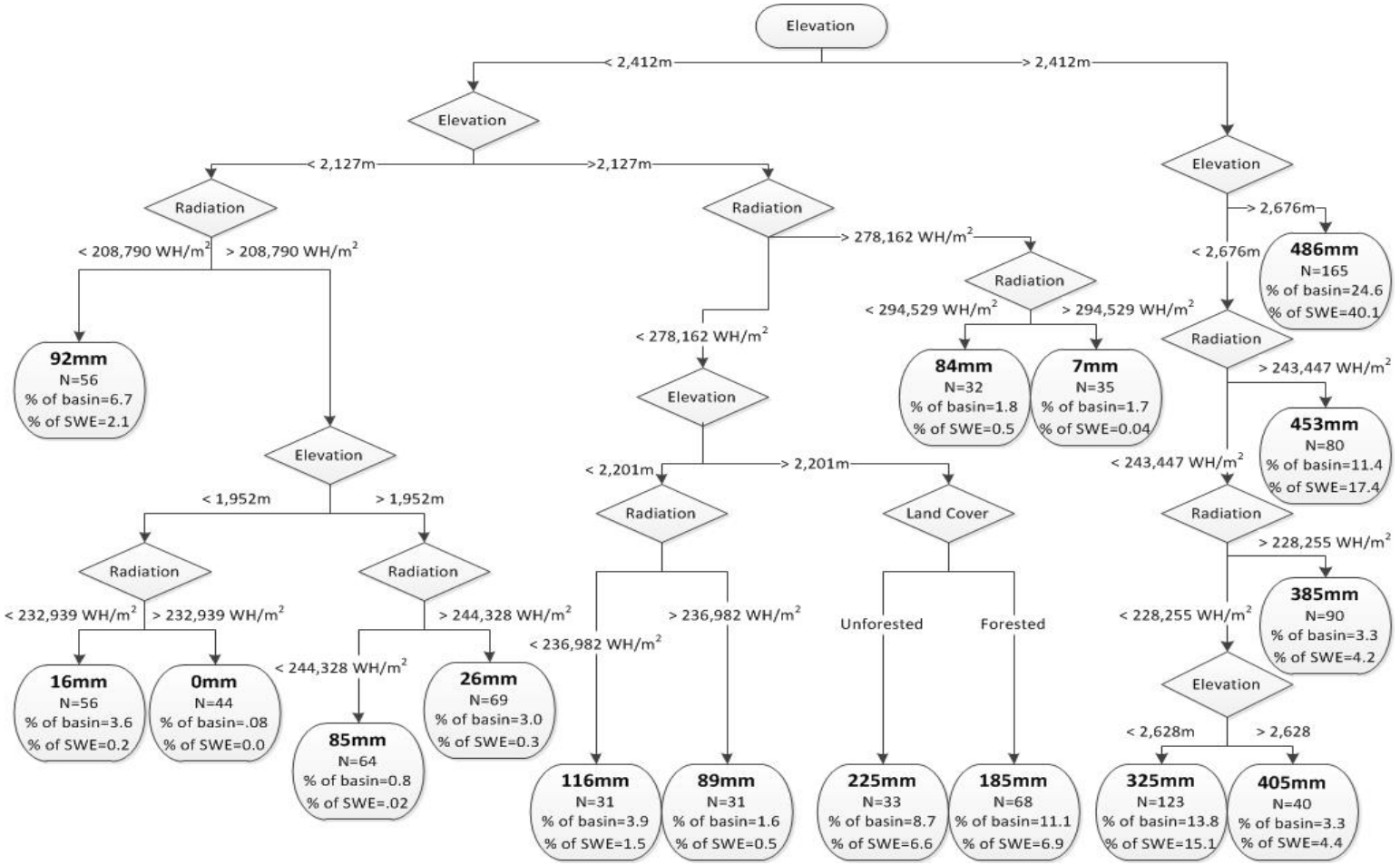


Figure 21. 16 node conditional inference tree describing modeled SWE depths based on physiography.

4.3.4 Model Comparisons

The three model structures utilized to estimate the spatial distribution of SWE modeled substantially different spatial distributions and ranges of SWE values but all estimated similar values of total basin SWE, to within approximately 1% of their average (Table 7). MEMR analysis yielded the widest range of modeled values (859mm) and that most similar to the range of measured values (965mm). The binary regression tree and conditional inference tree models provided similar ranges of values, 501mm and 486mm, respectively.

Table 7. Summary of modeled SWE values from all model structures

Model	Modeled total basin SWE (m^3)	Range of modeled SWE values (mm)	Number of unique modeled SWE values
MEMR	59,792,000	0 - 859	unique for each pixel
CI tree	60,935,000	0 - 486	16
Regression tree	61,195,000	43 - 545	7
Average of others	60,641,000	15 - 618	unique for each pixel

In addition to differences in the modeled ranges of SWE values, the manner in which SWE was distributed throughout the basin (Figure 22) also varied amongst the models. The MEMR model provided the smoothest distribution of values throughout the elevation range with the largest contrast being to the regression tree which modeled no SWE values between 162 and 359mm, a range of values which contains the mean and median for all measured and modeled values.

The patterns in which the different models estimated SWE at the points where samples were taken also displayed notable differences. Boxplot comparisons (Figure 23, left side) show the median values of the CI tree (225mm) aligning best with the median

of the measured SWE values (229mm), with the median from the MEMR model residing slightly higher (252mm) and the regression tree substantially higher than the rest at 359mm. This, however, is to be expected considering the substantial gap in modeled values near the measured median.

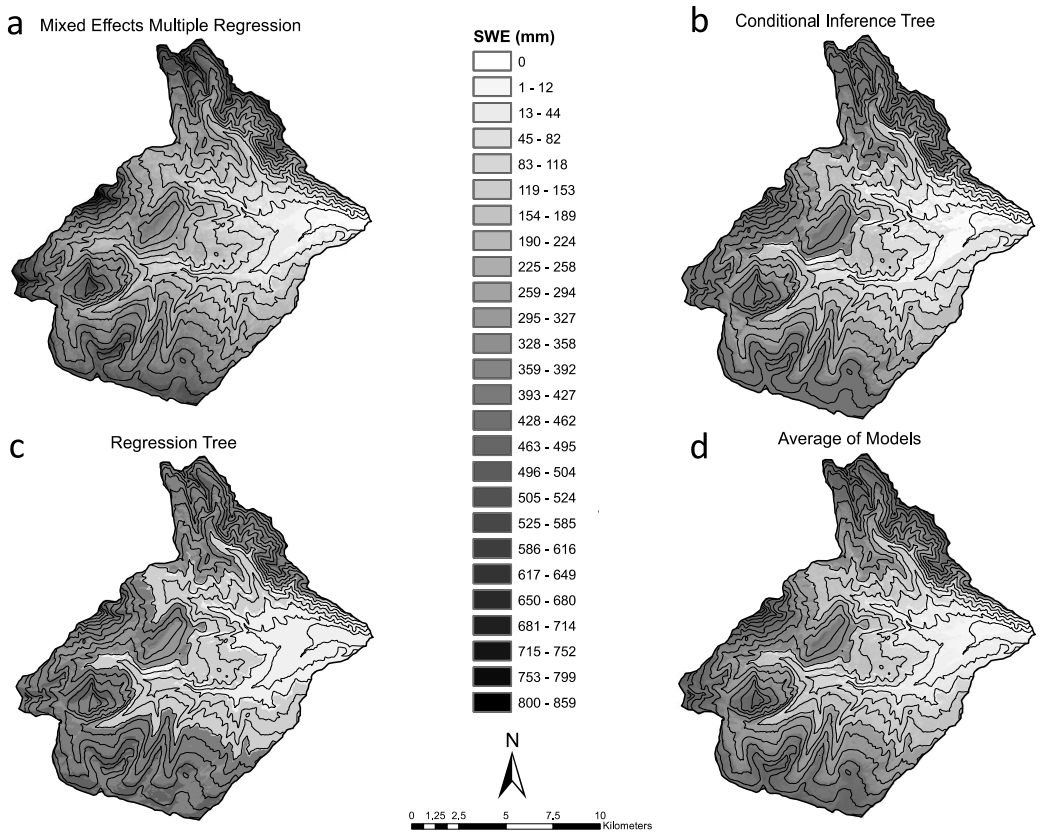


Figure 22. Comparison of three different modeling methods and an average of the three models. 22a shows a good representation of SWE at low elevations, but weights elevation heavily, likely leading to over-estimation at high elevation. 22b underestimates SWE at high elevation, while 22c over-estimates at low elevation. 22d, the average, accounts for the possible misrepresentations of the other models providing the most realistic view of the spatial distribution of SWE in the basin. 100m contour interval.

The inter-quartile and total range of measured SWE values was most closely matched by MEMR, with the other model structures displaying wider inter-quartile and

narrower total ranges. The right side of Figure 23 displays boxplots of the measured SWE values alongside boxplots of SWE values as modeled throughout the entire basin. The medians and inter-quartile ranges of the distributed values were higher than measured for all models, with MEMR providing the closest match for the median and at the tails but a relatively narrow inter-quartile range. Both of the tree based models provided more similar width of interquartile ranges to the measured values, but at higher range of values.

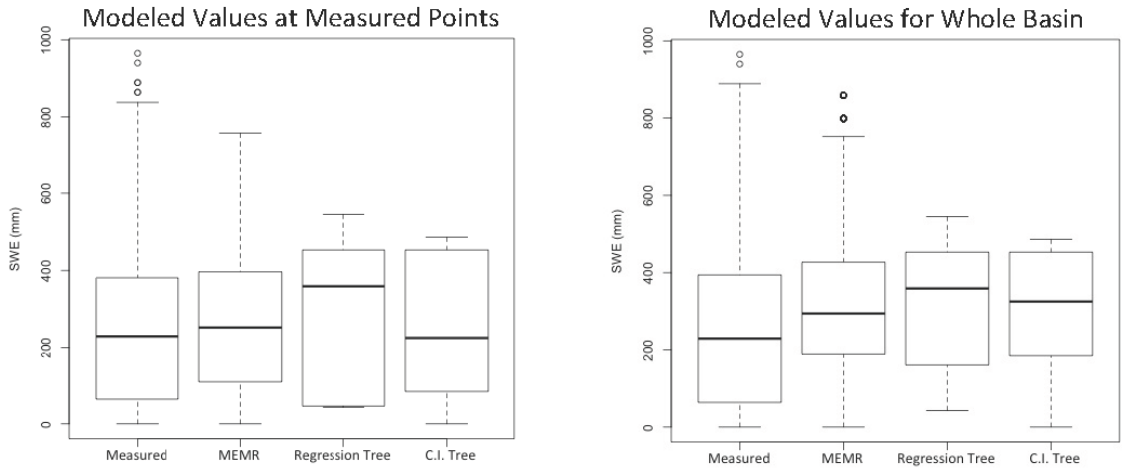


Figure 23. Boxplot comparisons of measured SWE values and modeled values of SWE at the locations of measured points.

Plots of measured and modeled SWE depths (at points where samples were taken) by elevation (Figure 24) provide another means to compare the differences between the various model structures. Most notable is the continuous distribution of the MEMR model across the elevation range compared to the discrete values estimated by the tree based models. While all models do display a similar trend of increasing SWE with elevation, the values estimated using MEMR visually appear to provide the most similar

distribution to the measured values, both in its continuous distribution and the general relationship of SWE to elevation.

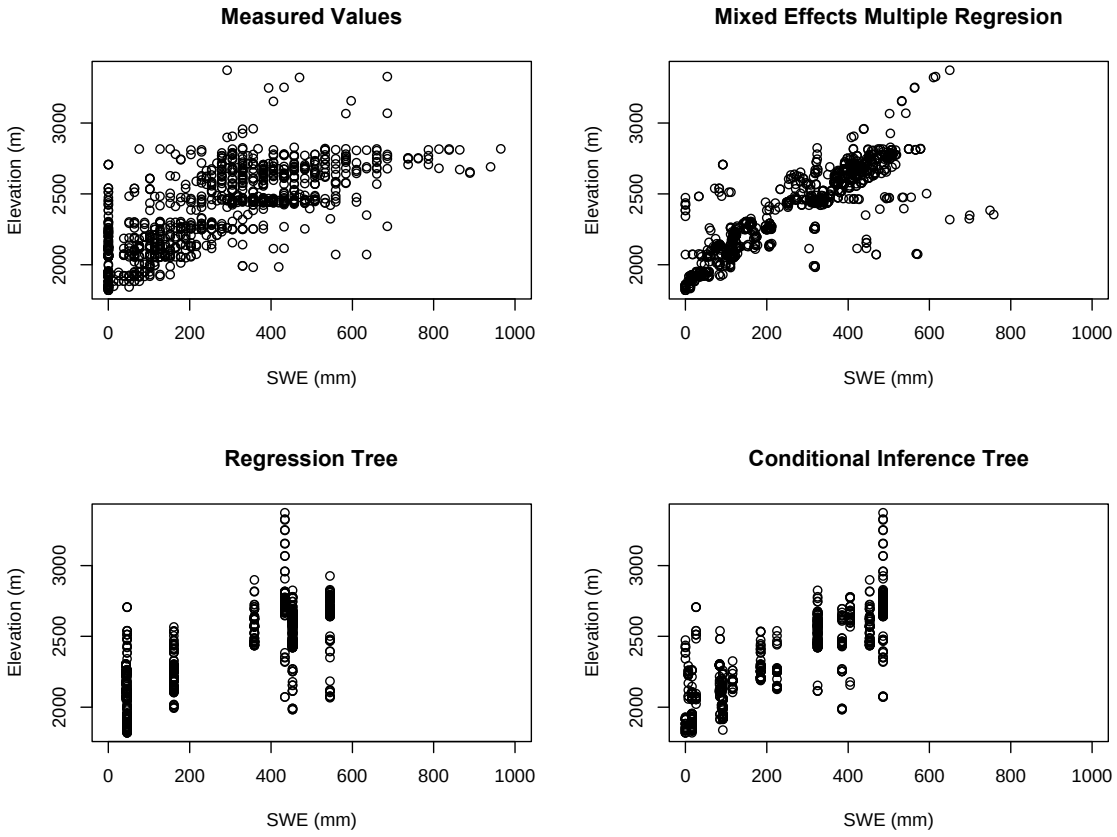


Figure 24. Comparisons of measured SWE values and modeled SWE values at the locations of measured points.

Plots of observed vs. modeled values (Figure 25) and the difference between modeled and observed values at measurement points (Figure 26) provide another means of exploring how the various models estimate SWE at the points where samples were taken.

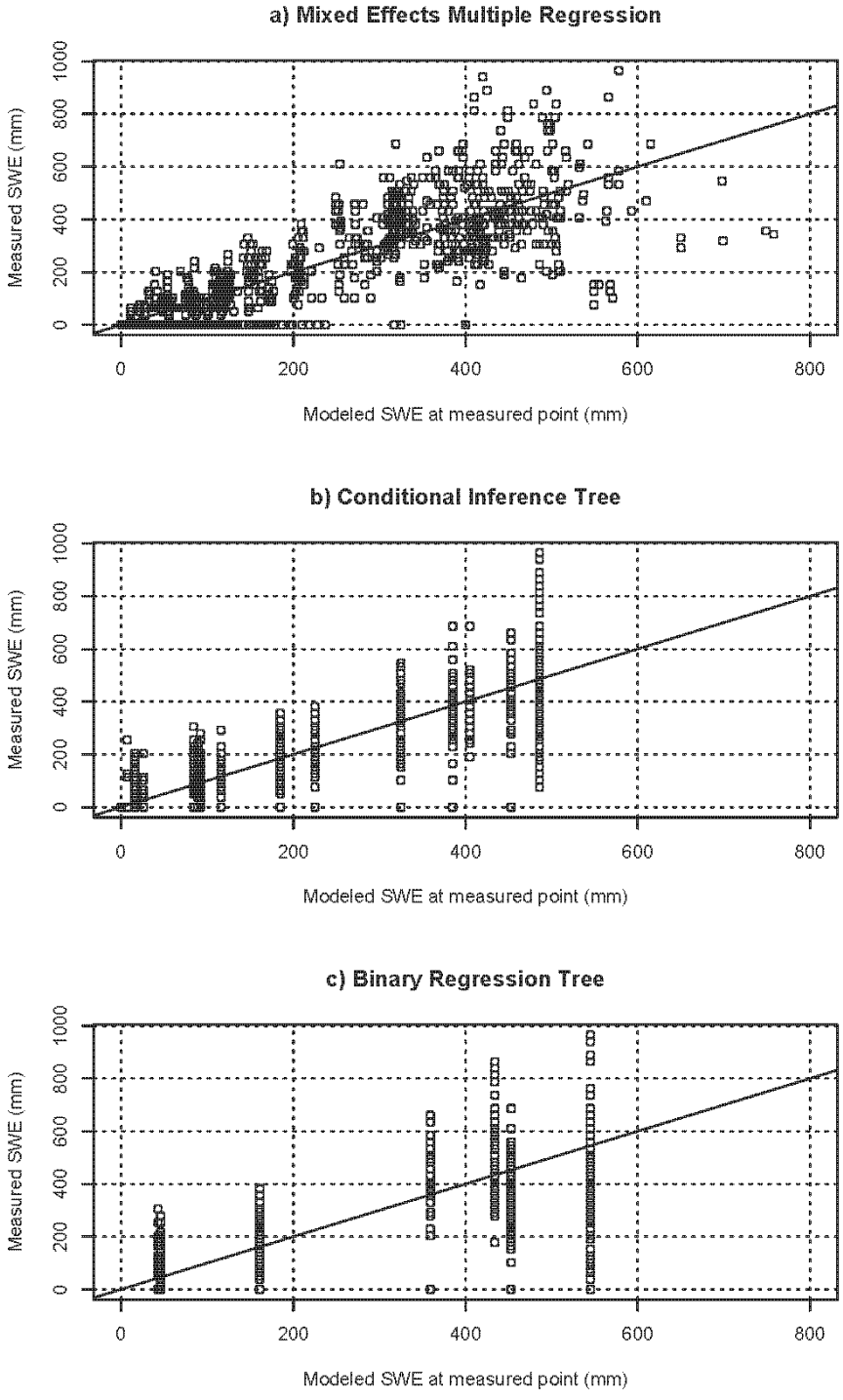


Figure 25. Observed vs. modeled values of SWE at measured points with the 1:1 line displayed.

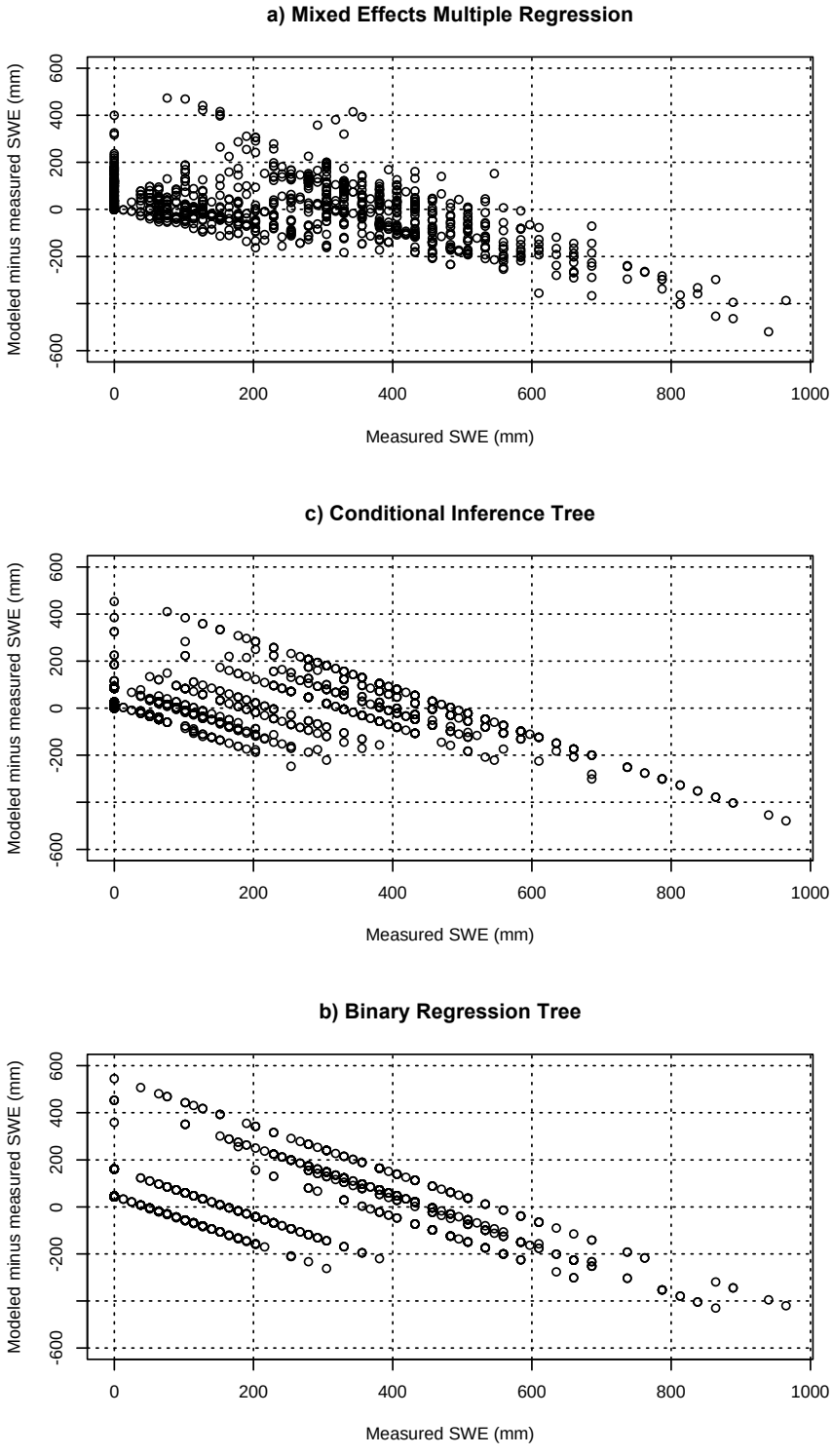


Figure 26. Residuals of modeled values from measured values at measured points

The more smooth distribution of values modeled by MEMR can also be seen in Figure 25, with the more dis-continuous values resulting from the tree based models also being evident. All three models display the general trend of modeled values increasing along with measured values. The MEMR (25a) and CI tree (25b) models do this particularly well while the regression tree (25c) models the widest range of values and does not display the continuous increase with the measured values as the others do. In general, modeled SWE depths are centered around the measured values throughout most of the range and underestimate the higher values and overestimate lower values (Figure 26). The MEMR and CI tree models also generally tend to model the measured values slightly more closely than the regression tree, likely due to the small number of unique values modeled by the regression tree as compared to the others.

A comparison of how the models estimate SWE across the elevation range relative to each other is shown in Figure 27 by plotting the various models' deviation from their average against elevation. Although direct quantification of these residuals is not comparable because it is from their own averages, the general trends of how they differ are easily seen. Notable differences are seen in the higher elevations (above ~3,000m) with MEMR displaying consistently higher than average values and the tree based models displaying consistently lower than average values. In general the tree based models follow a similar trend, which is inverse to MEMR.

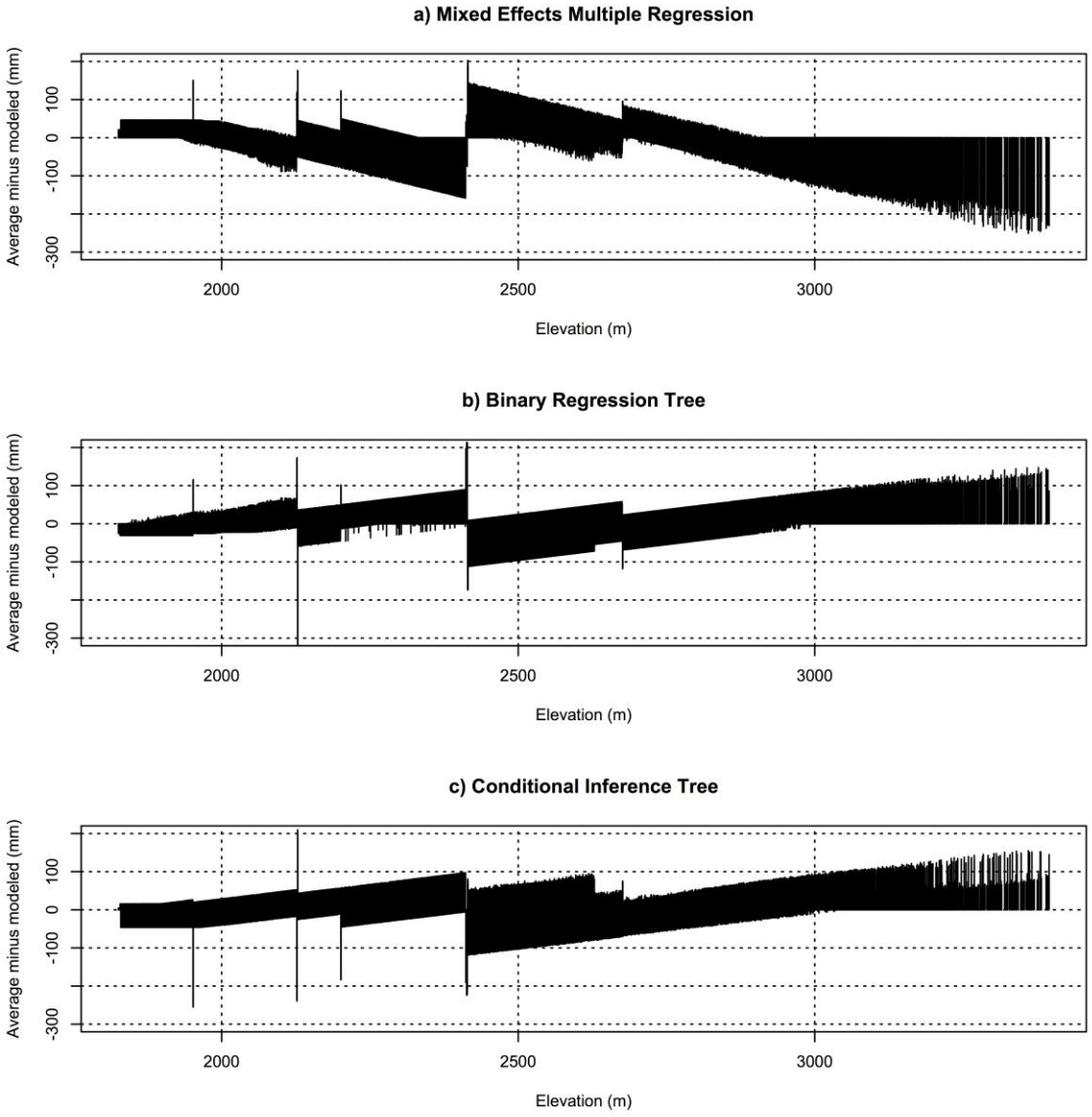


Figure 27. Comparison of modeled SWE values to their average, by elevation.

A similar comparison of how the spatial distributions of the various models compare to their average was also performed by subtracting the raster of the three SWE models from their average (Figure 28).

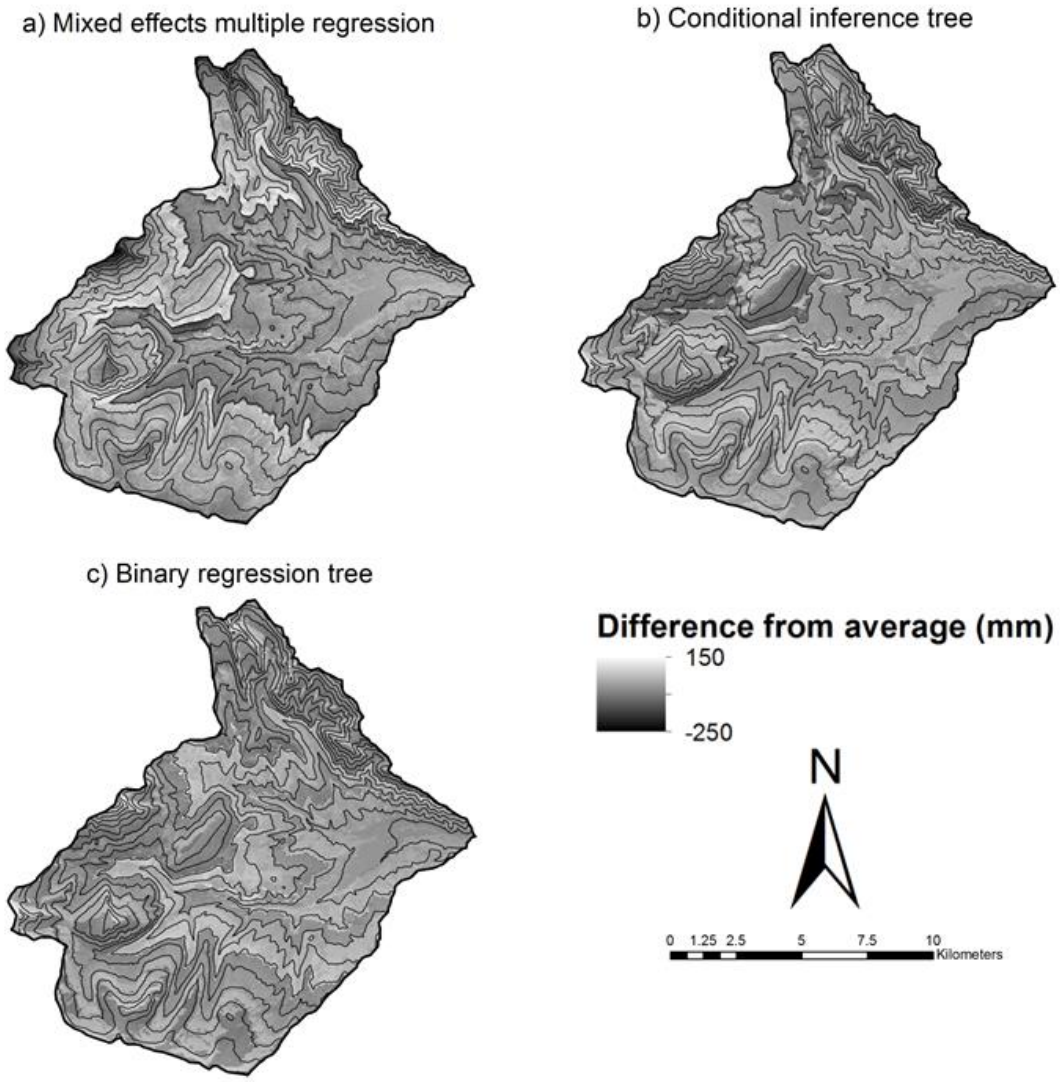


Figure 28. Spatial distribution of the differences between the three models and their average, with the models being subtracted from the average (i.e. positive values indicate less than average and vice versa). 100m contour interval.

The large negative values (darker colors in Figure 28) at high elevation in the MEMR model (Figure 28a) indicate that it modeled substantially higher values than the average in these areas. Alternatively, the binary regression tree (Figure 28c) and CI tree (Figure 28b) modeled SWE as being consistently less than average at high elevation. Of particular note, the MEMR model did not show as much difference from average with

respect to aspect (due to the varying effect of radiation in the different models) as did the two tree models. For the tree based models this effect is most prevalent in the higher elevations, estimating SWE as being higher than average in areas that receive higher levels of radiation (southern aspects) as compared to areas of similar elevation but with more northerly aspects. In general, modeled values in the lower elevation portions of the basin displayed less variation from average than in the higher elevation areas, which is likely related to the modeled values being overall less in these areas.

4.4 Results of Modeling the Spatial Distribution of Snow Density

The spatial distribution of snow density was modeled using two methods, multiple linear regression (MLR) and regression tree analysis. Both methods used elevation and potential incoming solar radiation as explanatory variables for estimating snow density at any given point in the basin in their final models. All physiographic parameters tested for modeling the spatial distribution of SWE were also tested for significance but these provided the greatest statistical significance, and no significant improvement to model performance was gained by adding additional parameters. Similar mean basin snow densities but substantially different ranges and spatial distributions were observed. Measured values of density displayed considerable variability with a mean of 349 kg/m^3 and standard deviation of 61 kg/m^3.

4.4.1 Results of Modeling Snow Density Using Multiple Linear Regression

The data for the analysis of the effect of physiographic parameters on the spatial distribution of snow density met all of the assumptions required for MLR [*Ramsey and Schafer*, 2002] so this method was used as opposed to the mixed effects model which was used for modeling SWE. First, simple linear regression (SLR) was performed using all available parameters to determine which had a significant correlation to snow density. Elevation, radiation, slope angle, and snow depth all had significant correlations to snow density (Table 8). Elevation had the strongest correlation, explaining 27% of observed variance. Snow depth also showed a strong correlation, explaining 18% of observed variance, which is expected due to its relation to elevation. Relative incoming solar radiation on its own explained 13% of observed variance, while that of slope angle was minimal.

Table 8. Summary of the results of SLR of physiographic parameters on snow density.

Model Structure	R^2	p-value
density ~ elevation	0.27	<2.20E-16
density ~ radiation	0.13	<2.20E-16
density ~ snow depth	0.18	<2.20E-16
density ~ slope angle	0.047	3.89E-10

Using the results of the SLR analysis, MLR analysis was performed to determine which combinations of parameters best estimate the spatial distribution of density. The model structure utilizing elevation and radiation provided the best fit for the data, explaining 39% of observed variance (Table 9). Using snow depth and radiation the fit

improved over just using snow depth, but was still only slightly better than the SLR of density as a function of elevation alone.

Table 9. Results of MLR models for snow density.

Model Structure	R^2	p-value
density ~ elevation + radiation	0.39	2.20E-16
density ~ snow depth + radiation	0.28	2.20E-16

A model utilizing elevation and snow depth together was not used due to their high level of autocorrelation. The multiple regression model that best describes the data is as follows:

*Snow density ~ 479.5 + -0.1104*elevation(m) + 0.0004878*radiation(WH/m^2)*

This indicates lower densities at higher elevations, higher densities with more radiation and vice versa. The spatial distribution of snow density based on this model is shown in Figure 29.

This model structure displays a wide range of snow densities from 184 to 406 kg/m^3. The lowest modeled densities are at the highest elevations on north facing slopes, while the highest densities are at low elevation on south facing slopes. Similar to the mixed effects model for SWE this method provided unique values of SWE for each pixel in the basin.

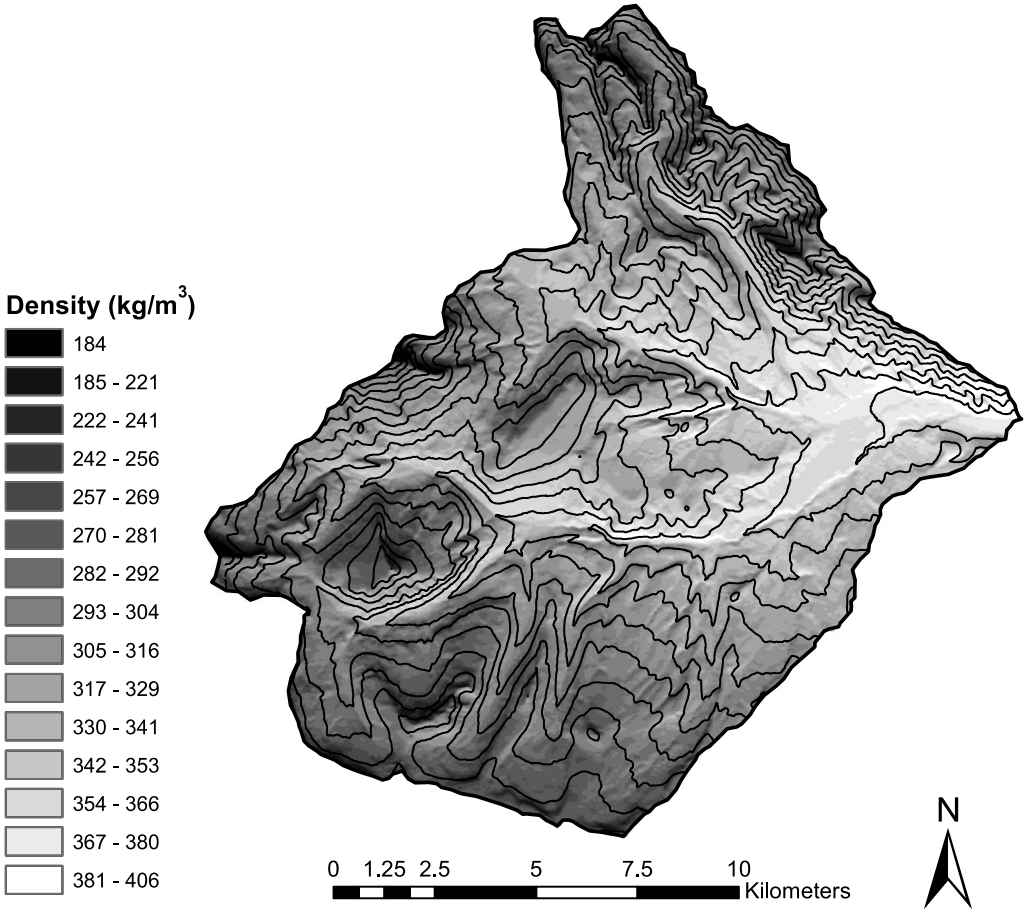


Figure 29. The spatial distribution of snow density using a multiple linear regression model. The range of modeled values is 184-406 kg/m^3. 100m contour interval.

4.4.2 Results of Modeling Snow
Density with Regression Tree Analysis

A nine terminal node regression tree (Figure 30) was used to model the spatial distribution of snow density, utilizing the same tree building and pruning criteria as for the SWE model. The optimal tree for modeling density, just as the MLR model, utilized elevation and radiation to spatially distribute snow density throughout the basin. The optimal tree size for this model was determined by pruning the tree back to the value of

the complexity parameter at which additional nodes no longer reduced the 10-fold cross validated error. This method provided a much smaller range of estimated densities (270–347 kg/m^3) and a different spatial distribution (Figure 31) than the MLR model as well as a slightly improved R^2 value, explaining 41% of observed variance.

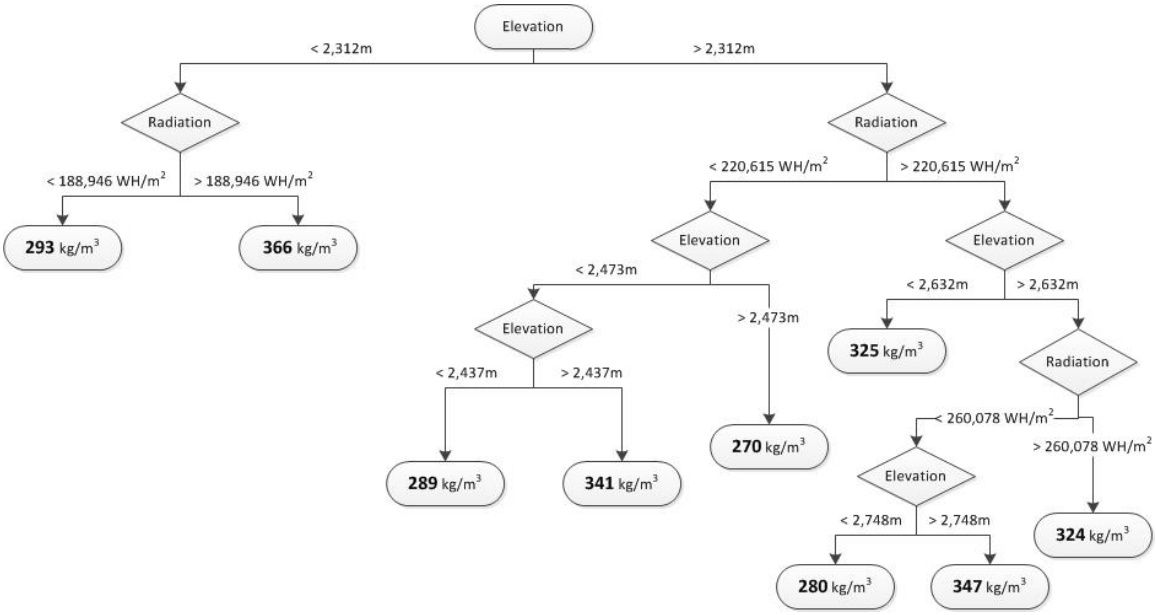


Figure 30. Binary regression tree utilizing nine terminal nodes to estimate the spatial distribution of snow density

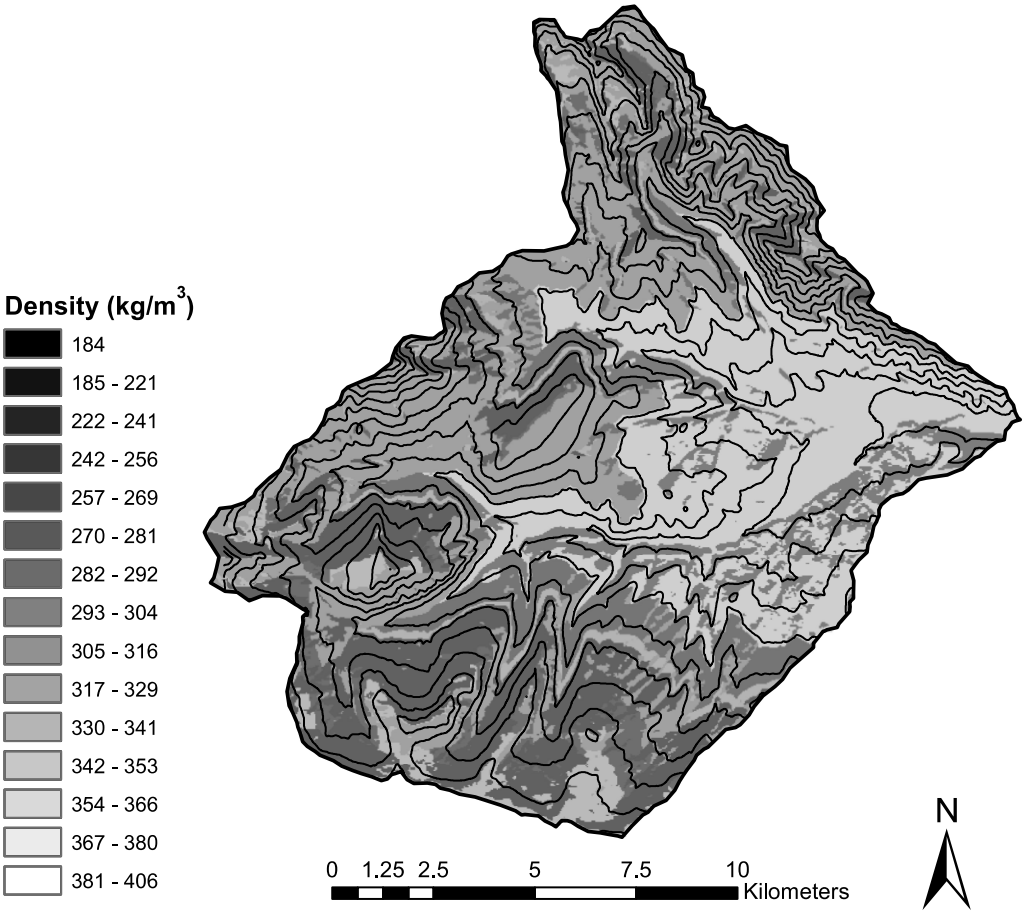


Figure 31. Modeled spatial distribution of snow density using a nine node regression tree. The range of modeled values is 270-366 kg/m^3. 100m contour interval.

4.4.3 Comparison of Modeled and Measured Snow Densities

Several key differences exist between the snow density values as modeled by the two different methods, and the densities measured in the field. The two different modeling methods displayed considerably different ranges and distributions of density values (Figure 32). The tails of the multiple regression model more closely matched the tails of the distribution of measured values, while the regression tree provided a more similar inter-quartile range. The medians of the modeled values were very similar both at

measured points and distributed throughout the basin, being slightly lower than measured values at the measured points, but similar to measured values when compared to the basin-wide distribution.

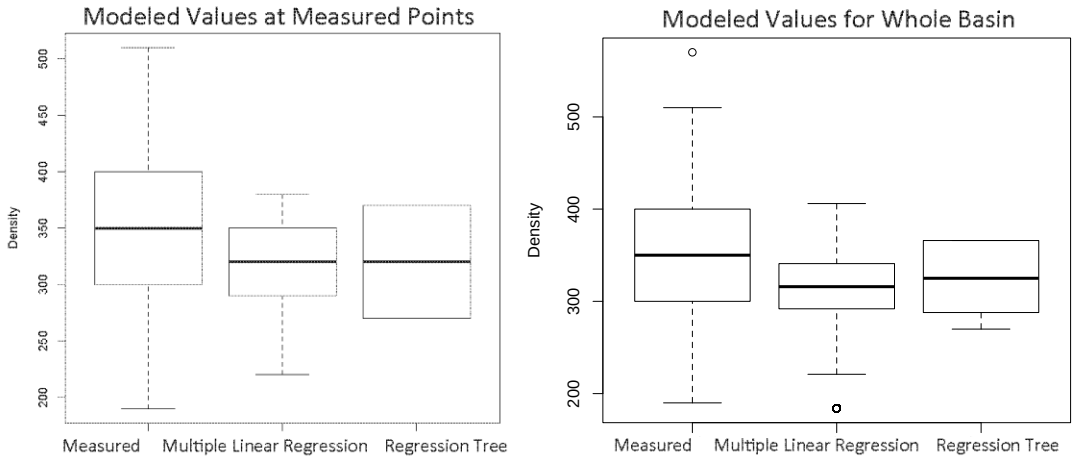


Figure 32. Boxplot comparisons of measured and modeled snow densities (kg/m^3).

In addition to the ranges of measured and modeled densities, considerable differences were also noted in the distributions themselves. Measured densities displayed a relatively normal distribution, which was well modeled by multiple regression, both in the shape and range of the distribution. Due to the nature of only modeling a limited number of unique density values (nine) the regression tree displayed a much narrower range of values. The largest portions of the basin were modeled by the highest and lowest densities to account for the values at the tails of the measure distribution, resulting in a very non-normal distribution (Figure 33) and relative under-representation of the most commonly measured densities (~275-375 kg/m^3). While the metrics used in this this comparison are not equivalent, the percent of basin (figure 33b) provides similar

information as a histogram of pixels for each value in the basin would, providing for a comparison of the general trends between measured and modeled values.

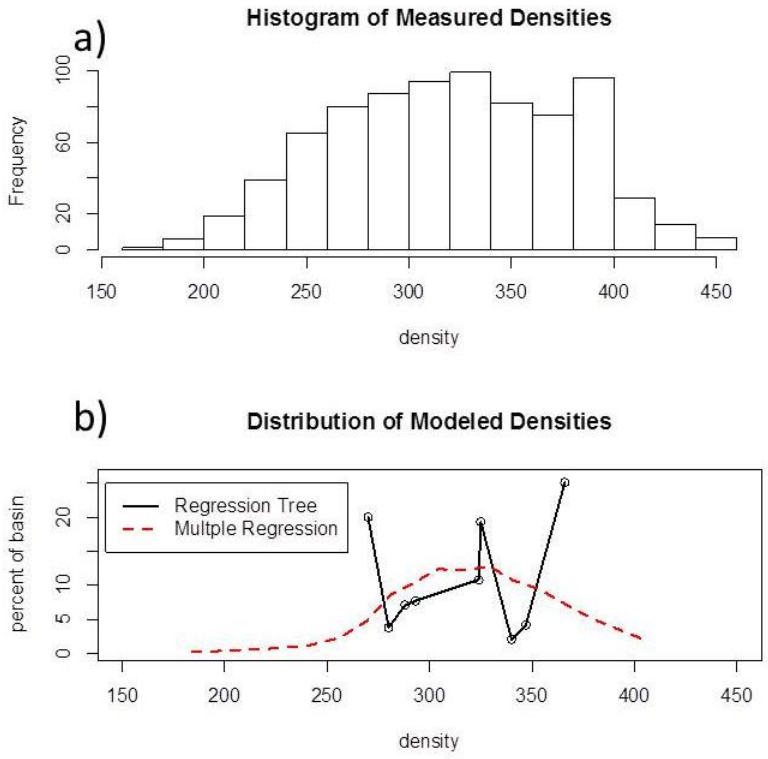


Figure 33. Figure 33a shows a histogram of measured density values. 33b shows the distributions (with % of basin being equivalent to a histogram of pixels in the spatial distribution) of density as modeled by regression tree and multiple linear regression. Multiple linear regression more closely models the distribution of the measured values, both in the center and at the tails.

4.5 The Effect of Density Parameterization on Estimates of Total Basin SWE

While proportionally the differences in density are conservative when compared to depth, when used to calculate SWE a relatively small change in density can have a very large impact on an estimate of total basin SWE, as also affirmed by *DeWalle and*

Rango [2008, pg. 87] with respect to estimating SWE volume from point measurements of depth. To illustrate this, the spatial distribution of snow depth was modeled using both MEMR and a binary regression tree which were then used to estimate total basin SWE using the basin average snow density and the two modeled spatial distributions. These estimates of total basin SWE were then compared to the average of total basin SWE as calculated by the three models that utilized direct SWE measurements (60,641,000 m^3) as is shown in Table 10.

Table 10. The effect of varying depth and density parameterizations on estimates of total basin SWE.

Depth Model	Density Model	Modeled Total SWE (m^3)	% Difference from mean of measured SWE models
MEMR	MLR	55,973,813	-8.3
MEMR	Regression tree	56,728,045	-6.9
MEMR	Average of measured	59,409,463	-2.1
Regression tree	MLR	61,088,312	0.7
Regression tree	Regression tree	61,574,372	1.5
Regression tree	Average of measured	64,398,753	5.8

When utilizing basin average density the MEMR model of snow depth yielded a relatively similar estimate of total basin SWE to the average of the SWE models (2.1% less), but when the distributed models of density were applied to this depth model, estimates of total basin SWE were 6.9% (regression tree) and 8.3% (MLR) less. Alternatively a five terminal node regression tree of snow depth modeled 5.8% more total basin SWE than the average of the SWE models, when basin average snow density was used. When total basin SWE was estimated using the regression tree for depth as well as the regression tree for density the estimates vary by only 1.5% compared to the average of the SWE models, and by 0.7% if the MLR model for density is used.

4.6 Comparisons to the Lone Mountain SNOTEL Site

The Lone Mountain SNOTEL site (NRCS #590) provides the only continuous SWE data for the West Fork Basin and is a major data source for streamflow forecasting for the upper Gallatin River (at the USGS Gallatin at Gateway Gauge). Because of its importance, comparisons were made between measured values at the site to measured and modeled values throughout the physiographic strata that it occupies (strata 3310, see Table 1 for description) as well as modeled values at the site itself. These analyses also provide insight into the measured and modeled variability in SWE and snow density in areas of physiographic similarity throughout the basin. During the time of sampling measured SWE at the SNOTEL site was 450 mm and the density was 370 kg/m^3. Summary statistics of the measured and modeled SWE depths and snow densities in the strata that contain the SNOTEL site are given in Table 11.

Table 11. Comparisons of modeled SWE values (mm) and snow densities (kg/m^3) to that measured at the Lone Mountain SNOTEL site and comparisons between modeled and sampled SWE and density values throughout strata 3310.

Data	Mean	Median	Standard Deviation	Modeled at SNOTEL

Regression Tree: SWE	460	453	60.9	453
CI Tree: SWE	449	453	32.9	453
MEMR: SWE	348	358	53.3	327
Sampled SWE values throughout strata 3310	485	508	126	n/a
Regression Tree: density	316	325	19.3	325
MLR: density	316	317	11.5	325
Sampled density values throughout strata 3310	316	329	49	n/a

The regression tree and CI tree happened to model very similar values to that measured at the SNOTEL site, as well as have very similar means and medians of values in the same physiographic strata throughout the basin. The MEMR model provided substantially lower estimates both at the site and in the same strata throughout the basin. Measured values in this strata had means and medians larger than those measured at the site and estimated my any models. Mean densities of modeled and measured values were all the same. The medians showed more variation with the measured values being closest to, but still 41 kg/m^3 less than was measured at the SNOTEL site.

5.0 DISCUSSION

This paper presents the effect of the physiography of a basin on the spatial distribution of SWE and snow density near peak accumulation using a variety of different modeling methods. A sampling plan was utilized that sampled a large and complex basin in areas that were physiographically proportional to the whole (with approximately 25% of the total basin area being sampled) in a semi-random structured manner to ensure the most representative sample possible. All modeling methods used were determined to be similarly accurate with respect to estimating total basin SWE and appropriate for this type of study. However, these statistical approaches provided widely varying representations of the spatial distributions of SWE and snow density. These differences can provide insight into the appropriateness of the various model types depending on the purpose of a study. For example, if one were looking to estimate total basin SWE without regard for how it is spatially distributed any model would appear to be equally appropriate. However, if a model of the spatial distribution of SWE is to be put into a distributed watershed model for the purpose of estimating runoff timing and volume perhaps the MEMR model would be a better choice than the others due to its closeness to measured values with regard to the smooth distribution of SWE depths throughout the elevation range.

5.1 The Spatial Distribution of Snow Water Equivalent

The spatial distribution of SWE was modeled using the well accepted method of binary regression trees [*Balk and Elder,* 2000; *Elder et al.,*1998; *Erxleben et al.*; 2002; *Winstral et al.*, 2002; *Molotch et al.*, 2005] as well as two methods previously unused for this type of study, mixed effects multiple regression, and conditional inference trees. All three methods provided estimates of total basin SWE to be within approximately one percent of their average (Table 7) but in very different spatial arrangements (Figure 20). The MEMR model provided the widest range of modeled values SWE (0-859mm) as well as unique values calculated for each pixel in the raster grid of the basin. The regression tree and CI tree models provided seven and 16 unique values of modeled SWE, respectively, and a smaller range of modeled values than did MEMR. The regression tree model had seven terminal nodes and a range of modeled values from 43-545mm and the CI tree had a range of 0-486mm, compared to measured SWE values of 0-965mm.

Optimal tree size for the regression tree model in this study was very similar to those used by *Molotch et al.* [2005], who found them to be between five and eight nodes for snow depth. This however is much smaller than the tree sizes used for analysis by other similar studies. *Elder et al.* [1998] used a 25 node regression tree to model the spatial distribution of snow depth and *Balk and Elder* [2000] developed an 18 node tree to model snow depth. The size of the CI tree used in this study fell into the middle of these values. Although other studies have not used CI tree, the 16 node tree used in this study is similar in size to that of *Winstral et al.* [2002] who used a binary regression tree pruned to 16 terminal nodes for their analysis, and slightly larger than *Erxleben et al.*

[2002] who utilized trees with 9-12 terminal nodes to describe the spatial distribution of snow depth at their respective study sites.

While these types of studies are not directly comparable because they are performed in different watersheds, during different years, with different datasets, and R^2 values increase with increased terminal nodes [*Molotch et al.,* 2005], R^2 can still be a useful tool for comparison tool as long as the associated assumptions of its interpretation are understood. Based on an R^2 value of 0.71 the results of the regression tree model in this study are strong compared to previous similar work, particularly when considering the relatively large basin and small tree size. An average regression tree model fit of 0.37 was obtained by *Molotch et al.* [2005] in the 19.1 km^2 Tokopah Basin in the Sierra Nevada Mountains of California and *Erxleben et al.* [2002] had an average R^2 of 0.25 in their three 1km^2 plots. In a 6.9 km^2 catchment in Colorado *Balk and Elder* [2000] yielded an R^2 value of 0.59 through the use of an 18 node regression tree. To express the influence basin size has on an R^2 value, *Elder* [1995] increased an average R^2 value of 0.4 over the whole Tokopah basin to between 0.6 and 0.8 by developing independent models for the two sub-basins that comprise it (between 0.69 and 1.78 km^2).

While studies from *Balk and Elder* [2000] and *Elder* [1995] appear to show that a smaller basin size have correlation with a larger R^2 value, this study found otherwise. The large R^2 in this study could likely have relation to the large basin size (207 km^2) which provided a wide elevation range (1575m) and considerable physiographic diversity. This physiographic diversity, combined with a large number of samples (n=1017) collected in a physiographically proportional manner possibly allowed for a stronger statistical

relationship between the physiography of the basin and SWE depth than would be possible in a smaller basin, both of which agree with statements made by *Erickson et al.* [2005] regarding factors that can influence R^2 values.

When determining optimal tree size and structure, as well as generally understanding how the model functions it appears to be valuable to analyze the influence each individual terminal node has on the total modeled spatial distribution of SWE and estimated total basin SWE. The two tree based models displayed substantially different characteristics in this respect, with the regression tree showing a more even distribution of SWE across the terminal nodes (Figure 10) than the CI tree (Figure 12). Five of the 16 nodes represented 56% of total basin area and 81% of total basin SWE (with a single node representing 24.6% of basin area and 40.1% of basin SWE) while five others only represented 6.8% of basin area and 1.8% of total basin SWE. Although this type of analysis has not been published in previous studies, the author believes it can be a valuable tool for obtaining the best overall understanding of what a given tree model is describing. The quantification of the percent of basin area and total basin SWE that each terminal node represents adds substantially to the information given by a map of SWE depths throughout a basin. By quantifying the total SWE represented by each terminal node a more conceptually three dimensional quality to the model as a whole can be attained. By making the connections from a statistical model, to a spatial distribution, to a quantification of total volume of SWE held in a given portion of the basin the most information and a more complete understanding of what exactly the model is describing can be attained.

While all of the parameters found to be significant in this study are well accepted to have a substantial influence on the spatial distribution of SWE [*Clark et al.*, 2011] there were no parameters used directly correlated to snow redistribution due to wind. Both aspect (due to prevailing westerlies) and curvature of the land surface were tested, due to potential re-distribution from convex areas and deposition in concave areas. While the observations of *Golding* [1974] and *Woo et al.* [1983] of wind removing snow from convex ridgelines and depositing it in topographic depressions was observed, this in this study no statistically significant correlations were found to these parameters. This lack of correlation was possibly due to the parameter choice of the degree of convexity or concavity as the only parameter analyzed relating to wind re-distribution or the relatively small portion of basin area where wind would be a dominant influence. Based on the results of *Winstral et al.*[2002] and *Erickson et al.* [2005] it is likely that a more specific wind re-distribution related parameter could have improved the explanatory and predictive power of the models used in this study, particularly in the higher elevation alpine portions of the basin where wind is likely to have the greatest influence.

The manner in which the different models characterized the effect of radiation throughout the elevation range also showed much variation. With the MEMR model utilizing a single negative β value to characterize the effect of radiation on SWE depth higher radiation was correlated with less SWE throughout the basin, which complies with a well accepted perceptual model of the process. In the regression tree model this was the case below 2415m, but had the opposite interpretation above this elevation (Figure 17). One possible explanation for this is the effect of radiation on SWE depth is lessened as

elevation and SWE depth increase, however further research would be required to verify this. The CI tree also displayed this characteristic, but only in one terminal node (453mm).

Comparisons of model predictive power were made between the regression tree and MEMR models using the average prediction error resulting from a 10 fold cross validation. Both performed similarly, but the regression tree had a slightly improved average prediction error of 109mm over the 118mm error given by the MEMR model. A directly comparable cross validation method was not available for the CI tree model. Despite their differences one major similarity between the CI tree and regression tree models exists in that their initial split was made at very similar elevations and both models produced very similar estimates of SWE above those elevations. The CI tree modeled 81% of basin SWE above 2412m and the regression tree estimated 83% of SWE above 2415m. While their spatial distributions and ranges of modeled SWE values show notable variation, they both modeled total basin as well as total high elevation SWE in a fairly similar fashion.

Each model type displayed substantially different spatial patterns yet estimated very similar volumes of total basin SWE, each having their own pros and cons. The regression tree provided no zero values and only provided seven unique SWE values, yet appears to provide a simple and statistically defendable estimate of total basin SWE. MEMR provided unique values of SWE for each pixel in the basin, and a good representation of SWE at low elevations but due to its heavy weighting of elevation likely over-estimates SWE at many high elevations. The CI tree modeled low SWE values more

accurately than the regression tree, but its highest modeled value was only 486mm, much lower than many field observations. Based on these differences, and average of the three models (Figure 20d) was determined to provide the most realistic overall model of the spatial distribution of SWE throughout the basin (based on quantitative and qualitative field observations), particularly with respect to elevation.

All three methods of modeling SWE estimated very similar quantities of total basin SWE, but did so providing considerably different spatial patterns and ranges of modeled values. Given this and the relatively similar prediction errors of the regression tree and mixed effects multiple regression models, it is recommended that close attention should be paid to what types of models are used to spatially distribute SWE in future work depending on the purpose of a study. For instance, if the goal was to simply estimate the total SWE stored in the West Fork Basin at peak accumulation it seems any of the models would be appropriate. If, however, the goal was to estimate the spatial distribution or total SWE stored in a particular sub-basin, or to estimate the timing and volume of snowmelt runoff, the choice of model would then be more critical due to the varying spatial patterns estimated by the different models. While they all model similar total basin SWE volumes in the entire West Fork Basin, the models all exhibit varying degrees of spatial averaging to achieve this. For these reasons MEMR would likely be a more appropriate choice for estimating the spatial distribution of SWE in a small high elevation sub-basin than the CI tree because the CI tree would likely model the entire sub-basin as having 486mm SWE uniformly throughout it, which is unlikely to the reality in the field. Additionally, if a model of the spatial distribution of SWE in a basin is to be

used for the purpose of modeling or estimating a runoff hydrograph resulting from snowmelt the manner in which SWE is spatially distributed throughout the basin can have a very large impact on the resulting modeled hydrograph, on both diurnal and seasonal scales, as is evidenced by the work of *Lundquist and Dettinger* [2005].

5.2 The Spatial Distribution of Snow Density

Most of the previous research on quantifying the spatial distribution of SWE has primarily measured snow depths and calculated SWE using comparatively few density measurements. Multiple linear regression has been used to estimate the spatial distribution of snow density to calculate total basin SWE, but with varying results. Both *Erxleben et al.* [2002] (using 13, 15, and 17 density measurements) and *Molotch et al.* [2005] (using 19, 66, and 76 density measurements) found no statistically significant correlation between physiography and snow density during their respective sampling campaigns and therefore used the mean density from each campaign to calculate SWE. More similar to *Elder et al.* [1998], using MLR this study did find significant correlations between snow density, elevation, radiation, and slope angle. *Elder et al.* [1998] was able to explain 70% of observed variance using those three parameters based on 10 density measurements. This study utilized only elevation and radiation as explanatory variables, due to autocorrelation between slope angle and radiation, and was able to explain 39% of observed variance in snow density. Using the same variables a binary regression tree was able to explain 41% of observed variance. Direct comparison of these results is difficult due to the differences in variable choice and the considerable difference in number of

observations used for the regression, n=1017 for this study and only n=10 for *Elder et al.* [1998].

The range of modeled densities of the regression tree was 94 kg/m^3 and the range of modeled densities of the MLR model was 222 kg/m^3. The range of densities in the multiple regression model was more than twice that of the regression tree but the portion of the basin represented by the wider range (seen in the tails of the distribution outside the range of the tree model) of values was much smaller in comparison, accounting for 11% of the total basin area. While visually the regression tree does appear to under-represent the most commonly observed densities (Figure 31), all modeled values are still within the range of the inter-quartile range of the measured values. The tree model provided a good representation of the most commonly observed values, but failed to model the tails of the distribution.

The nine node regression tree that utilized elevation and radiation as explanatory variables was able to explain 41% of observed variance in snow density, slightly more than with MLR (39%). Both methods estimated essentially the same basin mean snow density multiple linear regression modeled a much wider range of values (184–406 kg/m3) than did the regression tree (270-347 kg/m3). The wider range of values resulting from the multiple regression model appear to be due to its linear relationship with elevation, with higher elevation areas displaying low density values and low elevation areas displaying the highest values. With only nine unique values the regression tree model displayed a more conservative range of values, likely underestimating density at

low elevation and overestimating in higher portions of the basin but providing a good representation of the most commonly observed densities.

It is relatively well accepted that during the melt season snow density varies considerably less than snow depth so fewer density measurements are required. However, the results of this study also support the statement of *Elder et al.* [1991] that before the basin wide onset of melt, snow density exhibits considerable variability. Given the results of this study, that considerable, but explainable, spatial variability in snow density still exists near the time of peak accumulation the implication exists that careful consideration should be given to how the spatial distribution of snow density should be modeled in future work, as snow density will continue to change spatially and temporally as the melt season progresses. Much of this variability is likely due to the large elevation range (compared to previous work) of this study, which emphasizes the practical importance of this issue because both large elevation ranges and spatial extents of mountainous basins are characteristic of the type of terrain where operational water supply forecasts generally derive from. If the total basin SWE (and the spatial distribution of SWE) is to be estimated by applying a density value (or range of values) to a modeled spatial distribution of snow depth, the nearly 12% range (representing 8,425,000 m^3 of water) of estimated total basin SWE values exhibited by these different strategies exhibits the importance of carefully evaluating how snow density is to be incorporated.

6.0 CONCLUSIONS

Quantifying smaller areas of the basin which are physiographically proportional to the whole in which to sample appeared to be an effective way to sample a large and complex drainage basin for the purpose of modeling the spatial distribution of SWE and snow density. As such, sampling methods such as these can be an effective tool for being able to accurately expand these types of studies over larger spatial extents, which is essential for being able to apply such research to improving the accuracy and precision of operational water supply forecasting. The methods described here and provide an easily replicable template for being able to conduct a similar study over a wide range of spatial scales and landscape types while only sampling a relatively small percentage of the basin (the exact percent would vary basin to basin).

This research shows that in a basin with a large elevation range snow density can vary widely near peak accumulation and should be adequately sampled for in future work, particularly if the snowpack in the entire basin has yet to become completely ripe. Small differences in density can have relatively large impacts on estimates of total basin SWE if snow depth is the primary data being collected, so accurate parameterization of snow density is of great importance in such studies.

The various model types utilized in this study displayed notable differences in the manner in which the spatial distribution of SWE and snow density were estimated. The most notable difference being that the tree based models only produce a limited number of discrete values as outputs, whereas MEMR and MLR provide more continuous estimates throughout the range of modeled values. This characteristic of the MEMR and MLR models led to their continuous estimates throughout the elevation range and range

of modeled values at measured points, which was generally far more similar to what was observed and measured in the field than was estimated by the tree based models. Tree based models have the advantage of potentially being able to model the influence of the various parameters differently throughout the basin, whereas MEMR and MLR generally model the same parameters as having a similar influence (positive or negative) throughout. While the inclusion of interaction terms could potentially be utilized to account for this, these were not shown to improve model performance in this study. This characteristic of tree models could be advantageous for accurately modeling field data, but also potentially dis-advantageous if this is modeled based on some correlation inherent in the data but is not necessarily the primary driving factor (as could possibly be the case with how the regression tree model for SWE treated radiation differently in this study). All of the model structures presented in this study were determined to be appropriate for the data and generally the purpose of estimating the spatial distribution of SWE and snow density based on basin physiography. They all have advantages and dis-advantages for various purposes and the results of this research suggest that great care should be given to the choice of model used to estimate the spatial distribution of SWE and snow density depending on the goals of a study.

7.0 CHALLENGES, IMPROVEMENTS, AND RECOMMENDATIONS

7.1 Sampling Plan

There are many challenges that arise in conducting field based snow research, particularly when working with predetermined dates and a short timeline. This section addresses many of the challenges experienced during the case study of the West Fork basin as well as suggestions and improvements that can make such a study operate more efficiently and effectively in the future.

7.1.1 Lack of Access Due to Low Snowpack

Challenges due to lack of access can be addressed in several ways. First, the risk of this occurring can be minimized through obtaining as much knowledge of the area as possible during the planning stages. This can be done by either the researcher observing patterns of snow cover distribution over many different snowpack conditions, or through accessing local knowledge from individuals who have observed a wide range of conditions. This process would allow the researcher to identify which sampling areas are at risk of minimal access if snow depths happen to be less than ideal during the data collection campaign. Given this information, alternate sampling areas can be identified which have similar physiographic characteristics but would still be accessible during low snow conditions.

7.1.2 Avalanche Hazard

A second major challenge that was faced in this study, as well as by *Winstral et al.* [2002], was the inability to access certain areas due to safety concerns, primarily avalanche hazard. In this study all avalanche terrain and runout zones outside of controlled ski resorts were avoided due to very dangerous conditions during the sampling campaign. While this is more challenging to plan for due to the fact that avalanche terrain likely comprises unique strata and may be difficult to replace, a similar strategy as mentioned for the lack of access due to low snow can be employed to ensure a quality data set is still obtained regardless of avalanche hazard. By using GIS to identify avalanche terrain (primarily by slope angle) alternate sampling areas can then be identified that are not in avalanche terrain but in strata that are as similar as possible to the ideal sampling areas, or utilizing remote methods of estimating SWE in these areas [e.g. *Kerr et al.*, 2013].

7.1.3 Access to Sample On Private Land

During the initial planning stages, portions of the basin that are potential sampling areas that lie in private land must be identified. If any private land lies within a proposed sampling area access must be requested from the landowner as early as possible to ensure that legal access can be obtained or if an alternate sampling areas must be considered. In the West Fork Basin various resorts owned much of the large tracts of private land that were in, or provided access to, ideal sampling areas and access was granted through contact with these owners. This however may not always be the case and this process should be started well in advance as it may require significant amounts of time, or alternative areas to sample may need to be identified.

7.1.4 Changing Weather Throughout Sampling Campaign

One of the most significant challenges to be considered in a study of the spatial distribution of SWE is variable weather during the sampling campaign. Ideally, a "snapshot" of how SWE is distributed throughout the basin near maximum accumulation will be obtained. If a multi-day data collection campaign is to be undertaken, any significant precipitation or ablation that takes place during the middle of the data collection process can potentially negatively impact the accuracy of the results of the analysis, which is of particular concern in a basin with a large elevation range. In this study weather did not have an impact of the collection of an unbiased "snapshot" of the basin. Throughout the data collection process temperatures remained near freezing and only traces of precipitation occurred throughout the basin. Measures were taken to minimize the potential of a weather related bias being introduced into the data. This was primarily accomplished through the use of numerous field assistants to ensure data was collected over the shortest possible time period.

7.1.5 Precisely Defining Sampling Areas

One final consideration for the planning stages is to be able to define the areas to be sampled as narrowly as possible to ensure the data that is collected is most representative of the basin as a whole. The more narrowly the sampling areas are defined during the planning stages (primarily the analysis of representativeness) the higher confidence the researcher can have that the resulting data set will be as physiographically representative of the whole basin as possible.

7.2 Analysis and Modeling

One potential way that this study, as well as future similar work, could be strengthened is through further analysis of the influence that various tree sizes would have on the results an interpretation of the models. While the sizes of the final CI and binary regression trees used in this study were determined to be most appropriate for this data, a detailed examination of the influence of varying the tree sizes could potentially add helpful insight into both the phenomena being observed on the ground as well as the optimal ways to model it. As an example, increasing the significance level required for a split to occur in the CI tree until it had the same number of terminal nodes as the regression tree would provide further interesting comparisons between how the two models would are structured if they are the same size. While it was not directly the focus of this research, further detailed analysis of the differences between CI trees and regression trees, and how they compare to methods such as MEMR, for their use in the field of snow hydrology could be an interesting and important contribution.

Very steep slopes in the high alpine regions could be better characterized, while representing only a small portion of the basin they were generally modeled as holding large amounts of SWE, when in reality slopes this steep will often lose much of their snowpack to sloughing [*Kerr et al.*, 2013] and be heavily affected by wind [*Winstral et al.*, 2002]. The seemingly differing effect of forest cover and radiation on SWE depth (with an apparent greater influence at low elevation than high elevation) throughout the elevation range could also be further analyzed and potentially better characterized in the

models. The regression tree model and much of the exploratory analyses that were performed show this to likely be the case, however none of the models utilized in the final analysis of this study can quantify or account for this phenomena very well.

7.3 Recommendations for Future Research

There is much opportunity for future research regarding the phenomena that influence the spatial distribution of SWE and snow density in mountainous terrain. In a general sense, continuing to expand the spatial extent on which the spatial distribution of SWE can be accurately and precisely measured and modeled, from hillslope, to catchment, to regional scales is of great importance. Currently much of the operational water supply forecasting that occurs in the Western United States utilizes point measurements to forecast for large and physiographically diverse watersheds. By improving the understanding of how and why SWE is distributed throughout expansive mountainous regions, the opportunity for increasing the accuracy of water supply forecasts is greatly increased. Similarly, using that information, methods for utilizing point measurements of SWE (e.g. SNOTEL and snow courses) to better estimate total basin SWE at peak accumulation could be developed which have potential for being valuable tools in increasing the accuracy of water supply forecasts. Overall, there is much opportunity for important research to be done in this field which would ideally lead to a better understanding of the role of snow in the hydrologic system on spatial scales of meters to hundreds of kilometers and on temporal scales from minutes to years. Connecting the understanding of snow hydrologic processes across all of these scales,

while an imposing task, is of critical importance for the best possible understanding, modeling, and management of water resources in the snow dependent Western United States.

REFERENCES CITED

Balk, B. and K. Elder (2000), Combining binary decision tree and geostatistical methods to estimate snow distribution in a mountain watershed. *Water Resour. Res., 36,* 13-26.

Blöschl, G. (1999), Scaling issues in snow hydrology, *Hydrol. Proces.,* 13, 2149-2175.

Blöschl, G., and M. Sivapalan (1995), Scale issues in hydrological monitoring: a review, *Hydrol. Proces., 9*, 251-290.

Breiman, L., J. H. Friedman, R. A. Olshen, and C. J. Stone (1984), Classification and Regression Trees. *Wadsworth*, 358 pp.

Campos, N., R. Lawrence, B. Mcglynn, and K. Gardner (2011), Using Quickbird and Landsat imagery to analyze temporal changes in mountain resort development: Big Sky, MT 1990-2005, *Journal of Applied Remote Sensing*, *5*, 053541-1 – 053541-14

DeWalle, D.R. and A. Rango (2008), Principles of snow hydrology, *Cambridge University Press.*

Clark, M.P., J. Hendrikx, A.G. Slater, D. Kavetski, B. Anderson, N.J. Cullen, T. Kerr, E.Ö. Hreinsson, and R.A. Woods (2011), Representing the spatial variability of snow water equivalence and land surface models: a review, *Water Resour. Res., 47*, W07539 1-23.

Doeksen, N.J. and A. Judsen, The snow booklet: a guide to the science, climatology, and measurement of snow in the United States, *Dep. Of Atmos. Sci., Colo. State Univ., Fort Collins*, 1996.

Elder, K. (1995), Snow distribution in alpine watersheds, PhD dissertation, University of California, Santa Barbara, CA; 309pp.

Elder, K., J. Dozier, and J. Michaelsen (1991), Snow accumulation and distribution in an alpine watershed, *Water Resour. Res., 27*, 1541-1552.

Elder, K., W. Rosenthal, and R.E. Davis (1998), Estimating the spatial distribution of snow water equivalence in a montane watershed, *Hydrol. Process., 12*, 1793-1808.

Erickson, T.A., M.W. Williams, and A. Winstral (2005), Persistence of topographic controls on the spatial distribution of snow in rugged mountain terrain, Colorado, United States, *Water Resour. Res., 41*, w04014 1-17.

Erxleben, J., K. Elder, and R. Davis (2002), Comparison of spatial interpolation methods for estimating snow distribution in the Colorado Rocky Mountains, *Hydrol. Process., 16*, 3627-3649.

Golding, D.L. (1974), The correlation of snowpack with topography and snowmelt runoff on Marmot Creek Basin, Alberta, *Atmosphere, 12*, 31-38.

Hothorn, T., K. Hornik, and A. Zeileis (2004), Unbiased recursive partitioning: a conditional inference framework, *Research Report Series: Wirtschafts Universität, 8*, 1-16.

Jost, G., M. Weiler, D. Gluns, and Y. Alila (2007), The influence of forest and topography on snow accumulation and melt at the watershed scale, *Journal of Hydrology*, 347, 101-115.

Kerr, T., M. Clark, J. Hendrikx, and B. Anderson (2013), Snow distribution in a steep mid-latitude catchment, *Adv Water Resour (2013)*, http://dx.doi.org/10.1016/j.advwatres.2012.12.010, (in press)

Kronholm, K. and K. Birkeland (2007), Reliability of spatial sampling plans for snow surveys, *Computers and Geosciences*, 33, 1097-1110.

Lohr, S.L. (1999), Sampling: Design and Analysis, Duxbury, Pacific Grove, CA.

Lundquist, J.D. and M.D. Dettinger (2005), How snowpack heterogeneity affects diurnal streamflow timing, *Water Resour. Res, 41*, W05007, 1-14.

Molotch, N.P. and R.C. Bales (2005), SNOTEL representativeness in the Rio Grande headwaters on the basis of physiographics and remotely-sensed snow cover persistence, *Proceedings of the Western Snow Conference, 2005*, 73-86.

Molotch, N.P., M.T. Colee, R.C. Bales, and J. Dozier (2005), Estimating the spatial distribution of snow water equivalent in an alpine basin using binary regression tree models: the impact of digital elevation data and independent variable selection, *Hydrol. Process*, *19*, 1459-1479.

Ramsey, F.L. and D.W. Schafer (2002), The Statistical Sleuth: A Course in Methods of Data Analysis, Duxbury, Pacific Grove, CA.

Skøien, J.O. and G. Blöschl (2006), Sampling scale effects in random fields and implications for environmental monitoring, *Environmental Monitoring and Assessment*, DOI: 10.1007/s10661-006-4939-z .

Trujillo, E., J.A. Ramirez, and K.J. Elder (2007), Topographic, meteorologic, and canopy controls on the scaling characteristics of the spatial distribution of snow depth fields, *Water Resour. Res.,43*, W07409, 1-17.

United States Department of Agriculture (USDA) (1984), Snow survey sampling guide, *Agriculture Handbook, 169*, 1-32.

Watson, F.G.R., T.N. Anderson, W.B Newman, S.E. Alexander, and R.A. Garrott (2006), Optimal sampling schemes for estimating mean snow water equivalents in stratified heterogeneous landscapes, *Journal of Hydrology*, *328*, 432-452.

Winstral, A., K. Elder, and R.E. Davis (2002), Spatial snow modeling of wind-redistributed snow using terrain based parameters, *Journal of Hydrometeorology, 3,* 524-538.

Woo, M., R. Heron, P. Marsh, and P. Steer (1983), Comparison of weather station snowfall with winter snow accumulation in high arctic basins, *Atmos.-Ocean, 21,* 312-325.

Zuur, A.F., E.N. Ieno, N.J. Walker, A.A. Saveliev, and G.M. Smith (2009), Mixed effects models and extensions in ecology with R, *Springer*, 574.

APPENDICES

APPENDIX A

DATA USED FOR ANALYSIS

SWE (mm)	Elevation	Land cover	Radiation	Curvature	Aspect	Slope angle	Depth (mm)	Density (kg/m^3)
64	1980.4	0	163321	0.46	28	5	152	383
64	1982	0	174890	3.41	336	10	152	383
64	1992.5	10	171549	-2.88	322	20	152	383
279	2115.8	0	155776	15.26	68	9	813	316
254	2114.7	0	155512	6.81	165	5	711	329
127	1987.6	0	179899	6.36	347	6	432	271

152	1994.4	10	170331	2.5	330	3	432	325
76	1993.2	10	171549	33.56	312	23	279	251
0	1992.3	10	170331	11.24	316	13	0	
102	1992.2	10	174593	9.01	21	8	318	294
127	1993.6	0	171623	2.21	33	16	457	256
0	2006.5	10	168265	6.7	294	3	0	
152	2003.4	0	164786	-7.5	357	15	521	269
114	2009.5	0	164786	-8.34	316	23	394	267
89	1997.8	0	163299	11.39	252	9	330	248
0	1846.7	0	210398	12.07	77	8	0	
0	1839.9	10	225990	26.51	70	10	0	
0	1884.2	0	210263	-7.4	47	2	0	
0	1883.7	0	212386	-5.18	328	3	0	
0	1882.8	0	208320	-4.94	132	4	0	
0	1881.8	0	210111	-10.34	74	3	0	
0	1948.7	0	211542	-3.39	215	22	0	
64	1945.3	0	232939	-17.94	90	7	152	383
0	1945.2	0	232939	-21.18	215	13	0	
0	1948.2	0	232939	-23.67	213	17	0	
64	1953.4	0	222820	-6.32	140	5	152	383
0	1920.1	0	216577	-12.41	273	6	0	
0	1920.2	0	215704	-0.24	45	3	0	
0	1930.7	0	211505	15.76	29	1	0	
0	1930.7	0	211505	2.81	65	2	0	
0	1931.1	0	212421	13.62	159	3	0	
64	1983.8	0	182988	-7.23	338	5	152	383
0	2059.8	0	207884	11.28	70	11	0	
0	2055.8	0	205687	6.74	70	15	0	
0	2054.9	0	201359	-36.16	180	9	0	
0	2054.3	0	194713	13.09	39	19	0	
0	2048.6	10	188871	31.47	27	21	0	
140	2061	0	211918	-12.74	66	9	356	361
64	2062.1	0	212164	7.18	42	3	152	383
64	2065.4	0	212164	-0.88	87	8	152	383
127	2064.7	0	212233	0.34	53	6	330	354
191	2066.6	0	207488	-12.74	67	9	406	431
140	2066	0	212233	-2.91	84	7	356	361
76	2064.6	0	212169	1.76	95	5	152	460
152	2063.6	0	212169	-33.86	73	8	356	394

152	2062.8	0	212037	15.41	70	12	356	394
64	2073.9	0	215276	5.27	126	9	152	383
64	2072.2	10	212182	6.27	187	25	152	383
152	2074.3	0	212182	3.32	131	3	356	394
0	2075.6	0	212182	0.63	160	7	0	
0	1846	0	210398	-3.66	173	15	0	
0	1846.8	0	210700	14.65	143	4	0	
0	1843.1	0	210398	2.8	118	9	0	
0	1884.4	0	210263	-5.07	31	1	0	
0	1884	0	209940	-7.23	114	2	0	
0	1884.2	0	210300	-2.64	89	2	0	
13	1884.2	0	210300	-16.69	68	1	38	307
0	1885.3	0	210208	3.72	224	5	0	
51	1882.5	0	210208	25.67	338	23	152	307
38	1882.8	0	208996	-3.38	334	18	102	345
64	1881.6	0	208996	19.31	333	21	178	329
13	1882.6	0	208996	-3.43	333	20	25	460
38	1883.2	0	208996	6.23	328	20	102	345
0	1912.7	0	231378	2.53	94	4	0	
25	1913.3	0	231675	2.99	71	7	76	307
51	1914.9	0	224197	25.94	57	14	140	335
0	1914.9	0	224197	-2.25	68	9	0	
64	1916.5	0	224197	-9.94	62	19	152	383
76	1917.1	0	224197	-11.1	54	18	203	345
51	1919	0	224197	1.78	55	15	127	368
0	1921.9	0	223619	-16.77	118	10	0	
0	1925.2	0	230108	-14.25	134	6	0	
38	1924	0	220421	4.21	69	15	102	345
64	1921.7	0	220421	-26.45	61	14	152	383
38	1918.2	0	218039	-14.23	74	9	114	307
76	1918.5	0	218039	-16.46	56	13	203	345
0	1916.1	0	226585	-5.51	152	5	0	
25	1914.2	0	231675	-0.37	107	3	51	460
38	1950.2	0	200470	-0.73	68	10	102	345
76	1951.1	0	200470	2.29	66	9	203	345
89	1950.6	0	196892	0.9	63	13	254	322
0	1951	0	196892	4.72	41	11	0	
76	1949.7	0	196892	-4.46	42	12	229	307
76	1946.4	0	204096	-10.56	56	14	229	307

102	1946.3	0	204096	-11.4	47	13	330	283
76	1948.5	0	204096	-3.06	60	14	203	345
89	1950.2	0	196892	-14.67	61	12	254	322
64	1951.3	0	196892	-13.65	49	12	152	383
76	1951	0	196892	2.29	62	14	178	394
25	1950.4	0	200470	10.01	48	8	64	368
89	1955.4	0	208353	-0.71	55	7	254	322
89	1955.7	0	208353	0.39	61	8	229	358
0	1919.4	0	216577	6.31	25	2	0	
0	1919.1	0	215653	5.38	160	1	0	
0	1918.7	0	216706	-7.93	27	3	0	
0	1918.9	0	215653	-1.59	130	2	0	
0	1930.5	0	211505	-7.52	91	2	0	
0	1930.3	0	210505	-9.45	344	3	0	
0	1930.9	0	212358	-12.54	319	2	0	
0	1931.1	0	212421	6.97	0	3	0	
0	2018.6	0	190716	-8.9	337	11	0	
76	2016.4	0	190716	-5.81	337	8	178	394
152	2056.7	0	208790	-1.95	16	9	381	368
140	2056.6	0	208790	-1.2	33	6	368	349
114	2056.9	0	208790	-8.79	27	3	305	345
140	2061.7	0	212164	-5.05	46	6	356	361
127	2062.4	0	206781	11.33	48	5	330	354
152	2064	0	206781	-8.72	53	10	394	356
114	2065	0	206781	-0.32	54	9	318	331
178	2066.2	0	206781	0.42	51	9	457	358
127	2066.4	0	207488	-25.78	65	9	330	354
203	2067.8	0	203422	-1.1	50	9	483	387
140	2069.2	0	203422	10.52	51	11	394	326
140	2068.8	0	207488	12.43	48	11	381	337
152	2068.3	0	207488	4.03	61	8	356	394
114	2074.9	0	230216	3.39	105	7	254	414
114	2074.1	0	230216	6.03	99	7	279	376
64	2073.7	10	230216	-2.59	170	10	152	383
140	2075.2	0	231213	-17.02	94	11	330	389
64	2057.9	10	207468	1.25	94	8	152	383
64	2072	10	215276	4.66	89	4	152	383
64	2071.9	10	215276	4.66	89	4	152	383
0	1847.5	0	210398	12.76	258	1	0	

0	1846.9	0	210398	-1.2	83	12	0	
203	2057	0	208790	-9.57	84	7	483	387
0	2057.1	10	211957	4.76	9	10	0	
0	2056.5	10	211957	-1.73	351	5	0	
127	2056.6	10	208790	15.26	93	3	356	329
102	2056.3	10	209699	-7.1	51	3	254	368
76	2056.6	10	211913	-11.74	75	5	178	394
0	2056.4	10	211913	4.83	36	3	0	
114	2057.1	10	211913	2.49	91	9	279	376
178	2057.7	0	211913	-3.32	84	4	445	368
178	2056.9	0	211913	3.64	90	4	445	368
0	2055.9	10	211913	-6.86	80	8	0	
0	2055.8	10	211913	-14.62	109	4	0	
76	2055.6	10	210656	8.25	96	5	191	368
0	2052.6	10	210656	8.91	112	7	0	
0	2051.1	10	205298	-2.51	99	11	0	
140	2052.5	10	210656	2.86	99	7	305	422
165	2053.1	10	210656	-8.57	83	7	406	374
51	2056.5	10	210656	-8.45	90	5	102	460
191	2072.1	10	230767	-16.97	74	7	432	406
140	2071.8	10	230767	2.81	118	5	305	422
114	2072	10	230767	4.83	193	3	279	376
0	2125.3	10	248798	23.27	142	12	0	
127	2113.8	0	242300	9.96	150	9	305	383
76	2113.8	0	242300	-11.21	153	9	203	345
0	1832.7	0	272527	-4.06	154	5	0	
0	1913.3	0	249740	6.49	124	5	0	
0	1919.4	0	263758	-2	203	26	0	
0	1934.2	0	261736	28.75	187	12	0	
0	1930.3	0	258043	-5.48	218	25	0	
0	1925.5	0	258043	-25.04	227	25	0	
0	1920.1	0	253860	-13.84	213	6	0	
0	1923.2	0	242604	2.75	126	3	0	
0	1924.8	0	216587	8.78	141	7	0	
0	1917.3	0	239514	-6.02	100	4	0	
0	1912.7	0	239525	3.89	149	3	0	
64	1949.8	0	219587	12.93	64	10	152	383
51	1948.6	0	211542	-7.65	26	10	127	368
0	1951	0	236110	-0.32	151	3	0	

0	1952.3	0	231879	6.58	161	5	0	
64	2022.1	0	243792	2.51	191	5	152	383
0	2056.1	0	261533	1.78	161	14	0	
64	2054.5	0	261533	-3.54	162	10	152	383
0	2057.8	0	261533	-5.96	134	8	0	
64	2105.7	0	262556	-9.11	216	7	152	383
0	2104.2	0	266021	8.37	176	9	0	
64	2105.2	0	260910	0.44	172	11	152	383
0	2121.5	10	259522	10.67	164	13	0	
0	2095.3	0	270182	-5.42	172	26	0	
0	2095.7	0	266584	-2.71	178	16	0	
64	2095.5	0	264285	1.86	114	13	152	383
64	2078.1	0	237222	18.55	148	23	152	383
0	1832.4	0	272527	16.75	164	13	0	
0	1836.9	0	283370	1.65	184	21	0	
0	1855.5	0	278277	-1.1	168	20	0	
0	1860.7	0	274211	-3.43	183	19	0	
0	1836.6	0	288865	-2.06	195	25	0	
0	1832.1	0	272527	10.57	173	14	0	
0	1921	0	241170	0.02	113	10	0	
0	1921.6	0	241170	4.71	132	8	0	
0	1920.1	0	241170	35.91	138	9	0	
0	1920.5	0	250959	12.4	165	8	0	
0	1916.9	0	250959	11.63	166	15	0	
51	1950.3	0	200470	15.39	53	5	127	368
0	2076.2	0	259219	-20.04	227	27	0	
0	2076.2	0	259219	-10.4	240	27	0	
0	2076.1	10	259219	3.47	231	30	0	
51	2070.9	0	253510	2.54	184	9	127	368
127	2056.3	0	242740	-21.78	210	9	305	383
114	2066.3	10	242740	5.54	222	9	279	376
89	2056.2	10	242740	5.83	116	7	216	379
38	2061.6	0	261285	-6.08	202	10	89	394
102	2061.9	0	261285	-22.73	189	11	305	307
203	2067	0	252173	6.93	139	7	546	342
0	2105	10	258948	-24.37	207	12	0	
0	2105	0	258948	19.78	195	8	0	
0	2106.8	0	258948	-15.58	162	12	0	
102	2114.9	0	260671	-7.54	171	15	254	368

114	2116.6	0	263536	-8.81	176	16	279	376
38	2117.9	0	267979	9.11	172	20	76	460
0	2117.9	0	267979	-10.94	163	14	0	
76	2121.8	0	267979	-4.52	170	13	178	394
203	2127.6	0	259637	-24.15	141	12	508	368
165	2129	0	259343	-1.56	150	11	457	332
0	2096.1	0	270182	11.01	172	30	0	
152	2073.7	10	239463	9.86	123	7	356	394
127	2073.5	10	239463	10.11	138	5	305	383
216	2079.3	0	237222	20.41	158	10	508	391
64	2115.8	10	242406	4.81	145	8	152	383
102	2115.8	10	242406	4.1	133	8	254	368
0	2121.6	10	240802	-0.68	98	8	0	
114	2116.5	0	242406	4.44	137	8	279	376
76	2116.3	10	242289	-5.71	162	10	178	394
38	2119	10	242289	-5.57	143	7	89	394
0	2122	10	242289	-0.42	157	12	0	
0	2120.9	10	248798	-30.71	143	15	0	
0	2123.5	10	248798	8.08	152	14	0	
165	2126.5	10	244328	3.59	148	7	406	374
140	2126.9	10	244328	-25.32	163	11	330	389
114	2128	10	244328	1.73	124	5	254	414
76	2126.4	10	244328	-24.51	152	12	178	394
127	2129.4	10	234825	2.64	168	10	305	383
0	2123.8	10	234825	9.47	163	14	0	
0	2126.3	10	248798	16.53	139	13	0	
0	2122.5	10	242289	24.41	146	16	0	
0	2123.6	10	242289	9.38	163	14	0	
0	2121	10	242289	-18.38	149	21	0	
0	2118.9	0	234578	-38.67	151	15	0	
51	2115.7	0	234578	-0.95	158	10	127	368
0	2110.3	0	262735	-30.69	174	17	0	
114	2125.6	10	256154	-11.04	156	4	419	251
0	2061.7	10	253510	11.33	149	6	0	
0	1842.7	10	276328	17.15	233	31	0	
0	1838.5	10	243796	-13.57	133	30	0	
0	2100	10	247327	-4.61	240	30	0	
0	2101	0	274637	-2.49	207	17	0	
0	1841.5	0	245066	26.68	102	20	0	

0	1848.5	10	281180	11.08	262	20	0	
0	1857.6	10	236487	-3.67	242	23	0	
0	1845.6	10	270540	-33.23	126	28	0	
0	2127.6	0	266008	0.76	154	18	0	
0	2127.6	10	265645	-9.08	104	32	0	
0	2125.8	0	248797	-2.05	252	25	0	
0	2127.1	0	297843	-4.61	201	33	0	
0	1838.5	0	286225	-3.65	180	30	0	
0	2100	0	283008	-3.03	170	23	0	
64	2101	0	282727	-12.08	147	21	152	383
0	1841.5	0	283370	-3.48	190	23	0	
0	1848.5	0	285493	-3.23	189	27	0	
0	1857.6	0	291295	-5.53	205	36	0	
0	1845.6	0	283370	7.51	195	27	0	
0	2127.6	0	280275	-5.49	153	9	0	
0	2127.6	0	280275	2.49	161	11	0	
165	2125.8	0	280275	-20.53	160	15	432	352
76	2127.1	0	278444	-4.86	148	9	178	394
0	2101.2	0	269186	21.17	177	26	0	
0	2108.2	0	281619	15.23	171	16	0	
38	2107.9	0	281619	-25.07	186	10	76	460
51	2109.4	0	281619	-3	165	8	127	368
38	2108.5	0	283008	-12.01	126	5	76	460
51	2103.7	0	283008	-25.46	162	25	127	368
0	1860.4	0	296363	13.65	149	26	0	
0	1855.8	10	287264	-3.27	203	19	0	
0	1916.9	10	292511	7.54	176	32	0	
0	1950.3	0	304451	-14.94	208	35	0	
0	2076.2	0	311315	-3.64	171	32	0	
0	1866.8	10	297843	1.81	208	45	0	
0	1853.6	0	285493	5.97	202	26	0	
0	1860.4	10	285493	13.82	213	28	0	
0	1855.8	0	291295	3.5	204	36	0	
0	1916.9	10	309229	4.93	198	34	0	
0	1950.3	10	288124	-14.4	216	31	0	
0	2076.2	10	306640	-0.32	224	34	0	
0	2076.2	10	303840	1.2	212	30	0	
0	2076.1	10	291328	-3.15	217	40	0	
0	2070.9	10	295547	-9.13	225	40	0	

0	2056.3	10	292305	-8.74	217	29	0	
0	2066.3	10	310615	1.71	180	22	0	
0	2056.2	0	309053	17.75	231	41	0	
0	2061.6	10	299472	-17.59	220	39	0	
0	2061.9	0	306705	1.17	182	31	0	
0	2067	10	295300	-16.78	190	31	0	
0	2105	10	308205	-7.28	197	35	0	
0	2016.5	10	269219	8.4	125	36	0	
0	2116.3	10	290392	-3.54	220	21	0	
0	1919	0	302765	26.83	204	34	0	
0	2099	10	273667	2.56	186	19	0	
0	2120.9	10	313287	-13.18	160	34	0	
0	2123.5	0	283897	-8.03	201	38	0	
546	2421.8	0	179051	-5.3	10	13	1283	392
356	2423.7	0	179051	-0.66	61	6	1029	318
229	2185.2	10	145117	-2.56	347	17	838	251
292	2178.8	0	150488	-43.73	343	20	953	282
102	2385.7	10	148277	1.42	47	37	305	307
178	2383.7	10	148277	-8.54	43	32	508	322
152	2330.8	10	109646	-23.12	43	31	559	251
127	2326.4	10	109646	-5.69	37	30	419	279
165	2261.3	10	146917	17.07	334	22	559	272
216	2259.6	10	146917	1.81	294	18	851	233
102	2237.2	10	127254	14.55	311	34	330	283
229	2233.3	10	127254	-7.28	341	18	762	276
305	2384.1	10	179168	11.77	322	12	914	307
356	2353.8	10	158944	-23.83	320	25	1092	300
229	2348.9	10	150567	7.93	307	24	737	286
292	2324.3	10	166210	22.9	310	19	851	316
203	2318.8	10	176643	-3.56	335	19	724	258
356	2252.4	0	234823	6.42	39	2	787	415
356	2250.5	0	226284	3.86	77	7	787	415
330	2249.4	0	226284	-29.91	40	5	711	427
330	2249.2	10	241404	15.97	118	5	711	427
406	2420.3	0	224012	20.09	53	6	1168	320
381	2420.4	0	224012	-6.32	68	3	1054	333
533	2441.8	0	186939	-29.08	39	18	1473	333
419	2447.9	0	230268	-6.74	236	13	1194	323
330	2445.7	0	230268	11.16	291	15	991	307

457	2447.3	0	230268	2.2	243	11	1143	368
330	2446.1	0	230268	-27.15	249	12	1003	303
381	2444.6	0	230268	12.3	240	12	1092	321
381	2443.5	0	230268	6.15	224	12	1118	314
457	2448.9	0	231297	15.21	254	11	1194	352
406	2449.4	0	231297	2.91	254	8	1092	342
432	2448.5	0	231297	10.67	246	12	1130	351
89	2155.6	0	187177	-14.99	113	26	368	222
127	2154.1	0	205839	-0.9	104	26	406	288
229	2406.5	0	199534	13.11	290	17	724	291
330	2422	0	196609	-3.25	315	3	940	323
305	2422.1	0	196609	-6.01	346	5	991	283
381	2422.5	0	196609	-9.18	337	8	1143	307
152	2174.1	0	229350	6.59	109	13	381	368
76	2252.9	0	241425	-9.81	101	7	254	276
254	2395.5	0	217548	1.17	94	25	1067	219
152	2349.5	0	204788	54.79	292	27	635	221
203	2142.2	0	229394	1.59	112	9	483	387
178	2151.7	0	232910	-25.44	127	10	483	339
203	2171.7	0	229350	-4.44	117	9	483	387
0	2148.4	0	185901	2.83	277	26	0	
64	2193.5	10	238497	-19.92	105	6	152	383
102	2200.9	10	238497	15.11	102	11	267	350
127	2196.6	10	233728	-10.6	112	12	318	368
152	2195.4	10	233728	-6.69	103	16	356	394
89	2196.7	10	233728	-1.12	112	12	229	358
102	2196.9	10	230680	-6.67	101	10	267	350
165	2196.8	10	230680	-3.17	99	12	381	399
89	2193.5	10	230680	3.98	95	12	203	403
102	2186	10	230683	-4.59	100	12	267	350
114	2189.6	10	230683	15.28	118	13	305	345
64	2183.7	10	233554	8.01	86	10	165	354
127	2182.7	10	233554	22.8	83	10	330	354
102	2182.7	10	233554	10.89	88	9	267	350
165	2185.6	10	230683	8.79	84	13	406	374
38	2185.9	10	230683	-2.69	100	11	89	394
114	2186.9	10	230683	-3.69	82	8	279	376
140	2179.6	10	230683	-2.05	79	10	330	389
76	2183.7	10	230683	3.61	81	18	178	394

432	2438	0	180909	-22.53	99	13	1041	381
330	2433.8	10	203630	-7.86	81	19	965	315
305	2417.1	10	210408	20.14	79	28	991	283
191	2412.3	10	210408	-5.91	83	21	711	246
229	2405.9	10	182441	-16.33	296	18	787	267
292	2387.3	10	189920	9.74	317	12	940	286
305	2434.9	10	187447	-9.42	348	9	978	287
279	2435	10	187447	-5.57	351	7	953	270
254	2435.4	10	187447	-3.32	337	9	864	271
0	2158.8	10	232910	3.61	176	22	0	
127	2187.6	10	224411	-2.98	332	9	343	341
0	2196.5	10	245937	-39.14	242	25	0	
394	2438.4	10	240560	5.93	176	6	1334	272
419	2441.6	10	240560	9.55	132	6	1321	292
457	2441.5	0	240560	-40.97	138	6	1346	312
318	2442.2	0	240560	-19.43	130	11	1143	256
394	2442.3	0	240560	11.67	104	4	1219	297
381	2442.3	0	243443	8.62	128	9	1168	300
394	2447.6	0	243443	20.68	112	8	1245	291
368	2444.7	0	243443	-11.47	172	6	1130	300
394	2444.4	0	243443	0.88	231	8	1130	320
394	2440.8	0	247489	0.61	250	8	1130	320
0	2302.2	10	274388	5.54	162	7	0	
381	2260.5	0	238667	1.66	86	10	826	425
292	2254.1	0	247152	-16.14	108	8	635	423
279	2257.1	0	247152	-11.87	114	13	597	431
229	2260.8	0	247152	12.7	127	12	508	414
229	2252.8	0	247185	7.79	114	11	508	414
229	2253.1	0	245521	9.77	121	15	622	338
254	2248.8	0	241800	0.51	106	7	610	383
114	2250.3	0	241800	-1.95	121	9	254	414
178	2247.8	0	241800	-1.88	111	9	406	403
229	2248	0	241800	1.1	126	13	533	394
0	2247.8	0	243811	1.86	120	16	0	
229	2247.5	0	243811	3.49	116	14	533	394
305	2249	0	243811	7.47	122	6	711	394
279	2252.7	0	234823	-14.53	92	7	635	405
305	2249.5	10	251775	-2.37	128	8	737	381
216	2259.6	0	239074	-14.77	77	8	483	412

165	2268.4	0	245551	-9.86	121	7	406	374
178	2272.1	0	240734	-2.86	137	8	470	348
279	2271.6	0	240734	-0.9	100	10	622	413
102	2199	10	245598	13.09	253	22	254	368
89	2193.3	10	236471	5.76	97	10	203	403
330	2445.4	0	235723	-2.54	227	12	1041	292
419	2444.1	0	235723	8.94	263	13	1105	349
381	2443	0	235723	-14.48	247	15	1194	294
305	2442.3	0	240298	13.43	260	11	927	302
305	2442.9	0	240298	13.43	260	11	927	302
381	2441.8	0	240298	-9.01	250	12	1143	307
559	2438.3	0	240298	7.52	224	29	1549	332
305	2432.8	0	241027	8.59	220	8	1029	273
432	2442.5	0	235723	-21.9	264	14	1270	313
508	2441.9	0	235723	-34.64	213	14	1372	341
406	2440.7	0	235723	-5.08	259	13	1207	310
381	2440.3	0	240298	-1.51	288	11	1143	307
330	2440.1	0	240298	4.66	261	14	1041	292
610	2437.4	0	241027	12.65	205	14	1524	368
483	2442.3	0	243366	-8.01	261	17	1321	336
267	2439.9	0	243366	18.24	257	13	1143	215
559	2438.4	0	250435	-13.92	241	15	1321	389
0	2133	0	267571	4.13	148	21	0	
152	2271.3	0	245570	-4.59	148	8	521	269
254	2268.1	0	245551	5.03	146	8	711	329
330	2252.7	0	241425	11.91	78	6	940	323
216	2253.3	0	241425	-6.42	116	13	622	319
203	2254.1	0	241425	-0.73	122	10	635	294
114	2138	0	264183	-4.47	187	9	279	376
76	2138	0	265665	-13.18	186	9	216	325
191	2217.2	0	273885	2.93	194	15	457	383
140	2224.3	0	276523	27.25	188	14	356	361
114	2225.6	0	276523	0	178	15	305	345
0	2264.3	10	317727	-23.95	259	39	0	
203	2273.8	10	278143	4.98	143	12	572	327
203	2273.7	10	278143	-0.44	127	9	572	327
229	2277.8	10	278143	17.8	130	10	660	318
152	2278.8	10	261358	1.95	142	13	483	291
254	2280.8	10	261358	-16.94	115	10	584	400

229	2283.8	10	252511	3.27	110	12	483	436
0	2286.2	10	252511	1.54	105	10	0	
89	2288.7	10	252511	5.79	101	9	203	403
279	2290.6	10	254484	2.93	121	12	660	389
229	2291.8	10	278162	-23.97	137	13	584	360
127	2295.8	10	278162	-9.84	138	12	432	271
178	2292	10	278162	-3.61	154	11	457	358
254	2290.2	10	278162	-12.48	143	9	533	438
229	2289	10	254484	6.49	139	11	533	394
64	2281.4	10	251477	-14.77	110	12	152	383
203	2282.1	10	251477	22.63	101	12	495	377
254	2278.2	10	251477	13.53	126	11	597	391
254	2255.4	10	240458	5.27	100	7	584	400
229	2255	10	238398	-0.68	78	11	533	394
279	2254.6	10	238398	-11.69	84	9	686	375
191	2254	10	239292	-3.59	124	11	572	307
203	2254.4	10	239292	1.2	92	19	559	335
305	2256.4	10	240954	2.69	99	15	826	340
178	2255	10	240954	14.21	107	16	457	358
203	2254	10	240954	-11.23	116	16	559	335
203	2261.7	10	243434	-27.95	87	15	559	335
178	2252.9	10	243434	3.25	117	14	483	339
127	2253.1	10	245133	-11.69	90	15	330	354
229	2248.8	10	241404	7.86	123	6	572	368
191	2213.6	10	241044	2.56	187	9	470	373
152	2212.1	10	243722	-1.44	192	10	381	368
178	2213.4	10	243722	-4.66	142	6	432	379
127	2210.5	10	243722	-5.79	184	10	305	383
114	2210.7	10	243722	-0.83	201	11	279	376
102	2210	10	243722	-3.52	199	12	254	368
152	2210.4	10	243722	-19.17	200	12	368	381
267	2208.4	10	244482	2.47	98	9	622	394
241	2207.9	10	244482	3.56	89	14	584	380
203	2207.8	10	244482	6.86	90	10	508	368
267	2208	10	244482	1.12	150	16	622	394
191	2208.1	10	247246	-30.35	132	5	483	363
0	2199	10	236982	-13.21	250	19	0	
0	2198.9	10	240182	-25.51	250	19	0	
89	2188.9	10	240182	3.03	248	19	203	403

51	2199	10	240182	-7.23	249	25	127	368
0	2199.1	10	236982	-9.25	255	24	0	
0	2193.9	10	246267	-0.63	235	15	0	
483	2437.4	10	247456	5.93	168	6	1321	336
483	2437.1	10	247456	1.2	199	6	1372	324
381	2435.1	10	247456	-4.49	209	5	1156	303
457	2436.8	10	247456	-8.33	210	2	1270	331
432	2428.3	10	247456	3.32	222	4	1283	310
229	2434.2	10	238611	5.3	219	5	864	244
381	2436	10	238611	-7.1	203	8	1080	325
457	2435.8	10	238611	12.7	220	4	1219	345
432	2436.7	10	238611	-20.68	190	7	1257	316
457	2436	10	236666	-1.93	155	4	1283	328
0	2158	10	266585	-18.65	59	16	0	
254	2435.4	10	232177	1.1	125	13	914	256
178	2128.4	10	251944	3.59	96	3	432	379
114	2129.8	10	251182	6.1	159	5	381	276
89	2135.2	10	245204	-7.54	114	13	330	248
0	2138	10	243508	1.39	195	7	0	
114	2137.2	10	243508	3.66	198	6	419	251
102	2135.3	10	245539	-10.28	179	6	439	213
76	2133.6	10	247376	2.59	206	10	279	251
127	2135.4	10	250520	-1.51	153	7	318	368
102	2142.2	10	261715	2.66	171	11	318	294
0	2145.9	10	261081	12.94	155	12	0	
51	2148.4	10	261984	1.9	147	13	203	230
102	2152.1	10	261831	-15.41	141	16	318	294
76	2149.3	10	252785	1.56	161	7	305	230
241	2142.8	10	250821	-21.48	152	11	559	397
216	2141.9	0	242921	-4.96	93	10	584	340
127	2133.4	10	242237	-6.71	120	5	584	200
178	2130.1	10	252873	-13.94	111	10	406	403
0	2230.7	10	278351	1.46	234	27	0	
0	2292.4	10	272929	4.17	231	22	0	
0	2299.8	10	274877	6.54	108	32	0	
0	2305.8	10	238720	-12.48	260	24	0	
0	2291.9	10	265069	4.64	122	29	0	
0	2232.3	0	283668	3.37	191	13	0	
0	2132.4	0	278444	-5.47	176	17	0	

102	2142.2	0	292341	-13.09	196	17	254	368
102	2229.1	10	282876	-15.7	194	17	254	368
191	2237.5	0	294469	9.03	192	15	432	406
0	2259.9	10	332408	-8.89	195	38	0	
0	2214.5	10	327670	9.69	197	32	0	
0	2145.6	10	322901	-1.95	178	29	0	
0	2230.7	0	297955	-18.14	191	37	0	
0	2292.4	0	305311	-13.65	152	34	0	
0	2299.8	10	297506	-11.94	216	36	0	
0	2305.8	0	279263	43.7	229	37	0	
254	2299.4	10	267617	1.22	150	11	597	391
152	2300	10	267617	19.24	143	8	457	307
127	2301.6	10	274388	14.09	164	13	330	354
51	2304.3	10	291773	2.27	178	16	127	368
0	2301.3	10	291773	-35.18	173	13	0	
64	2300.2	10	294319	-8.72	185	14	152	383
0	2297.6	10	294319	15.89	178	15	0	
89	2304.2	10	294319	-1.49	170	15	203	403
178	2304.9	10	279843	4.76	174	13	483	339
127	2299.1	10	274388	14.4	157	15	356	329
305	2305.8	10	280811	4.69	155	17	787	356
305	2300.6	10	292254	11.13	153	18	711	394
254	2299.8	10	292254	4.35	158	19	559	418
64	2300.2	10	292254	1.9	153	18	152	383
127	2299.1	10	292217	-24.9	136	23	305	383
165	2297.3	10	292217	-4.86	152	19	381	399
203	2292	10	291392	6.69	160	21	508	368
254	2291.9	10	294829	-8.72	180	17	610	383
178	2292.5	10	291773	-0.42	168	15	432	379
51	2291.9	10	291773	2.22	163	15	114	409
0	2292.4	10	286362	-48.68	187	20	0	
0	2170.3	0	312540	-15.45	149	25	0	
0	2241.7	10	300918	0.42	192	26	0	
0	2260.1	10	304234	-6.98	203	27	0	
0	2230.7	10	282876	7.62	176	17	0	
0	2235	10	294469	-1.59	199	17	0	
0	2249.2	10	302220	8.08	184	19	0	
0	2249.9	10	302220	10.28	173	21	0	
127	2261.1	10	304234	22.12	199	29	330	354

0	2260.1	10	304234	12.01	184	31	0	
0	2259.7	10	311181	-3.03	195	32	0	
0	2259.9	10	311181	-1.44	192	28	0	
114	2265.2	10	304234	-11.87	193	29	419	251
0	2230.7	10	308164	-3.49	199	28	0	
0	2292.4	10	319224	5.69	192	24	0	
0	2299.8	10	313721	-0.22	202	32	0	
0	2305.8	10	313721	-0.22	202	32	0	
0	2291.9	10	321373	3.42	234	34	0	
0	2300.2	10	299119	5.59	225	36	0	
0	2170.3	10	314919	-2	231	34	0	
0	2304.3	0	333666	2.29	178	51	0	
0	2292.5	10	330561	-4	196	30	0	
0	2249.2	10	327056	12.74	236	37	0	
0	2300.2	10	297773	-0.29	234	26	0	
0	2297.6	10	281666	11.08	247	34	0	
0	2241.7	10	318452	14.11	210	30	0	
0	2291.9	10	297535	2.93	223	26	0	
0	2304.9	10	285775	-9.45	227	28	0	
0	2235	10	284803	3.61	135	31	0	
0	2299.1	10	281000	-10.01	230	34	0	
0	2297.3	10	315600	19.9	167	24	0	
0	2301.3	10	298182	3.91	136	25	0	
0	2292	10	292614	-6.32	141	28	0	
0	2304.2	10	294852	-1.61	215	15	0	
0	2300.6	10	310582	3.88	194	29	0	
0	2299.1	10	301300	46.12	199	36	0	
0	2260.1	10	287936	-3.59	220	41	0	
610	2677.2	0	170967	2.39	32	12	1930	291
889	2696.6	0	167387	-0.76	15	12	2388	343
203	2612	0	168421	33.96	345	16	533	350
254	2564.9	0	161831	-9.69	307	22	864	271
241	2562.7	0	161831	16.5	307	23	711	312
279	2539.4	0	167627	4.22	327	6	991	259
229	2540.3	0	167627	-4.91	340	16	1016	207
356	2660.4	0	186266	-71.39	33	26	1092	300
686	2660.5	0	186266	5.64	26	30	1854	340
432	2633.7	0	169553	13.53	60	19	1295	307
330	2633.4	0	169553	38.55	66	26	1321	230

343	2609.5	0	156937	-15.67	215	9	1016	311
330	2609.9	0	156937	3	297	6	1067	285
330	2607	0	155654	-19.82	352	12	1283	237
330	2483.9	10	161230	3.17	3	14	813	374
178	2482.9	10	161230	-10.45	358	11	940	174
381	2743.2	10	162070	2.05	333	9	1295	271
432	2610.2	0	168421	24.49	344	33	1245	319
279	2533.5	0	183809	-7.96	318	17	889	289
241	2530.8	0	183809	-2.42	318	16	838	265
305	2484.5	0	174974	4.17	315	24	940	298
368	2484.1	10	174974	13.35	321	19	965	351
305	2467.3	10	171839	-2.98	331	19	927	302
305	2450.4	10	151532	0.42	314	20	902	311
279	2447	10	151532	6.54	318	25	914	281
330	2539	0	165942	14.45	22	14	1118	272
495	2744.7	0	143402	-10.23	9	11	1880	242
381	2779.8	10	139205	17.7	24	27	1575	223
635	2706.4	0	173824	6.42	24	11	1880	311
330	2706.6	10	163885	5.37	23	13	1118	272
457	2706.9	10	163885	-2.73	30	11	1727	244
165	2482	10	161230	4	2	14	686	221
0	2451.6	0	227527	3.81	269	14	0	
495	2452.4	0	239129	-19.8	227	16	1334	342
305	2452.1	0	239129	-5.52	253	13	991	283
508	2452	0	231297	8.74	247	13	1168	400
267	2451.4	0	231297	-3.56	260	14	1168	210
394	2450.7	0	231297	-7.23	257	13	1143	317
356	2450.8	0	198034	7.59	78	10	1029	318
394	2467.8	0	218753	-0.17	72	12	1080	336
406	2470.3	0	218753	6.54	23	11	1194	313
381	2478.5	0	220050	7.3	16	28	1245	282
318	2483.2	0	220050	-0.12	12	12	1384	211
368	2490.9	0	208550	1.44	70	23	1168	290
318	2498.2	0	208550	-7.5	47	28	1118	261
470	2473.3	0	195995	-10.35	41	13	1346	321
432	2473.6	0	207694	14.5	36	12	1321	301
0	2452.7	0	227527	14.11	264	14	0	
356	2450	0	230268	-0.29	253	14	1054	310
419	2453.6	0	225300	-4	266	14	1168	330

343	2454.6	0	225300	-5.4	258	15	1067	296
394	2455.4	0	225300	-22.14	255	16	1092	332
406	2456.1	0	225300	-19.38	252	16	1041	359
432	2458.7	0	231644	7.5	260	19	1080	368
356	2462.2	0	231644	-7.69	263	19	1092	300
330	2463.6	0	231644	4.47	255	19	1041	292
356	2464	0	222317	-15.01	252	20	1080	303
406	2465.8	0	222317	-4	244	23	1143	327
305	2465.5	0	230262	-13.33	239	22	991	283
508	2614.3	0	209895	3.13	94	12	1448	323
406	2630.6	0	215077	-7.84	85	15	1295	289
508	2645.2	0	201486	-1.17	111	5	1575	297
521	2646.8	0	199680	-4.03	95	9	1600	299
432	2655.3	0	207762	1.9	36	7	1270	313
889	2689.2	0	187668	12.45	29	21	2540	322
406	2706.8	0	192398	2.08	29	9	1295	289
381	2720.5	0	204754	1.15	6	9	1270	276
419	2722.8	0	200555	-4.88	13	6	1422	271
483	2732	0	184506	-14.92	357	9	1638	271
508	2740.8	0	175579	-3.71	21	11	2032	230
610	2735.6	0	210840	-18.24	30	9	1905	294
406	2733.6	10	223536	1.17	63	11	1295	289
483	2677.8	0	217509	-1.2	95	15	1600	277
508	2691.2	0	202741	17.29	43	18	1778	263
406	2645.5	0	229899	4.15	96	6	1321	283
432	2645.5	0	229899	4.15	96	6	1422	279
432	2618.7	0	196920	13.6	79	12	1448	274
787	2753.4	0	238911	-5.79	201	1	1981	366
686	2753.1	10	214919	1.73	44	10	2057	307
762	2750.5	0	214062	11.94	56	9	2286	307
737	2751.3	0	214062	1.78	34	8	2108	321
762	2747.8	0	218898	6.13	352	2	1905	368
660	2724.6	0	233737	-5.96	84	9	1854	328
356	2453.1	0	225300	7.2	255	18	1092	300
381	2456.5	0	225300	-7.23	269	18	1054	333
432	2458.7	0	225300	9.79	256	17	1067	372
432	2460.4	0	227527	-11.16	262	15	1080	368
432	2461.8	0	225247	22.95	267	19	978	406
406	2464.2	0	225247	12.38	258	23	1029	363

508	2466.7	0	225247	-8.08	265	22	1181	396
508	2469.4	0	225247	-2.32	260	27	1181	396
356	2472.9	0	220716	1	255	28	889	368
381	2461.9	0	225247	-3.22	269	20	991	354
305	2457.3	0	189240	4.86	16	9	673	417
305	2457.5	0	189240	-1.37	347	9	673	417
305	2457.7	0	189240	1.44	14	10	711	394
330	2473.2	0	202982	2.12	71	3	737	412
229	2473.5	0	202982	12.7	69	5	787	267
178	2473.6	0	202982	-4.27	9	4	737	222
356	2522.2	0	203051	-3.91	39	7	1092	300
381	2522.4	0	203051	-0.24	9	5	1156	303
330	2522.2	0	203051	17.5	13	5	1029	295
254	2523.4	0	208463	-3.54	94	16	940	249
432	2524	0	208463	-5.59	94	18	927	428
356	2524	0	208463	-2.03	72	16	940	348
305	2542.4	0	220514	-2.66	36	12	1016	276
254	2542.9	0	220514	-4.2	32	11	838	279
254	2542.9	0	220514	21.29	33	8	889	263
279	2577.8	0	214433	3.25	56	9	864	298
279	2576.5	0	214433	-5.42	24	5	991	259
254	2576.7	0	214433	8.23	119	4	902	259
330	2596.5	0	202940	2.73	332	6	1219	249
381	2596.5	0	202940	2.05	318	8	1194	294
330	2613.7	0	195395	4.71	44	8	1219	249
330	2612.6	0	198694	-7.52	29	8	1118	272
330	2612	0	198694	-3.05	25	8	1156	263
381	2629.7	0	208868	-5.15	219	3	1067	329
406	2629.9	0	208868	-14.43	143	6	1092	342
381	2629.2	0	208868	2.08	91	6	1270	276
381	2639.9	0	195478	-13.75	299	5	1219	288
457	2640.6	0	195478	-15.84	47	2	1384	304
432	2640.4	0	195478	-0.93	62	6	1397	284
432	2673	0	194555	-6.1	5	15	1575	252
406	2672.1	0	190042	-12.11	327	19	1473	254
381	2673.7	0	194555	-17.07	317	8	1397	251
330	2628.7	0	207193	9.42	12	5	1168	260
406	2628	0	207193	21.17	51	13	1295	289
330	2627.7	0	207193	5.49	22	12	1168	260

483	2613.5	0	203095	-11.91	8	4	1549	287
330	2612.8	0	203095	-7.69	310	6	1219	249
279	2612.9	0	202050	-4.86	5	7	1041	247
330	2599.6	0	202856	0.81	48	9	1168	260
279	2598.1	0	202856	-3.64	35	6	991	259
152	2597.5	0	202856	11.47	38	11	660	212
330	2574.2	0	201911	10.91	25	12	1118	272
356	2574.2	0	204046	12.04	27	14	1092	300
432	2574.5	0	204046	-7.1	9	12	1321	301
279	2513.1	0	217264	1.61	27	9	991	259
305	2512.4	0	217264	15.58	48	8	1067	263
305	2511.7	0	217264	-1.56	34	10	991	283
432	2452.2	0	231297	-12.26	250	14	1194	333
483	2452.6	0	231297	-10.94	235	13	1168	380
381	2452.8	0	231297	-5.2	238	12	1041	337
330	2452.1	0	239129	17.21	285	14	1016	299
330	2453.3	0	239129	0.78	231	11	838	362
305	2453.6	0	239129	-7.4	255	11	940	298
432	2454.4	0	239129	-5.76	235	13	1219	326
356	2650.6	0	216465	-4.88	72	15	1295	253
305	2650.8	0	216465	5.62	66	12	1067	263
330	2606.2	0	205149	8.06	61	11	1143	266
330	2605.5	0	205149	-12.84	43	10	1194	254
356	2590	0	218080	-5.25	49	8	1219	268
381	2589.1	0	218080	-4.88	35	10	1270	276
356	2568.1	0	243447	8.06	114	12	1168	280
330	2567	0	243447	0.22	109	12	1219	249
356	2539.1	0	219624	2	65	15	1194	274
216	2503.6	0	201882	-16.19	55	24	1067	186
229	2501.6	0	199753	-16.77	72	18	940	224
432	2644	10	225692	-1.17	61	7	1473	270
483	2650.5	10	225983	11.89	71	6	1676	265
432	2666.2	0	191687	12.99	51	12	1270	313
508	2666.3	0	191687	12.99	51	12	1702	275
864	2694.6	10	225816	7.42	54	24	2540	313
457	2694.9	10	225816	23.88	55	19	1626	259
813	2693.9	10	225816	-44.29	73	26	2413	310
533	2674.4	10	183110	-7.08	28	13	1600	307
940	2668.8	10	183110	-12.45	22	14	2743	315

610	2681.9	10	201769	22.05	69	31	1930	291
508	2678.2	10	190287	19.78	69	29	1651	283
559	2679	10	189197	3.69	70	28	1753	293
838	2725.6	0	228750	6.52	110	4	2032	380
533	2724.4	0	230764	-1.61	71	5	1575	312
254	2536.5	10	227471	-5.52	97	27	813	288
191	2624	0	182953	6.93	345	25	559	314
305	2623.6	0	182953	25.66	348	29	889	315
305	2459.4	10	171839	7.91	347	20	940	298
356	2445.6	10	193502	-0.73	14	4	775	422
254	2446	10	193502	5.83	334	9	838	279
305	2446.1	10	193502	-1.49	348	6	1067	263
305	2556.8	0	214110	-2.22	338	8	1003	279
305	2556.4	0	214110	-2.05	84	6	914	307
305	2555.4	0	214110	16.72	13	6	991	283
0	2572.2	10	213712	4.74	334	9	0	
406	2664.8	0	194736	48.14	9	7	1334	280
432	2667	0	194736	0.46	312	6	1422	279
381	2665	0	194736	-30.96	346	9	1372	256
330	2681.6	0	196951	-6.69	318	4	1143	266
305	2683.8	0	196951	1.71	279	13	1029	273
254	2684.7	0	196951	20.58	356	9	889	263
279	2704.3	0	214353	-10.08	334	4	1092	235
381	2705.2	10	214353	-17.65	21	8	1346	260
432	2705.6	0	214353	13.16	48	8	1448	274
292	2712.2	10	213441	-1.66	6	4	1080	249
305	2712.6	10	213441	-9.08	21	12	1080	260
318	2713	10	213441	6.57	4	16	1181	247
483	2713.1	10	218150	-16.06	35	5	1524	291
381	2713.9	10	218150	-1.66	357	9	1384	253
381	2712.6	10	218150	13.11	4	11	1422	246
356	2704.9	10	221976	-0.54	41	9	1295	253
356	2706.5	10	221976	-15.8	27	7	1219	268
356	2701.9	10	218803	-9.3	55	8	1257	260
394	2698.3	10	215349	9.67	47	8	1397	259
343	2697.8	10	214346	4.74	55	8	1194	264
343	2698.6	10	214346	-3.47	33	12	1232	256
356	2683	10	208964	10.23	326	15	1321	248
381	2677.6	10	208964	-20.73	23	10	1308	268

381	2682.1	10	208964	5.25	337	13	1270	276
381	2677.4	10	210734	-3.39	343	13	1346	260
279	2659.2	10	213417	-7.74	327	13	1092	235
330	2672.2	10	210734	1.12	6	11	1219	249
508	2746.3	10	182181	14.53	71	34	2057	227
406	2532.8	0	176643	4.08	50	5	1283	291
381	2533	0	176643	6.86	27	7	1321	265
305	2753.8	10	205921	4.98	7	11	1219	230
279	2751.1	10	205921	3.25	347	17	1092	235
305	2750.5	10	205921	-5.64	3	15	1245	225
229	2675.9	10	204412	-11.94	32	15	940	224
267	2676.1	10	204412	-15.06	10	7	1041	236
279	2676.1	10	213429	-7.2	50	8	1067	241
279	2663.5	10	226853	8.96	86	7	1219	211
330	2661.8	10	226853	1.98	58	9	1168	260
279	2664.4	10	228255	-3.37	68	12	1067	241
254	2660.3	10	228255	-0.37	62	11	1041	224
241	2620.4	10	205726	-5.83	42	11	914	243
279	2624.5	10	205726	2.47	51	13	1016	253
254	2475.4	0	194100	3.25	55	16	1118	209
241	2474.8	0	194100	-11.3	59	13	1041	213
292	2454.5	0	240359	-1.71	241	13	927	290
318	2454.3	0	240359	1.17	247	13	1067	274
356	2453.9	0	239129	3.32	250	15	1067	307
318	2453.2	0	239129	-0.15	246	12	978	299
292	2452.6	0	239129	1.56	252	13	953	282
229	2635.7	0	234781	6.54	302	4	800	263
292	2635.3	0	241687	0.34	259	7	991	271
508	2627.4	0	254939	-13.7	191	6	1422	329
533	2627.2	0	254939	14.99	99	25	1524	322
279	2622.8	0	269222	-8.72	144	7	965	266
584	2693.6	0	235204	15.23	95	16	1702	316
508	2679.9	0	245875	-8.72	100	17	1549	302
508	2666.8	0	238386	1.9	53	10	1613	290
406	2670.4	0	248596	-8.28	112	9	1346	278
457	2671.1	0	248816	10.69	77	7	1422	296
457	2671.1	0	248816	10.69	77	7	1422	296
381	2672.1	0	245164	-5.03	89	7	1295	271
381	2675.3	0	239660	6.54	93	12	1321	265

406	2680.6	0	242324	2.71	84	10	1346	278
406	2651.8	0	255596	6.27	148	4	1321	283
483	2458.8	0	243804	-21.83	222	14	1321	336
483	2460.3	0	239494	-0.32	238	12	1219	364
457	2460.7	0	243804	5.96	225	15	1194	352
432	2487.5	0	253436	-3.44	241	18	1295	307
533	2485.2	0	257000	11.65	251	23	1524	322
483	2487	0	257000	-0.76	247	21	1372	324
330	2572.7	10	255956	-21.97	257	8	1067	285
508	2569.1	0	255577	10.69	157	5	1397	335
508	2568.9	0	255577	8.72	138	4	1422	329
483	2570.6	0	255577	5.74	129	11	1372	324
584	2579.8	0	245680	-2.78	181	6	1600	336
457	2585.7	0	249790	-15.09	160	11	1295	325
508	2579.7	0	249790	-3.13	162	7	1422	329
660	2627.9	0	281349	-15.16	228	26	1829	332
559	2619.6	0	281349	3.83	232	20	1499	343
559	2618	0	255719	11.94	241	22	1626	316
660	2679.5	10	263421	0.17	208	10	1727	352
610	2682	0	263421	3.76	183	7	1676	335
584	2684.5	0	263421	0.32	212	11	1600	336
787	2753.5	0	238911	-13.4	90	3	2032	357
737	2753.6	0	221350	-0.56	274	2	1905	356
737	2747.8	0	218898	-4.3	44	4	1981	342
660	2747.8	0	218898	-13.06	160	2	1829	332
610	2710.8	0	247985	-0.15	122	7	1753	320
660	2708.1	0	253463	2.61	121	6	1803	337
660	2709.2	0	244446	-6.08	147	2	1778	342
457	2623.4	0	244336	4.39	201	6	1346	312
533	2623.9	0	244336	1.27	271	5	1499	327
457	2623.9	0	244336	1.42	248	2	1270	331
483	2624.7	0	253669	6.1	226	7	1448	307
635	2627.7	0	259314	6.42	241	8	1524	383
533	2623	10	260117	-0.66	240	7	1499	327
457	2567.8	0	264584	3.91	250	8	1321	318
533	2568.6	0	260730	-0.44	228	5	1422	345
432	2565.9	0	248597	-2.08	293	4	1321	301
432	2464.6	0	243812	14.04	255	19	1118	355
381	2460.6	0	243812	-4.59	261	16	991	354

432	2460.9	0	243812	-0.22	257	14	1219	326
432	2449.7	0	239129	-2.71	283	14	1207	329
406	2450.7	0	239129	3.83	251	14	978	382
432	2451.5	0	239129	7.4	251	17	1054	377
457	2451.6	0	239129	4.52	236	18	1118	376
457	2452.1	0	240359	7.91	241	13	1041	404
457	2452.8	0	240359	-22.97	255	15	1016	414
381	2638	0	256825	17.65	104	19	991	354
330	2604.6	10	268171	-9.91	87	8	991	307
356	2565.8	10	256890	8.52	93	15	1041	314
279	2474	10	244005	13.53	93	17	914	281
368	2654.4	0	277120	-13.7	118	26	927	365
203	2510.8	0	244753	9.25	34	9	597	313
279	2510.9	0	244753	-11.65	42	8	737	349
406	2510.9	0	244753	-27.1	42	10	1168	320
381	2454.7	0	240359	-2.37	235	13	1080	325
381	2456	0	240359	-19.85	256	14	1054	333
330	2456.3	0	240359	-20.75	252	13	978	311
483	2458.8	0	240359	-10.33	250	13	1422	312
508	2460.3	0	241344	10.23	254	14	1384	338
457	2463.6	0	241344	10.28	257	19	1232	341
508	2465.5	0	243812	-6.88	254	21	1372	341
483	2466.9	0	243812	-9.81	251	21	1346	330
457	2469.4	0	242240	20.68	250	22	1295	325
381	2471.3	0	242240	23.71	255	25	1016	345
305	2473.7	0	242240	18.82	258	27	991	283
330	2475.7	0	242240	-4.15	247	24	991	307
305	2716.7	0	260040	-0.2	92	18	1270	221
279	2715.8	0	260040	10.74	95	17	1143	225
292	2712.2	0	252683	-12.55	97	17	1194	225
305	2711.3	0	239043	14.79	109	25	1346	208
178	2710.5	0	239043	4.93	77	13	787	208
279	2577.8	0	242836	9.89	73	1	838	307
165	2577.6	0	242836	-0.54	123	8	635	239
559	2610.1	10	250688	-10.96	194	8	1753	293
406	2646.1	10	200983	-1.56	41	8	1473	254
508	2726.2	10	234559	-2.76	22	9	1854	252
533	2720	10	247679	-5.1	43	7	1880	261
584	2716.4	10	254862	2.44	57	7	1930	278

457	2575	0	251460	-0.12	281	8	1448	291
381	2571.4	10	255956	14.33	274	9	1092	321
559	2642.3	10	249148	7.69	187	10	1448	355
584	2641	10	249148	-23.17	210	17	1651	326
229	2664.9	10	260117	-0.81	107	9	533	394
533	2650.5	10	260117	-3.88	165	8	1575	312
584	2660	10	244884	41.06	117	13	1600	336
660	2657.1	10	260117	-2.32	145	11	1473	412
508	2676.3	10	270958	17.33	211	18	1321	354
457	2684.7	10	270958	6.49	219	17	1346	312
533	2671	10	270958	8.98	206	13	1422	345
686	2706.5	10	260138	-0.44	193	1	1905	331
660	2706.7	10	264966	17.26	230	8	1753	347
635	2707.2	10	260138	-5.79	221	5	1676	348
660	2692.3	10	253618	-7.5	177	6	1778	342
584	2693.8	10	253618	-11.28	215	6	1676	321
559	2691.1	10	253618	10.94	188	2	1626	316
330	2488.2	10	253505	2.66	240	13	889	342
457	2489.5	10	253390	9.08	246	13	1118	376
457	2487.4	10	254288	-14.53	240	12	1270	331
394	2614.2	0	278090	-25.05	129	10	1067	340
495	2590.3	10	276967	-3.69	104	25	1245	366
432	2478.6	0	242240	2.32	253	27	1194	333
279	2742.2	0	248434	4.54	103	7	1219	211
279	2741.3	0	248434	-7.86	97	16	965	266
279	2740.6	10	248434	5.96	105	14	1143	225
279	2717.9	10	257194	6.98	91	16	1245	207
406	2519.3	0	285821	-1.54	159	15	1118	335
483	2519.1	0	283608	-51.56	173	17	1295	343
457	2521.7	0	283608	-2.83	168	18	1168	360
559	2526.4	0	287570	7.62	156	19	1219	422
508	2527	0	287570	-16.19	179	17	1245	376
356	2530.3	0	287570	-3.27	181	18	965	339
457	2567.7	0	287538	2.42	176	12	1270	331
457	2569	0	287538	2.17	186	13	1270	331
559	2571.3	0	287538	1.83	184	16	1295	397
483	2746.4	0	295177	1.29	216	11	1651	269
457	2747.6	0	286404	6.67	205	16	1321	318
533	2749	0	286404	-14.6	245	16	1626	302

356	2725.1	0	304114	5.98	158	21	838	390
330	2724	0	301336	-4.71	159	26	864	352
305	2674.2	0	303618	-5.27	131	37	876	320
330	2653.2	0	277120	-12.23	114	26	1041	292
292	2672.5	0	303464	-18.12	143	35	826	326
330	2586	10	276967	7.86	152	18	965	315
102	2816.9	0	153974	3.59	346	25	419	223
152	2816.6	0	157721	-5.1	337	24	610	230
127	2817.1	0	157721	-17.85	341	28	610	192
533	2811.4	0	133051	6.01	345	21	1981	248
356	2790	0	156034	-1.78	338	28	1270	258
191	2789.5	0	156034	9.96	336	28	787	223
152	2789	0	142561	-1.76	345	34	584	240
965	2811.4	0	133051	23.61	356	23	2286	388
584	2811.9	0	133051	6.01	345	21	2134	252
864	2777.9	10	121757	-3.3	309	25	2083	381
533	2779.6	10	121757	7.2	309	25	1676	293
559	2779	10	121757	-3.3	309	25	1689	304
406	2785.1	10	124493	14.28	298	29	1575	237
406	2765.1	10	113495	0.56	357	21	1905	196
508	2765.6	10	113495	3.83	347	19	1930	242
432	2764.4	10	113495	0.27	359	25	1854	214
584	2768.5	10	132149	2.32	19	23	1295	415
305	2770.3	10	132149	4.05	28	32	1118	251
584	2771.4	10	139486	16.72	358	26	1956	275
584	2771.8	10	139486	13.16	352	23	1956	275
686	2772.7	10	131500	-2.66	345	33	2134	296
457	2774.6	10	131500	8.15	9	33	1791	235
457	2774.9	10	131500	-6.23	15	33	0	
406	2777.3	10	125196	-0.71	0	25	1422	263
483	2777.4	10	152796	2.44	36	32	1880	236
457	2778.1	10	152796	6.86	37	32	1829	230
305	2777.7	10	152796	5.91	30	38	1549	181
432	2777.8	10	162565	-2.88	318	3	1626	244
305	2770	10	162565	8.3	330	7	1245	225
305	2769.4	10	135212	11.69	57	32	1168	240
356	2797.4	10	170171	8.84	352	20	1092	300
508	2769.3	10	156782	5.13	16	20	1702	275
305	2769.5	10	161745	-11.82	8	21	1397	201

229	2768.5	10	161745	-5.62	6	23	965	218
432	2927.5	10	134610	7.76	38	36	2108	188
470	2829.3	10	134951	22.78	353	32	2032	213
610	2825.3	10	130205	-9.01	1	33	2261	248
686	2818.7	0	220313	-60.52	82	25	2083	303
127	2810.7	0	183903	-0.44	289	32	495	236
152	2810.4	0	183903	-0.44	289	32	686	204
432	2773.7	10	181749	5.2	66	26	1702	233
203	2816.1	0	189712	11.69	340	8	610	307
660	2816.1	0	257874	9.11	193	5	1829	332
533	2817.1	0	252198	7.57	102	3	1422	345
635	2816.8	0	256760	-39.84	257	9	1803	324
838	2807.8	0	265033	6.76	71	6	2184	353
813	2805.5	0	264944	4.86	79	5	2159	346
787	2807.1	0	264944	-6.71	54	10	2184	332
635	2818.3	10	243335	0.02	210	7	1854	315
559	2819.7	10	243335	0.07	188	6	1854	277
864	2818.2	10	243335	8.91	209	7	1829	434
584	2770.5	0	288722	-14.06	138	22	1803	298
356	2773.2	0	285278	13.65	137	21	1397	234
533	2776.1	0	292670	0.51	112	25	1651	297
737	2809.1	0	285107	-6.35	171	6	1956	346
559	2809.9	0	275198	2.37	173	7	1626	316
787	2810.9	0	274893	6.71	233	15	2032	357
686	3069.4	0	357321	-0.68	157	25	2337	270
470	3067.2	0	355484	7.98	164	28	1448	299
432	2959.9	0	332296	-10.16	164	23	1422	279
394	2957	0	335797	14.84	164	20	1194	303
597	2906.8	0	319122	-15.23	135	17	1702	323
406	2898.6	0	319122	-2.39	128	19	1105	338
584	2815.2	0	284379	14.26	133	18	1499	359
343	3321.5	0	343534	24.29	176	31	1067	296
318	3251.6	0	382112	-0.85	166	25	965	303
546	3248.1	0	381908	-16.02	173	37	1778	283
330	3156.7	0	368342	-2.73	150	29	1105	275
292	3152.9	0	368342	-10.42	146	35	914	294

APPENDIX B

CONDITIONAL STATEMENTS FOR SPATIALLY DISTRIBUTING SWE MODELS

Binary regression tree:

```
Con("w_fork_dem" < 2128 , 46, Con(("w_fork_dem" < 2415)  &  ("w_fork_dem" > 2128)  &  ("wfork_rad2" >= 278300),43,Con(("w_fork_dem" < 2415)  & ("w_fork_dem" > 2128)  & ("wfork_rad2" < 278300),161,Con(("w_fork_dem" > 2415) &  ("w_fork_dem" < 2676) & ("wfork_rad2" <243600),359,Con(("w_fork_dem" > 2415) & ("w_fork_dem" < 2676) & ("wfork_rad2" > 243600),453,Con(("w_fork_dem" > 2676) & ("wfork_rad2" < 218900),434,545))))))
```

Conditional inference tree:

Con(("w_fork_dem" < 2412) & ("w_fork_dem" < 2127) & ("wfork_rad2" <= 208790),92,Con(("w_fork_dem" < 2412) & ("w_fork_dem" < 2127) & ("wfork_rad2" > 208790) & ("wfork_rad2" <= 232939),16,Con(("w_fork_dem" < 2412) & ("w_fork_dem" < 2127) & ("wfork_rad2" > 208790) & ("w_fork_dem" < 1952) & ("wfork_rad2" > 232939),0,Con(("w_fork_dem" < 2412) & ("w_fork_dem" < 2127) & ("wfork_rad2" > 208790) & ("w_fork_dem" > 1952) & ("wfork_rad2" <= 244328),85,Con(("w_fork_dem" < 2412) & ("w_fork_dem" < 2127) & ("wfork_rad2" > 208790) & ("w_fork_dem" > 1952) & ("wfork_rad2" > 244328),26,Con(("w_fork_dem" < 2412) & ("w_fork_dem" > 2127) & ("wfork_rad2" <= 278162) & ("w_fork_dem" < 2201) & ("wfork_rad2" <= 236982),116,Con(("w_fork_dem" < 2412) & ("w_fork_dem" > 2127) & ("wfork_rad2" <= 278162) & ("w_fork_dem" < 2201) & ("wfork_rad2" > 236982),89,Con(("w_fork_dem" < 2412) & ("w_fork_dem" > 2127) & ("wfork_rad2" <= 278162) & ("w_fork_dem" > 2201) & ("cov_reclass5" < 5),225,Con(("w_fork_dem" < 2412) & ("w_fork_dem" > 2127) & ("wfork_rad2" <= 278162) & ("w_fork_dem" > 2201) & ("cov_reclass5" > 5),185,Con(("w_fork_dem" < 2412) & ("w_fork_dem" > 2127) & ("wfork_rad2" > 278162) & ("wfork_rad2" <= 294829),84,Con(("w_fork_dem" < 2412) & ("w_fork_dem" > 2127) & ("wfork_rad2" > 294829),7,Con(("w_fork_dem" > 2676),486,Con(("w_fork_dem" > 2412) & ("w_fork_dem" < 2676) & ("wfork_rad2" > 243447),453,Con(("w_fork_dem" > 2412) & ("w_fork_dem" < 2676) & ("wfork_rad2" <= 243447) & ("wfork_rad2" > 228255),385,Con(("w_fork_dem" > 2412) & ("w_fork_dem" < 2676) & ("wfork_rad2" <= 228255) & ("w_fork_dem" <= 2628),325,Con(("w_fork_dem" > 2412) & ("w_fork_dem" < 2676) & ("wfork_rad2" <= 228255) & ("w_fork_dem" < 2628),405))))))))))))))))